Neural dynamics of human motor control

Tjeerd Boonstra

The work presented in this thesis is part of the research program of the Institute for Fundamental and Clinical Human Movement Sciences (IFKB), and was carried out at the Faculty of Human Movement Sciences, VU University Amsterdam, the Netherlands. This research was financially supported by the Dutch Science Foundation (NWO grant #051.02.050).

ISBN: 9789086591268

Cover adapted from: W. Ross Ashby, Design for a brain, 1952
Design: Ruben van Nimwegen
Printer: Print Partners Ipskamp, Enschede

VRIJE UNIVERSITEIT

Neural dynamics of human motor control

ACADEMISCH PROEFSCHRIFT

ter verkrijging van de graad Doctor aan
de Vrije Universiteit Amsterdam,
op gezag van de rector magnificus
prof.dr. L.M. Bouter,
in het openbaar te verdedigen
ten overstaan van de promotiecommissie
van de faculteit der Bewegingswetenschappen
op donderdag 20 september 2007 om 13.45 uur
in de aula van de universiteit,
De Boelelaan 1105

door

Tjeerd Willem Boonstra

geboren te Wageningen

promotor: prof.dr. P.J. Beek
copromotor: dr. A. Daffertshofer

voor mijn opa

Contents

1. General introduction 9

2. Fatigue-related changes in motor-unit synchronization of quadriceps muscles within and across legs 25

3. Bilateral motor unit synchronization is functionally organized 49

4. Effects of sleep deprivation on event-related fields and alpha activity during rhythmic force production 65

5. Amplitude and phase dynamics associated with acoustically-paced finger tapping 79

6. Multivariate time-frequency analysis of electromagnetic brain activity during bimanual motor learning 97

7. Epilogue 113

Appendix A. Principal component analysis 129

Appendix B. MEG-compatible force sensor 131

References 137

Summary 159

Samenvatting 163

Dankwoord 169

List of publications 173

I.

General introduction

1.1 Panta rhei: a focus on change

The human brain is without doubt an intriguing and interesting scientific subject. It seems to conceal answers to vital questions that have puzzled mankind throughout history, such as "What is consciousness?", and "How is language produced?" Apart from being the subject of endless research, the brain is simultaneously the instrument used for its own analysis, which imposes a fundamental epistemological question (cf. Yates, 1980): "What can the brain know about itself?" Given that in most parts of my thesis I consider the brain as the primary object of research, let me here take the opportunity to reflect on the role of the brain as vehicle for scientific research.

In general, science is strongly influenced by positivism, a tradition based on empiricism that postulates experience as the sole source of knowledge. According to this tradition, strict methods of empirical science are the only means to acquire scientific knowledge and all knowledge should be based on logical inference from observable facts (Stent, 1975). This view agrees with the notion of the brain as a *tabula rasa*, i.e. a blank slate, whose entire knowledge base is gradually built up by merely combining simple and ultimate facts derived from sense experiences. Hence, from the positivist point of view, the objective nature of brain research is ensured, because the influence of the brain as an instrument of analysis is reduced to sheer associations of factual observations. However, the problem is that the number of properties of an object that may be perceived tends to infinity. Any two objects can thus be maximally similar to each other depending on the properties chosen for comparison. In consequence, differentiating between different classes of objects requires a selection of the to-be-compared properties (Keil et al., 1998). This problem of empiricism has been extensively discussed in the context of categorization theories in the field of psychology (Keil, 1981; Murphy and Medin, 1985), but has similar implications for a positivist position in science (cf. ter Hark, 2003). That is, classes as well as theories can only be formed if distinct properties of the objects are excluded *a priori* (Yates, 1980). Evidently, excluding or, more provocatively, ignoring properties is a subjective rather than an objective act.

It therefore seems sensible to investigate the grounds for selecting the relevant properties of the object under study, in casu the brain. Despite the need for a pre-selection of properties to investigate, science is by no means an entirely subjective endeavor (cf. Walter, 1971; Popper, 1972; Davies, 1995). Its

recognition only denotes the focus of research and, given this focus, the properties of the system (brain) are observed and analyzed objectively. The role of, and need for, a focus or perspective in scientific research is discussed in depth by Kuhn (1962), who identified the focus of a particular scientific community as a paradigm, i.e. the set of recurrent and quasi-standard illustrations of various theories in their conceptual, observational, and instrumental applications as manifest in textbooks, lectures, and laboratory exercises. A paradigm restricts the focus of factual scientific investigation to a small range of relevant problems and instrumental applications and thus forces scientists to investigate some part of nature in detail and depth that would otherwise be unimaginable. As such, an a priori focus seems indeed necessary and even beneficial for any scientific process and progress.[1]

What perspective or paradigm did I use for my thesis? To answer that question I shall thus discuss the essential concepts, observations, and instrumental applications that served to focus my research to a particular problem in the realm of neuroscience. Note that apart from limiting the field of research, a paradigm may also stipulate the approach needed to answer a certain question. Before discussing these more technical details, however, let me first step back and dwell on the scientific tradition the here chosen paradigm belongs to. In most general terms, the perspective of this thesis is on change. I assume that the brain can best be understood in terms of processes rather than compounds or things, i.e. in terms of modes of change instead of fixed constituents. This stance is part of the conceptions of process philosophy, which holds that processes are more fundamental than things (Rescher, 1996). In its more rigorous version, process philosophy regards all (physical) things reducible to (physical) processes, a position that goes all the way back to

[1] Paradigmatic research is not the only modus operandi and there can be scientific research without paradigms, namely when there is not a firmly based agreement upon the scientific achievements that serve as the foundation of a particular research area. About the pre-paradigmatic period Kuhn (1962, p. 46-47) states "The pre-paradigm period, in particular, is regularly marked by frequent and deep debates over legitimate methods, problems, and standards of solution, though these serve rather to define schools than to produce agreement." It may be argued that neuroscience is in its pre-paradigmatic period, inviting its contributors to describe their perspectives on the research topic and methods used. Alternatively, one might argue that the situation in neuroscience can be better captured by competing 'research traditions' (Laudan, 1977), similar to the situation in psychology (Gholson and Barker, 1985).

Heraclitus' famous aphorism *panta rhei*.[2] In contrast, Parmenides (ca. 515-450 BC) already stated that the reality of the world is an unchanging, ungenerated, indestructible whole. That is, at the very beginning of the western tradition of science, or arguably even before (cf. Heidegger and Fink, 1979), a dichotomy emerged regarding the nature of reality. This dissension of axioms is, however, not a relic of the past, but a recurrent theme in the history of philosophy and science. To indicate the relevance for modern-day neuroscience, let me discuss one of Heraclitus' fragments: "We both step and do not step in the same rivers. We are and are not." This poses the question how a river remains the same although its constituents change continuously. A river is clearly not defined solely by its constituents, i.e. water molecules, but particularly by the processes that organize the flow of the constituents in a more or less regular pattern – since the molecules themselves cause the flow pattern this relates to more recent ideas of self-organization (cf. Gare, 2002). Similarly, one may question how the brain is organized to function consistently and coherently despite, or because of, the continuous change of its components and/or environment.

Fortunately, the opposition in neuroscience is not as extreme as that between Heraclitus and Parmenides. Most neuroscientists will acknowledge that the brain has both more static and more dynamic characteristics. However, the focus of researchers may differ considerably and is found along most part of the continuum. For instance, Gall (1758-1828), the founder of phrenology, suggested that the brain is divided into separate organs each corresponding to a discrete human faculty or function. He further assumed that these faculties are innate and that the brain is composed of as many particular organs as there are faculties, tendencies, and feelings (Zola-Morgan, 1995). Accordingly, brain functioning can be explained by examining its constituents or parts, considering substance the primary grounds of description. In contrast to this atomistic view, James (1842-1910), for example, posited that human functions correspond to the entire activity of the brain (James, 1890), a stance that thus regards processes fundamental (cf. Rescher, 1996). Both ideas have profoundly influenced psychology and neuroscience and several derivates appear in contemporary neuroscience. In the present context, these ideas merely serve as an example and I shall not discuss other

[2] Although this statement has generally been ascribed to Heraclitus, this is probably erroneous (Russell, 1946). However, Heraclitus, as is apparent from his fragments cited by Plato and Aristotle, clearly acknowledged the universality of change and development through internal contradictions (Russell, 1946, Heidegger and Fink, 1979).

contributors to both standpoints. Such a discussion would most likely divert the argument made here, namely that the perspective of this thesis is a focus on change and stands in the scientific tradition that considers processes fundamental. Instead, I will focus on the concepts, empirical observations, and instrumental applications essential for investigating neural synchronization during human motor control and explain how it constrained the focus of my thesis.

1.2 Concepts: a focus on physics

Doing neuroscience with a focus on processes implies that the functioning of the human brain can be described best using concepts from the physics of complex systems. This relation to physics may seem trivial, but, when thinking of the more substance-oriented approach portrayed as exemplified by the afore-sketched ideas of Gall, it seems apparent that not all concepts in neuroscience are rooted in physics. For instance, if the state of each neuron is considered to be simply on or off, a system of multiple neurons could effectively be described by two-valued logic, i.e. on the basis of tertium non datur (like a conventional digital computer). Accordingly, the relations between different neuronal states can be captured just syntactically, i.e. in terms of formal relations, which has its roots in a so-called logical atomism (Churchland, 1980). In consequence, this approach cannot capture the dynamics of the system, because syntactic relations lack intrinsic temporality (cf. Clark, 1998). Note again, however, that this approach by no means denies the existence of dynamics in neuronal activity, it just regards it as belonging to a different level of organization which, as such, is irrelevant for describing human performance (Fodor, 1975; Newell and Simon, 1976; Marr and Poggio, 1977). In contrast, by approaching neuroscience in terms of complex systems in physics one considers the neural dynamics fundamental and one has to determine how the dynamics of the system are capable of brain functioning, i.e. information processing. To do so, one has to apply tools to recover potential information-bearing vehicles from highly complex webs of interrelated neural activity and to discern intrinsically temporal features of the system which may play representational and computational roles (cf. Port and van Gelder, 1995; Clark, 1998; Varela et al., 2001).

What seems important to note is that a complex systems approach in neuroscience does not imply a unidirectional reasoning from 'low level'

physical processes to 'high level' cognitive functions in terms of a troublesome reductionistic inference (Churchland, 1980). In fact, even in physics scientists seem to agree that microscopic processes may not necessarily yield the optimal or ultimate description of macroscopic processes. Instead, describing activity at a macroscopic level requires new concepts and generalizations supplementing the prevailing microscopic constraints. To find such concepts and generalization, so-called phase transitions form essential circumstances at which the system's macroscopic state or phase changes qualitatively while microscopic symmetries are broken.[3] Put differently, while the system's parts or constituents are constrained to maintain certain fixed relationships with each other, the symmetry only allows to obey as a whole in response to external forces (Anderson, 1972). In consequence, the laws describing the system's behavior at the microscopic level cover a range of states in which the system will never be present when the microscopic processes are grouped and constrained by a macroscopic process. Hence, the laws at the microscopic level do not always suffice to efficiently describe the system's behavior at a higher level and may therefore require new concepts (Pattee, 1973; Laughlin and Pines, 2000).

Concepts and tools used in the complex systems approach to neuroscience are mainly borrowed from non-equilibrium thermodynamics and nonlinear statistical mechanics (cf. Yates, 1980; Haken, 1996). In fact, concepts from these fields have been used across sciences and turned out to be interdisciplinary at heart, which becomes especially apparent when exploiting the common mathematical language of dynamical systems as formalized, e.g., in synergetics. Synergetics provides an interdisciplinary approach to principles underlying self-organizing processes by describing how microscopic features yield qualitative changes at the system's dynamics at a macroscopic level. For this sake, the couplings or interactions between different subparts turn out to be essential as they enable macroscopic processes to *enslave* microscopic processes (Haken, 1983). Under specific circumstances the system's qualitative properties are governed by so-called *order parameters* and, using these, the entire system can be described at the macroscopic level. In particular, in the immediate vicinity of the aforementioned phase transitions, the system's

[3] Noether's theorem is a central result in theoretical physics, which shows that a conservation law can be derived from any continuous symmetry. For every continuous symmetry there is a quantity which is conserved by its dynamics and, vice versa, symmetries are broken when this quantity is not conserved (Morrison, 1995).

subcomponents formally partition into at least two distinct groups that differ in their intrinsic rate of change: slowly varying order parameters and quickly relaxing modes. The first ones undergo the macroscopic change and, thus, change their stability, while the latter remain stable and, because they can rapidly adapt to the altered order parameters, become enslaved modes. In most cases the dynamics of the order parameters, the order parameter equation, is low-dimensional compared to the entire high-dimensional system and can be treated mathematically using concepts of nonlinear dynamical systems (Haken, 1983; Haken, 1996). As such, synergetics crucially builds on the formal separation of order parameters versus enslaved modes and the elimination of the latter from the system's dynamics renders the dynamics of large-scale systems like the human brain tractable. Synergetics provides a general framework for describing the formation of higher-level processes from interacting subsystems and can be expediently applied to neuroscience (e.g., Haken, 1996; Tass, 1999; Haken, 2006).

What is thus essential for the formation of a process at the macroscopic level, or *macrostates* (Freeman, 1975), is that the different microscopic processes are coupled: only when the microscopic processes are coupled is it possible for a macroscopic process to emerge. In biology, dynamical systems are always dissipative and, hence, systems settle onto an attractor, i.e. the part of the phase space of the dynamical system where the dissipation cancels out the driving force (Prigogine, 1978; Nicolis and Prigogine, 1981; Pikovsky et al., 2001). The characteristics of the attractor are determined by the differential equations describing the evolution of the system: changing the parameters of a dynamical system will change the shape of the attractor landscape (Abraham and Shaw, 1984). The kind of coupling will thus determine the order parameters and hence the macroscopic behavior of the system, i.e. whether the behavior is determined by a point, periodic, quasi-periodic, or strange attractor. Because a point attractor typically describes a system that is stationary, brain dynamics should be rather captured by periodic, quasi-periodic, or strange attractors that, by definition, display dynamical solutions. The simplest attractor of these is a stable limit cycle and the corresponding steady state behavior is periodic. A limit cycle can be described by a one-dimensional order parameter equation and due to enslavement the whole system shows a coherent synchronized behavior. It is not expected that the entire brain behaves as a global limit cycle, because the representational and computational capacity of such a system is rather limited. Consequently, the global brain dynamics is likely to display (a plenitude of) multistable or even strange attractors (Kruse and Stadler, 1995; Le Van Quyen, 2003). The

question is, however, how to the brain is organized to prevent the spreading of coherent synchronization to the entire brain as any group of neurons is potentially connected to many other groups of neurons (cf. Tononi et al, 1998).

In sum, a focus on processes calls for a physical or complex systems approach in neuroscience. The brain can be described as an open system, i.e. one that exchanges energy and information with is environment and consists of coupled processes. Using the mathematical tools of dynamical systems and synergetics, general properties of such a system can be determined. Specifically, because it is a dissipative system, the volume in state space captured by the behavior of the system will converge onto an attractor (cf. Stam, 2006). The attractor landscape of the system is determined by the parameters of the coupled differential equations and a small change in parameter value may result in large, qualitative changes in the attractor landscape, i.e. a phase transition. Particularly around such phase transitions, the behavior of the system can be described by a low-dimensional order parameter equation as the other modes become enslaved by the order parameters. The order parameters could thus operate as control constraints that limit the trajectory of the system in a regular way without a corresponding freezing out of its configurational degrees of freedom (Pattee, 1973). Hence, the response of microscopic processes to input from other processes, for instance perceptual input, will be changed and the qualitative change at the macroscopic level will therefore result in a change in its information processing capacities (cf. Koukkou and Lehmann, 1983; Lehmann, 1995; Tononi et al., 1998).

1.3 Empirical observations: a focus on synchronization

Synchronized neural processes are not only expected from a theoretical perspective, but have been shown extensively in empirical studies. Indeed, the formation of synchronized neural activation patterns is so widespread that Singer (1993) noted that neurons in cortical networks have a general tendency to engage in synchronous activity in different frequency bands whereby the probability of occurrence of synchronous activity in a particular frequency range depends on the central state of the brain, on the presence of sensory signals, and on the occurrence of motor acts. Hence, neural synchronization may play a functional role in information processing. In general, neural oscillations require the presence of both excitatory and inhibitory interactions between neural processes, either by coupling between excitatory and inhibitory membrane conductances within the same neuron or by network

architectures comprising inhibitory interneurons and feedback connections (e.g., Llinas, 1988; Singer, 1993; Pikovsky et al., 2001). Oscillations are thus a likely consequence of neural interactions and it actually becomes an important issue to understand how cortical networks can be prevented from entering states of global oscillation and, if they do, how these can be terminated (Singer, 1993). An important reason why the brain dynamics will not be found in a state of global oscillation is that neural processes are not uniformly coupled, but show a strong tendency to couple locally. That is, the brain has a structural make-up that favors the coupling between adjacent neurons forming structures that have been termed cell assemblies (Hebb, 1949; Palm, 1981). Indeed, it is this property of the brain that led the structure-oriented neuroscientists to propose that the brain is made up of individual organs. However, this structural property is also a fundamental principle for the process-oriented approach as it facilitates the local coupling or synchronization of neural processes, providing the system with the necessary degrees of freedom and flexibility to perform a large array of information processing functions (cf. Fujii et al., 1996). Because the brain is structurally organized at different levels (neurons, columns, hyper-columns, etc.), neural processes also display such a scaled organization. The different levels of organization have been referred to as the micro-scale, meso-scale, and macro-scale, respectively (Wilson and Cowan, 1972; Freeman, 1975; Nunez, 1995; Haken, 1996; Basar, 1998; Varela et al., 2001). More specifically, the micro-scale refers to the molecular and cellular level, i.e. the coupling of cellular processes resulting in the firing pattern of a neuron. At the next level, that of the meso-scale, the firing patterns of multiple neurons interact mostly locally, e.g., within hyper-columns in visual cortex (Kandel et al., 1991), to form dynamic cell assemblies showing macroscopic activity. Finally, the macro-scale comprises the collective activities of multiple neural assemblies distributed over the whole brain or CNS related to perception, cognition, emotion, motor control, etc. Hence, instead of a global and uniform coupling, neural processes are mostly coupled locally favoring neural synchronization of neuronal assemblies instead of the whole brain activity. Or in terms of synergetics, many local (unstable) order parameters appear capable of enslaving the (stable) remainder of the system. These order parameters may compete, coexist or cooperate resulting in different kinds of macro-scale activity (Haken, 1995).

Although the specific coupling and dynamics will be different at each scale, the dynamics at each scale can be described in a similar way (cf. McKenna et al., 1994). The specific form of the interactions resulting in macroscopic behavior has been studied most extensively at the micro-scale and

is understood in great depth. Numerous studies have been performed to examine how different cellular and molecular processes interact within a cell to predict the specific form of macroscopic behavior. In their pioneering work, Hodgkin and Huxley (1952) succeeded in casting the detailed empirical knowledge of the physiological properties of the giant squid axon into a dynamical systems framework. The Hodgkin-Huxley model is a set of conductance-based coupled differential equations incorporating sodium and potassium ion flows through their respective channels to accurately predict the action potential of a neuron. The seminal studies of Hodgkin and Huxley provided the appropriate conceptual framework for understanding spike propagation in axons and inspired others to extend and revise the original equations to describe the firing pattern of different neurons and for other ion channels (e.g., Llinas, 1988; Meunier and Segev, 2002; Breakspear and Jirsa, 2006; Rabinovich et al., 2006). Hence, there is a general consensus that different cellular processes interact and synchronize to produce macroscopic activity, i.e. spike generation, and that this process, i.e. the micro-scale, can be captured as a dynamical system.

Similarly, firing patterns of different neurons interact and result in meso-scale oscillations that have, for instance, been revealed in the visual system. For the cat's visual cortex, Gray and Singer (1989) showed that adjacent neurons have a strong tendency to synchronize resulting in oscillations of the local field potentials in the 35-50 Hz frequency band. Consequently, the local field potential reflects the synchronous activity of a population of neurons and may serve as a useful signal for analyzing the temporal dynamics of interacting populations of cells. Furthermore, the formation of oscillatory cell assemblies was stimulus specific, i.e. different combinations of neurons synchronize dependent on the orientation and direction of the visual stimulus. Hence, although anatomical connections are evidently a requirement for synchronization, they do not impose a certain synchronization pattern (Gray and Singer, 1989). Because formation of stimulus-specific synchronized cell assemblies has been generally confirmed, it is considered a solution to the binding problem (e.g., Eckhorn et al., 1988; Gray and Singer, 1989; Engel et al., 1992; Singer, 1999, von der Malsburg, 1999, Fries et al., 2001). That is, synchronization might integrate activities of spatially distributed neurons, each of which relates only to partial aspects of a perceived object, into a single percept. The essential advantage of assembly coding is that individual cells can participate at different times in different neural assemblies of synchronized activity and that the significance of individual responses depends entirely on the context set by the other members of the assembly (Singer, 1993).

Irrespective of its functional role, the synchronization of oscillatory activities results in the formation of dynamic cell assemblies (Fujii et al., 1996), which can again be considered a single oscillator (Tass, 1999).

Naturally, the next question that arises is whether the activities of different cell assemblies interact to form synchronized macro-scale activity (cf. Stam, 2006). As was already indicated, it is not expected that a single global oscillator entrains neural activity, but groups of cell assemblies might temporarily engage in synchronized activity. The formation of synchronized macro-scale activity has not received as much empirical support as neural synchronization at the micro- and meso-scale, but has recently attracted increasing attention. Different researchers have reported synchronized activity between distant cortical areas and between cortical and spinal activity. For instance in the visual cortex, neurons do not only synchronize between different columns, but also between neurons of the right and left cerebral cortex (Engel et al., 1991). Similarly, Rodriquez and colleagues (1999) showed that the perception of a face induced long-distance gamma synchronization corresponding to the moment of perception itself, whereas the perception of meaningless shapes did not induce such synchronization. Hence, this work supports the idea that neural synchronization acts as an integrative mechanism that may bring a widely distributed set of neurons together into a coherent ensemble underwriting the performance of a single cognitive act. Whereas neuronal synchronization related to perception generally occurs in the gamma frequency band, movement-related synchronization is particularly found in the beta band. For instance, the encephalographic activity recorded during movement production was found to be synchronized between different cortical areas (Gerloff et al., 1998a; Serrien and Brown, 2004), between cortical and motor unit activity (Conway et al., 1995; Salenius et al., 1997; Gross et al., 2000; Kilner et al., 2000), and between different motor unit pools (Farmer et al., 1993; Kilner et al., 1999). Rhythmic synchronization of neural activity might thus provide a mechanism for integration of the distributed motor activity and have the same functional role for motor control as for perception (Farmer, 1998).

The goal of my thesis is therefore to investigate how different neural assemblies at the meso-scale, i.e. coupled activity of multiple neurons resulting in a single neural oscillator, interact to form macroscopic dynamical processes that constrain human motor performance. More specifically, for effective hierarchical (motor) control to occur, the macroscopic neural process should constrain the individual elements, here end effectors, to force them into a collective behavior that is independent of the details of the dynamical behavior

of its elements (Pattee, 1973). According to Bernstein (1967), motor control can be defined as a problem of mastering the many, often redundant, degrees of freedom involved in any particular movement – of reducing the number of independent variables to be controlled. That is, the human body consists of multiple limbs whose relative positions are controlled by numerous muscles and hence involves numerous degrees of freedom. For effective motor control all these subsystems have to be coordinated, brought into proper relation to each other, such that the human body as a whole interacts with its environment in the intended way. The reduction of degrees of freedom may be accomplished if, following the pioneering work of von Holst (1937/1973), coordinated movement is achieved through coupled oscillators. Using the earlier explained mathematical tools it can be shown that coupled oscillators may behave under certain conditions as a single oscillator, thus reducing the number of independent degrees of freedom. Particularly, rhythmic movements have been modeled successfully in such a manner predicting many behavioral phenomena properly (e.g., Kelso, 1984; Haken et al., 1985; Turvey, 1990; Schmidt et al., 1991; Beek et al., 1995). Because the coupling between behavioral oscillators is considered mainly neural in origin and largely overlaps with the ideas on neural dynamics presented above, these two research fields might be merged. The question, then, can be formulated tentatively as "How does cortical motor activity modulate the coupling between these (spinal) oscillators?", or "How are these (spinal) oscillators entrained by the neural dynamics at the macro-scale?"

1.4 Instrumental applications: a focus on change

To answer such questions, one has to capture these macroscopic patterns and processes and develop strategies for investigating how the macroscopic patterns influence the microscopic processes (cf. Thompson and Varela, 2001). The formation of macroscopic activity can be examined using a broad variety of neuroimaging techniques, but electroencephalography (EEG), magnetoencephalography (MEG) and electromyography (EMG) appear particularly suitable for this purpose. These techniques have a high temporal resolution and measure electromagnetic changes related to the activity of large groups of neurons. They allow for the simultaneous recording of macroscopic neural activity combined with techniques that enable assessment of neural synchronization with high temporal resolution. These techniques therefore provide the opportunity to test whether neural synchronization serves as a

code for neuronal processing, i.e. which causal relation can be established between the occurrence of response synchronization in defined subgroups of neurons and particular functions that need to be assessed at the behavioral level (Singer, 1993).

In the work reported here, I used EMG and MEG to measure changes in synchronization at the meso- and macro-scale. With EMG one measures the action potentials of motoneurons traveling over a group of muscle fibers. The α-motoneuron together with the muscle fibers it innervates is summarized as a motor unit (MU). Such a MU is considered the functional unit of the neuromuscular system (Sherrington, 1925). The group of motor neurons in the spinal cord that innervates a single muscle is referred to as a MU pool and surface EMG measures the activity of the whole MU pool, or an extensive part of it. Because the recruitment of individual MUs is largely organized according to the size principle (Henneman, 1957), different MUs will have different fire frequencies given the same input. Hence, the MU pool does not have an intrinsic tendency to produce synchronized activity, in contrast to cortical neurons.

MEG measures magnetic fields that derive from the flow of ionic currents in the cortical neurons' dendrites (Hämäläinen et al., 1993). The local synchronized behavior of neural assemblies leads to fluctuations in local field potentials that can be measured using EEG and MEG (Lopes da Silva, 1991; Vrba and Robinson, 2001). Put differently, the fact that fluctuations of field potentials can be recorded with macro-electrodes from the scalp indicates that a large number of neurons must be engaged in synchronized rhythmic discharges at the oscillation frequency in question. Otherwise, the weak currents associated with synaptic activity and action potentials of individual neurons would not result in recordable macro-potentials or fields, but would cancel out (Singer, 1993).

Because EMG and MEG measure signals related to large groups of neurons, elaborate data analysis techniques are required to uncover underlying processes. Furthermore, additional factors influence the recorded signal to further complicate the assessment of neural synchronization. The chosen type of data analysis will also influence the kind of neural activity that is extracted from the recorded data. For instance, temporal aspects received comparatively little attention as a dimension for coding when a neuron was thought to be defined entirely by the amplitude of the response and its provenance. This was reflected by the fact that neuronal responses to sensory stimuli or activities occurring in relation to motor acts were commonly averaged over successive trials in order to improve the signal-to-noise ratio. This averaging procedure

destroys any temporal structure in the activation pattern that is not precisely locked to the stimulus or motor response (Tass, 2003). Hence, temporal codes were either ignored or undiscovered with the commonly applied methods of single unit analysis (Singer, 1993). Similarly, event-related averaging of encephalographic data removes those brain responses that are not phase-locked to the event (e.g., Pfurtscheller and Lopes da Silva, 1999).

1.5 Outline of the thesis

In the preceding, I have described the paradigm or research tradition that served as focus for the experimental work that will be presented in the next chapters. To clarify what this implies it is useful to turn to Popper (1972) who, following Selz (see ter Hark, 2003), used the apt term 'searchlight theory' to characterize a theoretically motivated focus for studying part of reality:

> "This is what I have called the 'searchlight theory of science' – the view that science itself throws new light on things; that it not only solves problems, but that, in doing so, it creates many more; and that it not only profits from observations, but leads to new ones. If in this way we look out for new observations with the intention of probing into the truth of our myths, we need not be astonished if we find that myths handled in this rough manner change their character, and that in time they become what one might call more realistic or that they agree better with observable facts." (p. 127-128)

In the following chapters the motor-related brain dynamics are investigated in various experimental designs to gain insight into the functional role of neural synchronization in human motor control. These experiments were meant to explore the macroscopic patterns present during motor control and to relate these to different task parameters. Although the tasks, recording techniques and data analysis methods differed between studies, the rationale behind all studies is consistent. That is, by varying task parameters attempts were made to induce a change in neural synchronization in order to uncover its functional role. If the recorded neural synchronization is an artifact or an epiphenomenon without functional significance for the task at hand, it would not be modulated in a task-dependent manner. Moreover, by changing task parameters the state of the system was changed which might have induced sudden changes in synchronization pointing at reorganization of neural dynamics. The behavior

of the participants was recorded simultaneously with the neural activity to link the induced changes in neural synchronization with specific changes in behavior to identify the functional role of neural synchronization.

To anticipate, in Chapters 2 and 3 neural synchronization between different MU pools was investigated using surface EMG during static isometric force production. During static isometric force production, synchronization between different MU pools was found (e.g., Farmer et al., 1993; Kilner et al., 1999) and we used a similar task to investigate the relation between MU synchronization and common drive by inducing different levels of fatigue. If MU synchronization is caused by a common drive to different muscles, it is expected to increase during fatigue as the drive to muscles is expected to increase with fatigue. In Chapter 2, changes in MU synchronization between different quadriceps muscles were investigated, whereas in Chapter 3, MU synchronization between the bilateral biceps and triceps muscles was compared. In Chapters 4 to 6, neural synchronization during rhythmic movement was examined using MEG and EMG and the effect of behavioral stability on neural synchronization was studied by varying task parameters. In Chapter 4, a synchronization-syncopation paradigm was used that is known to result in differential changes in stability with increasing movement tempo (Kelso, 1984; Kelso et al., 1992; Daffertshofer et al., 2000a). In addition, participants were sleep-deprived to induce further changes in synchronization. In Chapter 5, encephalographic data recorded during paced and unpaced tapping were further analyzed to investigate the changes in amplitude and phase in different frequency bands related to motor performance and auditory perception at different movement tempos. This data analysis method was further exploited in Chapter 6 to investigate how the amplitude and phase dynamics in different frequency bands are affected by motor learning. To this end, participants had to learn a bimanual polyrhythm resulting in a gradual increase in behavioral stability (Summers et al., 1993a; Swinnen et al., 1993; Peper et al., 1995b). Both MEG and EMG were recorded during the learning process to address the changes in neural synchronization that underlie the increased performance. The results of these studies are summarized further in the epilogue to elucidate their relation with the paradigm put forward in this introduction. In particular, the methodical and conceptual implications of these studies are discussed to evaluate and adapt this paradigm in future studies.

2.

Fatigue-related changes in motor-unit synchronization of quadriceps muscles within and across legs

Abstract

In this chapter synchronization between different groups of muscles is investigated. If different muscles cooperate in a task, their MUs are expected to synchronize due to common input. To this end, two experiments were conducted that examined the effects of muscle fatigue on MU synchronization between the quadriceps muscles of both legs. Muscle fatigue was expected to result in an increased common drive to different MUs of synergists within a leg and, hence, to increased MU synchronization. It was further expected that fatigue-related motor overflow might cause MU synchronization of homologous muscles of both legs. MU synchronization, quantified in terms of coherence between surface EMG, was found in two distinct frequency bands (6-11 and 13-18 Hz), more prominently so within a leg than between legs. The inter-limb synchronization in the 6-11 Hz frequency band increased with fatigue and resembled the increased motor overflow during unimanual contractions. As such, the two phenomena may be related in that they both indicate a fatigue-induced increase in bilateral coupling. MU synchronization at 13-18 Hz was clearly different and depended on posture.

Published as: T.W. Boonstra, A. Daffertshofer, J.C. van Ditshuizen, M.R.C. van den Heuvel, C. Hofman, N.W. Willigenburg and P.J. Beek (2007). Fatigue-related changes in motor-unit synchronization of quadriceps muscles within and across legs. *Journal of Electromyography and Kinesiology.* DOI:10.1016/j.jelekin.2007.03.005.

2.1 Introduction

The central nervous system exerts control over voluntary movements via the MUs of pertinent muscles and this control is considered oscillatory in nature (McAuley et al., 1997; Farmer, 1999; Morris et al., 2000; Gross et al., 2002). Apart from the cortical drive to the muscles, MU activity is influenced by several other neural factors at various levels along the neural axis, e.g., extracortical influences, reflex activity and various other sensory influences. Successful motor control can only be achieved by the properly orchestrated interplay of all participating neural subsystems. To gain insight into the corresponding neural interactions, we investigated MU activity using EMG recordings (see Farina et al., 2004, and references therein). The spectral decomposition of EMG has received much attention in studying the underlying physiology. For instance, conventional power spectra are known to be affected by the form of the MU action potential, the firing rate of MUs, and the correlation between firings of different MUs (De Luca and Forrest, 1973; Hagg, 1992).

Physiological changes have been studied extensively in the context of muscular fatigue. It is generally accepted that the mean amplitude of EMG increases with the level of fatigue due to the recruitment of additional MUs to compensate for the fatigue-related reduction in muscle contractility (Lippold et al., 1960; Viitasalo and Komi, 1977). Notice that, more recently, other factors have been found that may influence the EMG amplitude (Dimitrova and Dimitrov, 2003). The increase in EMG amplitude is accompanied by a spectral compression of EMG towards lower frequencies, typically quantified by a drop of the EMG's median frequency (Lippold et al., 1960; Kadefors et al., 1968; Viitasalo and Komi, 1977; Bigland-Ritchie et al., 1981). Several physiological factors have been identified that may contribute to this decrease in median frequency (see Hagg, 1992, for a review). For instance, progressive slowing of the conduction of intracellular action potentials along the muscle fiber may elongate the shape of the action potential and, thus, may cause a spectral shift towards lower frequencies in surface EMG (Mortimer et al., 1970; Lindstrom et al., 1977). The (relative) decrease of median frequency, however, often exceeds the (relative) decrease of conduction velocity, hinting at other factors contributing to the decrease of the median frequency (Bigland-Ritchie et al., 1981; Krogh-Lund and Jorgensen, 1993; Dimitrova and Dimitrov, 2003). For instance, MU synchronization may result in large low-frequency EMG

oscillations and thus to an increase in the relative spectral power in lower frequency bands (Loscher et al., 1996; Kleine et al., 2001).

MU synchronization can be quantified either by means of the cross-correlation of discharge times of individual MUs (Harrison et al., 1991) or by using coherence as frequency domain equivalent of the cross-correlation (Miller and Sigvardt, 1998). The cross-correlation histogram of MUs of the same muscle often contains a narrow central peak, referred to as short-term synchronization, that is caused by common pre-synaptic input from branched axons (Sears and Stagg, 1976; Kirkwood and Sears, 1978). Interestingly, MU synchronization has also been found between MUs of different muscles, be they synergistic arm muscles (De Luca and Erim, 2002), bilateral axial muscles (Carr et al., 1994), or bilateral homologous leg muscles (Gibbs et al., 1995). MU synchronization between distant muscles is more likely to be caused by pre-synaptic synchronization (Kirkwood et al., 1982), which can be understood as a neural strategy to simplify the simultaneous control of multiple muscles (De Luca and Erim, 1994; Gibbs et al., 1995; Mellor and Hodges, 2005). Coherence analysis has been proven to be a very useful method to link the synchronization features of single or multi MU intramuscular needle recordings and corresponding surface recordings (Christakos, 1997; Grosse et al., 2002). For instance, with coherence as frequency-dependent measure, MU synchronization was found in the beta band, i.e. 15-30 Hz, between EMG recordings of different hand muscles using rectified surface EMG (Kilner et al., 1999) and intramuscular needle recordings (Farmer et al., 1993).

To examine whether MU synchronization increases during fatiguing contractions, we simultaneously measured the surface EMGs of quadriceps muscles from both legs. If MU synchronization increases during fatiguing contractions as a result of an increased common drive, then MU synchronization can be expected to increase between MUs receiving common input. Besides MUs belonging to synergist muscles within a limb, we also expected MUs of homologous muscles to increasingly synchronize during fatigue, because an increase of bilateral co-activation had been found during unilateral contractions at high force levels (e.g., Zijdewind and Kernell, 2001; Aranyi and Rosler, 2002). Fatigue was induced in two tasks in which the quadriceps muscles of both legs had to cooperate for proper task performance, i.e. they had to act as a single functional unit (cf. De Luca and Erim, 2002). The design was used to promote synchronization between quadriceps muscles within (intra-limb coherence) and between legs (inter-limb coherence).

In a first experiment, different levels of fatigue were induced by means of changes in posture (knee angle). We expected a fatigue-related increase of synchronization at a specific frequency, reflecting the frequency of the increase in common input to both muscles. To investigate the relation between MU synchronization and tremor activity, we conducted a second experiment in which participants performed isometric knee extensions against force sensors at different force levels. Both tasks allowed for investigating fatigue-related changes in MU synchronization within and across legs and we expected intra-limb synchronization to be stronger than inter-limb synchronization.

2.2 Methods and Materials

Experiment 1

PARTICIPANTS Twelve healthy male students from VU University Amsterdam participated in the experiment (mean age: 22 years; range: 20-25 years). All participants signed an informed consent after the experimental procedures and the accompanying instructions had been explained to them. The Ethical Committee of the Faculty of Human Movement Sciences, VU University Amsterdam, had approved the experimental protocol before the experiment was conducted.

PROCEDURE Participants were invited to stand with their back leaning against a vertical wall with a smooth surface to minimize friction. To induce distinct levels of fatigue, participants were positioned with knees flexed at 90°, 120°, and 150°. Participants stood barefooted with their feet placed 20 cm apart and their lower legs in a vertical position. They were instructed to remain in contact with the supporting wall with both back and head while looking straight ahead (Fig. 2.1A).

At the beginning of the experiment, participants were asked to stand with a knee angle of 90° for 10 s in order to define a scale factor gauging the EMG (similar to a maximal voluntary contraction, see also Experiment 2). Subsequently, participants conducted three trials for each knee angle. Trials lasted 90 s and the order of trials was counterbalanced across participants. All participants maintained the required position for the duration of the trial. Between trials, participants rested for three minutes. Knee angles were determined with a goniometer.

DATA ACQUISITION Surface EMG was recorded from the rectus femoris (RF), vastus medialis (VM), tibialis anterior (TA), biceps femoris (BF), and gastrocnemius caput mediale (GM) of both legs. For the purpose of the present study, only data from VM and RF muscles were analyzed. The electrodes (Ambu® Blue Sensor N) were placed in a bipolar montage with an inter-electrode distance of about 2 cm with locations following SENIAM guidelines (Hermens et al., 2000). Data were amplified, band-pass filtered, and stored on disk (3-1000 Hz band-pass, 22-bit sampling depth, 2 kHz sampling rate, Porti 5-16/ASD, TMS International, Enschede, The Netherlands).

DATA ANALYSIS EMG data were filtered off-line (2^{nd} order bidirectional Butterworth band-pass filter: 5-300 Hz[4]), full-wave rectified using the Hilbert transform (cf. Myers et al., 2003), and normalized using the calibration at the beginning of the experiment, i.e. divided by the averaged rectified value of the initial 10 s recording at 90° knee angle. Every 90 s trial was split into 9 consecutive intervals lasting 10 s each. Per interval, mean power and median frequency were computed. The median frequency was calculated using the power spectral densities of the non-rectified EMG (Welch's periodogram method, Hamming windows: 1024 samples; overlap: 768 samples).

Power and coherence estimates for muscles belonging to the quadriceps group of both legs (VM_{left}, RF_{left}, VM_{right}, RF_{right}) were based on power spectral densities of the rectified EMG (again using Welch's periodogram method with the window setting given above; note that the dc-value was removed for each window before computing the Fourier transform). The power spectra were log-transformed and Fisher's transform was applied to the coherence spectra before conducting subsequent statistical tests (Halliday et al., 1995, Amjad et al., 1997). Both procedures 'stabilize' the variances of the underlying distributions and should be used before testing spectral estimates for statistical differences (Rosenberg et al., 1989; Farmer et al., 1993; Gerloff et al., 1998a).

STATISTICAL ANALYSIS Power and coherence spectra were compared using principal component analysis (PCA) to determine spectral components that were common across participants, conditions, and muscles. As mentioned above, we computed power and coherence spectra for different conditions, at

[4] We also tested larger high-pass cut-off frequencies to omit possible tremor-related movement artifacts potentially affecting subsequent coherence estimates. However, more rigorous high-pass filtering did not change the quality of coherence so that we decided to use this broad-band filter.

different time intervals, and for different muscles, which yielded many to-be-compared spectra (see below). Thus, PCA appeared an excellent approach having the capacity for dimensionality reduction in huge multivariate data sets by extracting major components; principal components are ranked according to the explained variance of the original data (see Daffertshofer et al., 2004, and references therein).

Applying PCA to sets of power and coherence spectra enabled us to quantify the strength of distinct frequency components in different conditions and muscles by comparing the corresponding coefficients of the major modes' eigenvectors (cf. Boonstra et al., 2005b, and Appendix A for more detail)[5]. This specific application of PCA allowed for comparing spectra of all different conditions without an a priori selection of relevant frequencies and corresponding scalar power values needed when applying more conventional statistical analyses. The general advantage of such a combined PCA is that effects of experimental conditions can be evaluated in a concise and readily interpretable manner, even when effects are small. Hence, frequency spectra of all participants and conditions were combined into a single signal vector. This combination resulted in three different high-dimensional signal vectors: a vector for power spectra with 12 (participants) × 3 (conditions) × 9 (intervals) × 4 (muscles) = 1296 signals, a vector for intra-limb coherence with 12 × 3 × 9 × 2 (VM_{left}-RF_{left}, VM_{right}-RF_{right}) = 648 signals, and a vector for the inter-limb coherence with 12 × 3 × 9 × 2 (VM_{left}-VM_{right}, RF_{left}-RF_{right}) = 648 signals.

For comparison with more conventional statistical approaches, we also analyzed effects of fatigue on amplitude, median frequency, and coherence by performing a two-way ANOVA (3 × 2; knee angle × interval) with repeated measures on the first and last intervals per trial. The design was completely balanced with equal record lengths across conditions. Coherence was evaluated in two frequency bands. The choice of spectral components was based on the PCA results, which revealed the presence of a lower (6-11 Hz) and a higher (13-18 Hz) frequency band (see Results). To facilitate the interpretation of significant results obtained with the ANOVAs, effect sizes (f) were calculated in terms of partial η^2 (Cohen, 1988). Whenever Mauchly's test of sphericity

[5] In general, the original spectra can be reconstructed as sum of modes, i.e. the summation of the products of eigenvectors with their corresponding projections – cf. Appendix A, equation (1). Restricting this sum to a small number of modes yields (at least) approximations whose qualities can be judged via the (sum of) corresponding eigenvalues that represent the modes' contributions to the total variance.

failed to indicate homogeneity of variance across conditions, the Huynh-Feldt's test was used.

Experiment 2

PARTICIPANTS Ten healthy male students from VU University Amsterdam participated in the experiment (mean age, 24 years; range, 21-27 years). Two participants also participated in the first experiment. All participants signed an informed consent after receiving instructions. The Ethical Committee of the Faculty of Human Movement Sciences, VU University Amsterdam, had approved the protocol of the experiment before it was conducted.

PROCEDURE Participants were seated in an adjustable chair in upright position and securely strapped by two belts to minimize the number of participating mechanical degrees of freedom. For each participant the chair was adjusted such that both hip and knee joints were flexed at approximately 90°. The exerted forces of knee extension of both legs were recorded with two force transducers (type KAP-E, Bienfait, Haarlem, The Netherlands) placed at the shin (Fig. 2.1B).

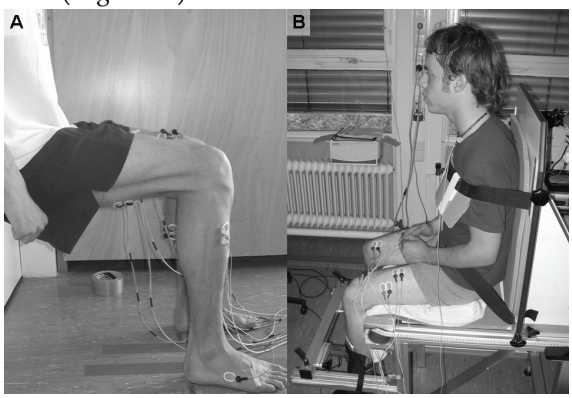

Figure 2.1 ***A****) Set-up of Experiment 1: Participant is leaning against the wall in the 90° condition.* ***B****) Set-up of Experiment 2. Participant is sitting in an adjustable chair with force sensors at shin level.*

First, the maximum voluntary contraction (MVC) was determined based on two consecutive 10 s recordings during which participants were instructed to gradually build up force and were verbally reinforced to exert maximal force. The maximum force of both recordings was used as MVC reference. Subsequently, participants were asked to produce forces at 10%, 35%, and 60% MVC to induce different levels of fatigue. Both the required and produced forces were displayed as horizontal lines on a screen located in front of the participants and they were instructed to tune their force output to the desired force level. To implicitly prompt participants to perform knee

extensions of both legs as a functional unit, the exerted force of both legs were summed and displayed as a single line.

Each participant conducted 12 trials of 60 s each. Trials consisted of two 30 s force plateaus with a different force level (10%, 35%, and 60% MVC). Participants were instructed to rapidly switch to the following force level and to stabilize there as fast as possible. Between trials participants were allowed to rest for two minutes. The order of force levels and trials was randomized over participants. The design allowed for analyzing effects of progressing fatigue on MU synchronization as function of force level and as function of preceding force level. For the latter we compared the effect of different force levels during the first plateau on the performance during the second plateau while keeping all other factors equal (cf. Statistical analysis).

DATA ACQUISITION Surface EMG was recorded from the rectus femoris (RF), vastus medialis (VM), and vastus lateralis (VL) of both legs. All technical settings were the same as in Experiment 1 except that the force signals were sampled at a rate of 1 kHz. Force and EMG data were synchronized using an additional trigger signal.

DATA ANALYSIS The two force plateaus of every trial were divided into 5 intervals of 5 s each (the first three and last two seconds of each plateau were discarded to omit transients). All subsequent analyses were identical to Experiment 1 expect now also force data were investigated in terms of their spectral power.

STATISTICAL ANALYSIS The power and coherence spectra of different force levels were compared using PCA as explained in Experiment 1 (for the force signals we only analyzed the corresponding power spectra). The vector of power spectra contained 10 (participants) × 3 (conditions) × 5 (intervals) × 6 (muscles) = 900 signals, while the vector of intra- and inter-limb coherence contained 10 × 3 × 5 × 6 (VL_{left}-VM_{left}, VL_{left}-RF_{left}, VM_{left}-RF_{left}, VL_{right}-VM_{right}, VL_{right}-RF_{right}, VM_{right}-RF_{right}) = 900 and 10 × 3 × 5 × 3 (VL_{left}-VL_{right}, VM_{left}-VM_{right}, RF_{left}-RF_{right}) = 450 signals, respectively.

Two statistical tests were applied to evaluate effects of fatigue on amplitude, median frequency, and coherence. First, we addressed the progression of fatigue during a trial with a two-way ANOVA (3 × 2; force level × interval) over the first and last interval of each plateau (cf. Experiment 1). Second, we eliminated temporal effects by comparing only the first interval of the second plateau after different force levels in the first plateau allowing for

a comparison between different levels of fatigue dependent on the force level history, while keeping all other factors constant. We used a two-way ANOVA (3 × 2; force level × history [low/high]) with repeated measures. The frequency bands, in which coherence was compared, matched those in Experiment 1 (i.e. 6-11 Hz and 13-18 Hz).

2.3 Results

Experiment 1

Amplitude and median frequency both showed marked effects of muscle fatigue. The EMG amplitude of the quadriceps muscles (RF and VM) increased significantly in time (Fig. 2.2, $p < 0.01$). This amplitude increase depended on condition, i.e. there was a significantly larger increase in the more difficult compared to the easier conditions as revealed by a significant angle by interval interaction for three out of four muscles ($p < 0.05$). As could be expected, EMG amplitudes were larger at lower knee angles, i.e. in more difficult conditions. Median frequencies of all muscles decreased significantly in time ($p < 0.01$). For the median frequency, the angle by interval interaction was not significant suggesting that the decrease was similar for different knee angles.

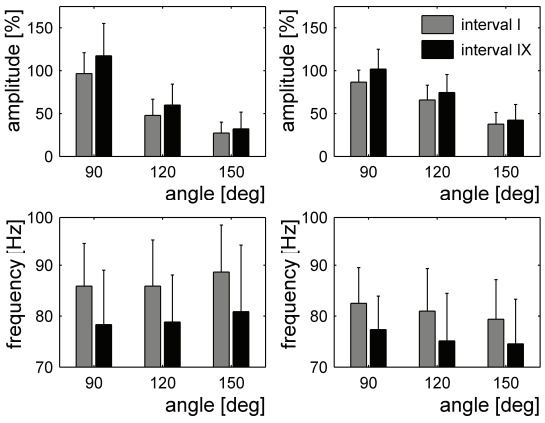

Figure 2.2 *Top panels: amplitude as percentage of reference measurement in the first and last 10 s interval for three conditions (left: RF_{left}; right: VM_{left}) of Experiment 1; lower panels: median frequency of the unrectified EMG in the first and last interval (left: RF_{left}; right: VM_{left}).*

The EMGs' power and coherence spectra revealed pronounced peaks around 10 and 14 Hz. The normalized power in the 6-11 Hz frequency band averaged over participants was 6.50 ± 0.72%, 6.06 ± 0.77%, and 5.91 ± 0.98%, for the 90°, 120°, and 150° conditions, respectively, compared to 6.40 ± 1.18%, 8.10 ± 3.16%, and 8.91 ± 4.09% in the 13-18 Hz frequency band ('±' refers to between-subject standard deviation; here, the normalized power denotes the

power in the 6-11 Hz as fraction of the total power). That is, the relative power in the 6-11 Hz frequency band was stronger in the 90° condition, whereas the relative power in the 13-18 Hz frequency bands was stronger at larger knee angles. The inter-subject variability was particularly high for the power in the 13-18 Hz frequency band. Figure 2.3 shows the power and coherence spectra for two participants with strong power and intra-limb coherence in the 13-18 Hz frequency band in the 150° condition (upper graph of each panel).

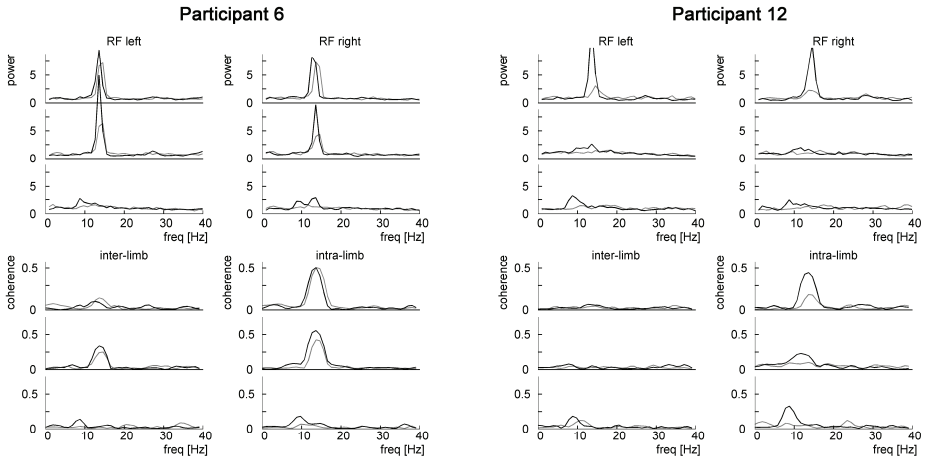

Figure 2.3 *Power and coherence spectra for two participants in Experiment 1. Top panels: the normalized power spectra of the rectified EMG for two muscles (bilateral RF) in three different conditions (from top to bottom: 150°, 120° and 90° knee angle) for the first (gray line) and last interval (black line). The graphs show the power at particular frequency as percentage of the total power. Lower panels: idem, but now for the coherence spectra.*

The PCA of the power spectra extracted the two frequency bands, i.e. 6-11 and 13-18 Hz, in different modes. Recall that PCA modes yield eigenvector coefficients that signify the strength of these frequency components in the individual spectra and hence allow for a comparison between conditions. As such, the first mode represented a spectral distribution common for all four quadriceps muscles with a pronounced peak around 14 Hz (first mode contained 64% of the total variance). The strength of this component, as revealed by the corresponding eigenvector's coefficients, increased with knee angle, i.e. it was strongest in the 150° condition. The second mode (which covered about 10% of the total variance) had spectral components located predominantly around 10, 20, and 40 Hz. In contrast to the first mode, these components clearly decreased with knee angle, that is, they were strongest in

the 90° condition. The first two modes hardly changed in time except in the 90° condition.

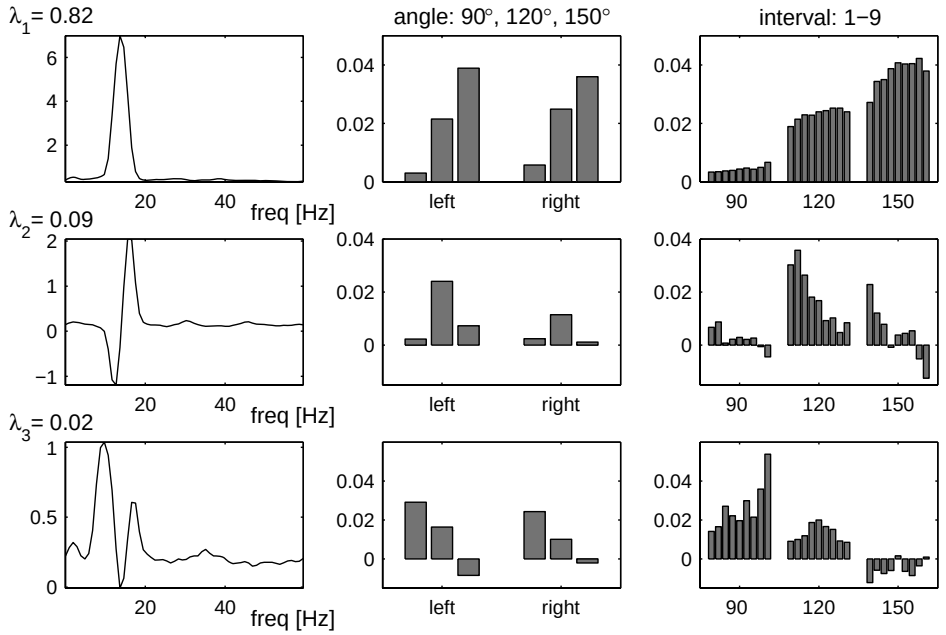

Figure 2.4.1 *PCA of intra-limb coherence in Experiment 1: left column: first three principal coherence spectra (eigenvalues 82%, 9%, and 2%); central column: coefficients of corresponding eigenvectors for coherences RF_{left}-VM_{left} and RF_{right}-VM_{right} at different knee angles; right column: mean coefficients for corresponding eigenvectors for knee angles 90°, 120°, and 150° at the nine time intervals*

Coherence was found between EMGs of a single leg as well as across legs in frequency regions that also displayed pronounced spectral power. Intra-limb coherence was generally stronger than inter-limb coherence, which prompted us to analyze them separately (cf. Fig. 2.3). PCA of all intra-limb coherence spectra yielded a first mode that covered more than 80% of the total variance (Fig. 2.4.1; first row). It displayed a peak around 14 Hz that was strongest in the supposedly easiest condition (150° condition; Fig. 2.4.1; second column) and seemed to increase in time (third column). The second mode (Fig. 2.4.1; second row) represented a modulation of the frequency of the peak of the first mode: the strength of this mode decreased with time corresponding to a shift of the 14 Hz peak towards lower frequencies. That shift was strongest for the 120° and 150° conditions (Fig. 2.4.1; third column). The third mode (Fig. 2.4.1; third row) exhibited a coherence peak around 10 Hz and a second

smaller peak around 20 Hz. This mode was strongest in the 90° condition and only in this condition the mode's strength increased in time (Fig. 2.4.1; third column).

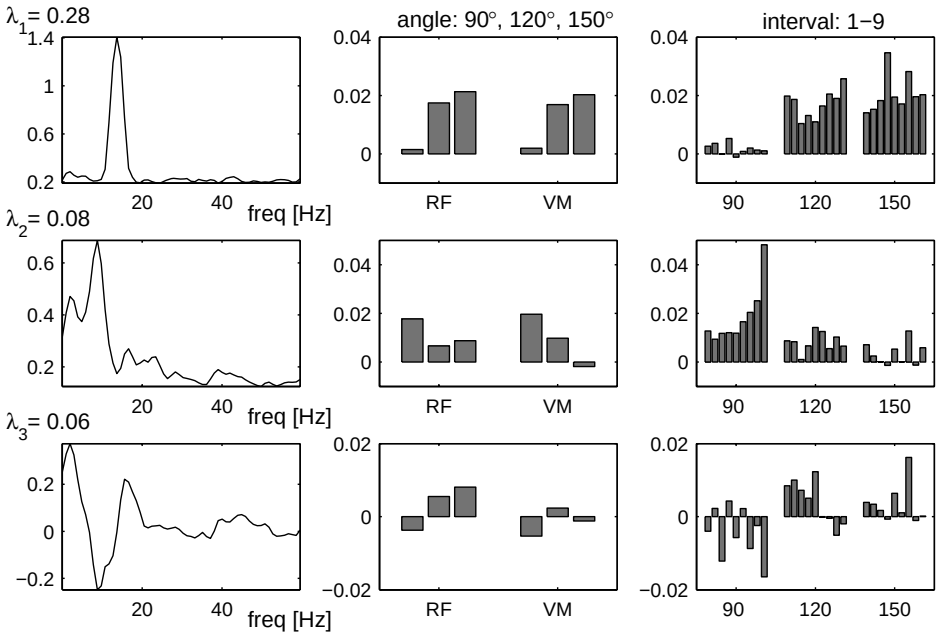

Figure 2.4.2 *PCA of inter-limb coherence in Experiment 1: left column: first three principal coherence spectra with eigenvalues 28%, 8%, and 6%; central column: mean coefficients of corresponding eigenvectors for coherences RF_{left}-RF_{right} and VM_{left}-VM_{right} at different knee angles; right column: mean coefficients for corresponding eigenvectors for knee angles 90°, 120°, and 150° at the nine time intervals.*

The decomposition of inter-limb coherence into different principal components revealed that the first, second, and third mode explained 28%, 8%, and 6% of the total variance, respectively. Complementary to the intra-limb case, the first mode showed a peak around 14 Hz that was strongest at 150° knee angle (Fig. 2.4.2; first row, second column). The second mode had a peak around 10 Hz and was strongest in the 90° condition. In this condition, the strength of the 10 Hz peak increased in time (Fig. 2.4.2; second row, third column). As the eigenvectors of the third mode did not display a comparably clear-cut structure, we abstained from further interpretation.

ANOVA of the coherence spectra agreed with the PCA results. The 6-11 Hz intra-limb coherence between RF_{right}-VM_{right} increased significantly in time

($F(1,11) = 5.98$; $p = 0.034$; $f = 0.73$; mean coherence: interval I, 0.031 ± 0.014; interval V, 0.048 ± 0.038) and this increase was strongest in the 90° condition ($F(2,22) = 4.85$; $p = 0.018$; $f = 0.66$; mean coherence 90°: interval I, 0.031 ± 0.009; interval V, 0.069 ± 0.049). In contrast, the 13-18 Hz intra-limb coherence was strongest in the 150° and weakest in the 90° condition in both legs ($p < 0.010$; mean coherence: 90°, 0.050 ± 0.039; 120°, 0.128 ± 0.122; 150°, 0.153 ± 0.145). No significant changes in time were found, probably due to the high inter-subject variability of the frequency component in question. Coherence spectra of the single participants revealed that, although most participants showed coherence in the 13-18 Hz frequency band, its values varied between 0.02 and 0.6. For the inter-limb coherence in the 6-11 Hz frequency band, the effects were similar to those observed for the intra-limb coherence. Coherence of the RF increased significantly in the 90° condition as revealed by the corresponding interaction ($F(2,22) = 3.47$; $p = 0.049$; $f = 0.16$; mean coherence 90°: interval I, 0.035 ± 0.017; interval V, 0.049 ± 0.030). There was also an almost significant effect of angle demonstrating largest coherence in the 90° condition ($F(1.3,14) = 4.31$; $p = 0.050$; $f = 0.63$; mean coherence: 90°, 0.042 ± 0.025; 120°, 0.029 ± 0.011; 150°, 0.030 ± 0.011). No significant effects in the 6-11 Hz frequency band were found for VM, although trends were similar to those for RF. The 13-18 Hz frequency band yielded no significant effects for inter-limb coherence.

Experiment 2

The EMG amplitude of the quadriceps muscles of interest showed similar effects of fatigue as in Experiment 1: amplitude increased in time and this increase was larger at higher force levels (Fig. 2.5A). Both effects were significant for all six quadriceps muscles (interval effect: $p < 0.001$, interaction effect: $p < 0.001$). However, effects of fatigue on median frequency were less obvious. Although the median frequency decreased over time in most conditions for most muscles, this effect was only significant for VL_{left} and RF_{left} ($p < 0.05$). The interaction between force level and interval was significant for VM_{left}: median frequency decreased at the 60% force level and increased at the 10% force level ($p = 0.001$). Median frequency was significantly higher at higher force levels for all muscles ($p < 0.01$). As already stated, we also studied effects of fatigue at the same force level and interval by comparing different force level histories. As expected, amplitudes were higher after a higher force level during the first force plateau (Fig. 2.5B) and significant for 5 of the 6 muscles ($p < 0.02$). The history effect was stronger for the 60% force level

during the second plateau ($p < 0.05$; same five muscles), i.e. the increase in amplitude after a higher force level of the first plateau was particularly strong in the 60% force condition of the second plateau. Again, effects for the median frequency were less clear-cut. For both VMs and VL_{left} , the median frequency was generally lower after a higher force level ($p < 0.02$; VMs and VL_{left}), whereas both RFs showed no history effect.

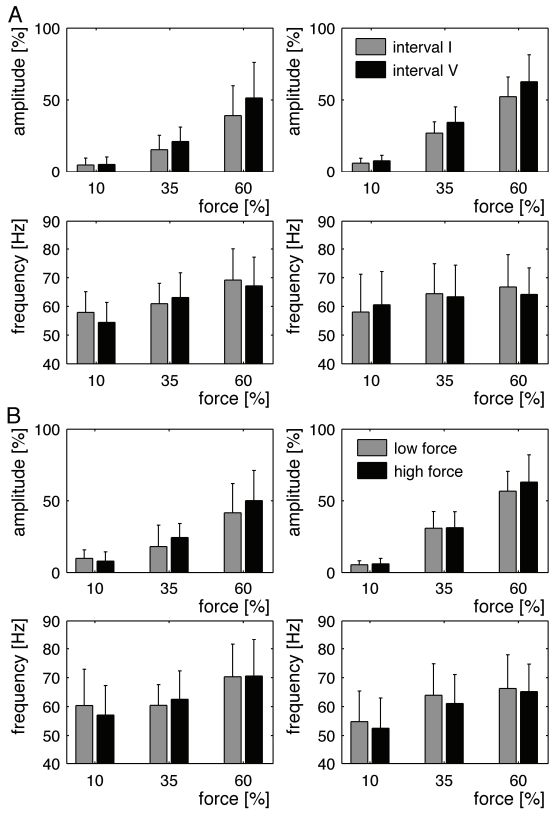

Figure 2.5 *A) Changes in mean amplitude (top panels) and median frequency of the unrectified EMG (lower panels) between interval I (gray) and V (black) of Experiment 2; the left column displays RF_{left} and right column VM_{left}; **B)** Mean amplitude and median frequency of interval I of plateau 2 after different force levels of plateau I (gray: low force, black: high force); similar to A the left column displays RF_{left} and right column VM_{left}.*

The power spectra of both the EMGs and force signals displayed peaks around 10 and 16 Hz. The mean normalized EMG power in the 6-11 Hz frequency band was 6.49 ± 0.59%, 6.12 ± 0.97%, and 6.27 ± 2.00%, for the 10%, 35%, and 60% condition, respectively, compared to 5.25 ± 0.55%, 8.98 ± 6.60%, and 10.69 ± 9.24% in the 13-18 Hz frequency band. The relative power in the 6-11 Hz frequency band remained steady across conditions, while the power in the 13-18 Hz frequency bands clearly increased at higher force levels. Again, the inter-subject variability was fairly high for the power in the 13-18 Hz frequency band, particularly at higher force levels. Figure 2.6 shows the power and coherence spectra for two participants, one of them showing strong

intra-limb coherence in the 6-11 Hz and the other in the 13-18 Hz frequency band in the 60% force condition (lower graphs of each panel).

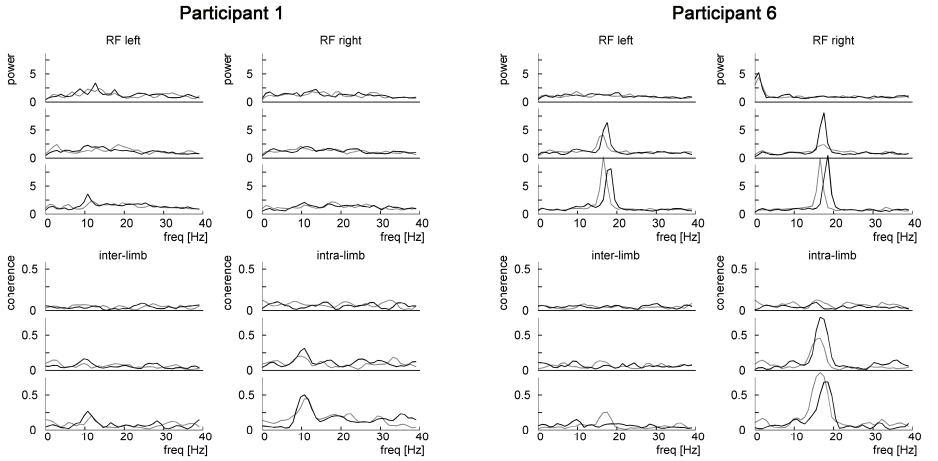

Figure 2.6 *Power and coherence spectra for two participants in Experiment 2. Top panels: the normalized power spectra of the rectified EMG for two muscles (bilateral RF) in three different conditions (from top to bottom: 10%, 35% and 60% force level) for the first (gray line) and last interval (black line). The graphs show the power at particular frequencies as a percentage of the total power. Lower panels: idem, but now for the coherence spectra.*

For the spectral power of the EMG, the first PCA mode, accounting for 51% of the total variance, displayed peaks at 10 and 16 Hz and was constant over conditions. The second mode (12% of the total variance) displayed a pronounced peak around 16 Hz and was stronger at higher force levels. The power spectra of the force signals were maximal around 2 Hz, but two peaks were clearly present around 10 and 16 Hz, particularly in the 60% condition. The mean normalized power in the 6-11 Hz frequency band was 5.40 ± 1.80%, 6.93 ± 3.48%, and 10.63 ± 4.37%, for the 10%, 35%, and 60% condition, respectively, compared to 2.00 ± 0.62%, 3.48 ± 5.86%, and 4.20 ± 6.91% in the 13-18 Hz frequency band, again showing high inter-subject variability in the 13-18 Hz frequency band.

Similar to Experiment 1, PCA of the coherence spectra revealed two distinct frequency bands in different modes: 6-11 and 13-18 Hz (Figs. 2.7). For intra-limb coherence, the first three PCA modes explained 60%, 15%, and 7% of the total variance (Fig. 2.7.1). The first mode exhibited coherence in the 13-18 Hz frequency band and was stronger at higher force levels. The second mode was a modulation of the first mode, whose strength increased in time,

pointing at a shift of the first mode's peak frequency towards higher frequencies in the course of a trial. The third mode covered the 6-11 Hz frequency band and was stronger at higher force levels. The ANOVA results were similar to those of PCA, revealing a significant increase of 6-11 Hz coherence at higher force levels in 5 out of 6 combinations ($p < 0.05$; mean coherence: 10%, 0.070 ± 0.026; 35%, 0.093 ± 0.064; 60%, 0.131 ± 0.093). The 13-18 Hz intra-limb coherence did not show a main effect of force level, although coherence levels were high and differed considerably between force levels (mean coherence: 10%, 0.069 ± 0.027; 35%, 0.137 ± 0.155; 60%, 0.185 ± 0.224).

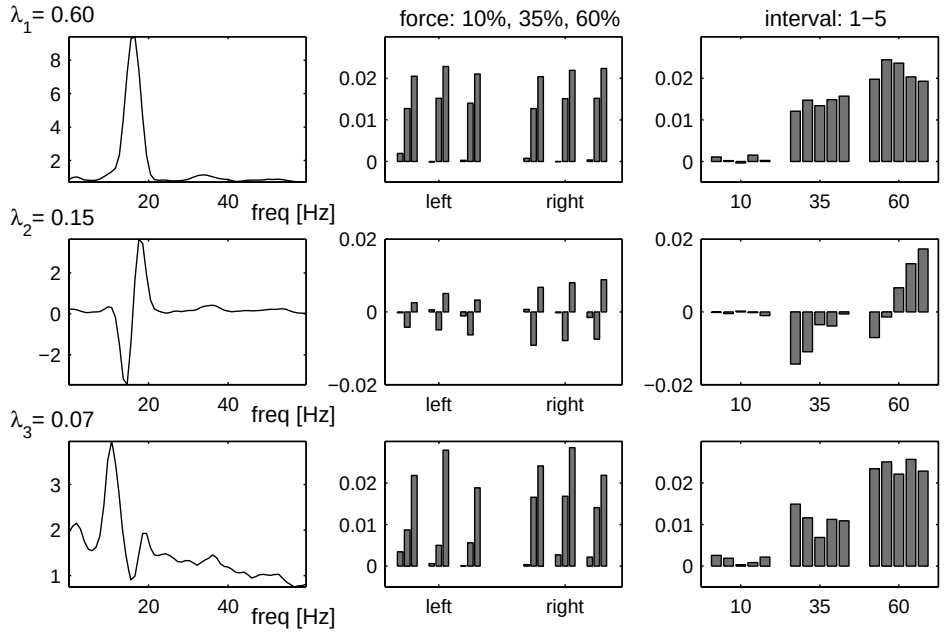

Figure 2.7.1 *PCA of intra-limb coherence in Experiment 2: left column: first three principal coherence spectra; central column: mean coefficients of corresponding eigenvectors for three coherences (left and right leg); right column: mean coefficients for corresponding eigenvectors for force levels 10%, 35%, and 60% at the five intervals.*

PCA of inter-limb coherence showed that the first, second, and third mode explained 19%, 8%, and 6% of the total variance, respectively (Fig. 2.7.2). The first mode had a peak around 16 Hz that was strongest at higher force levels. The second mode displayed a peak around 10 Hz that was strongest in the 60% condition, during which its strength increased with time. The third mode represented a modulation of the peak frequency of the first

mode (the eigenvector's coefficients were not clearly structured rendering their interpretation difficult). ANOVA confirmed the effects for the 6-11 Hz inter-limb coherence: VM_{left}-VM_{right} coherence was significantly higher at higher force levels ($F(2,18) = 4.40$; $p = 0.028$; $f = 0.70$; mean coherence: 10%, 0.063 ± 0.017; 35%, 0.062 ± 0.017; 60%, 0.082 ± 0.031) and increased in time in the 60% condition ($F(2,18) = 10.45$; $p = 0.001$; $f = 0.54$; mean coherence 60%: interval I, 0.066 ± 0.028; interval V, 0.097 ± 0.027). For RF_{left}-RF_{right} coherence only a significant interaction was found, showing an increase in time for the 60% condition ($F(2,18) = 5.91$; $p = 0.011$; $f = 0.40$; mean coherence 60%: interval I, 0.074 ± 0.024; interval V, 0.091 ± 0.036). Similar to the intra-limb coherence, the higher inter-limb coherence in the 13-18 Hz band at higher force levels was not significant.

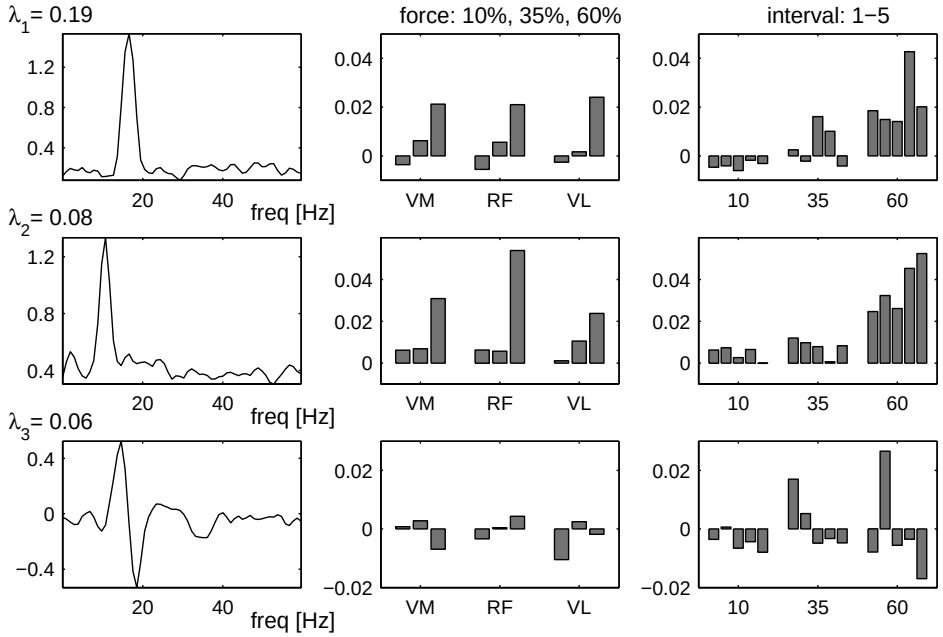

Figure 2.7.2 *PCA of inter-limb coherence in Experiment 2: left column: first three principal coherence spectra; central column: mean coefficients of corresponding eigenvectors for coherences VM_{left}-VM_{right}, RF_{left}-RF_{right}, and VL_{left}-VL_{right} at different force levels; right column: mean coefficients for corresponding eigenvectors for force flevels 10%, 35%, and 60% at the five intervals.*

The coherence spectra of the second force plateau were analyzed further in view of the different preceding force levels, i.e. the higher the force in plateau 1, the larger the resulting level of fatigue in plateau 2. A 3 × 2 ANOVA

(force level × history) revealed that 6-11 Hz inter-limb coherence was significantly higher after a higher force level during the first plateau for the VMs and the RFs ($p < 0.02$). For the VLs there was an equivalent trend that, however, failed to reach significance ($p = 0.08$). No significant main effect of force level or interaction was found for the 6-11 Hz inter-limb coherence. Statistical analysis of the 13-18 Hz frequency band and intra-limb coherence did not yield any significant effects, confirming that 13-18 Hz was not affected by muscle fatigue.

2.4 Discussion

Intra- and inter-limb coherence was found in two distinct frequency bands: 6-11 and 13-18 Hz. As expected, intra-limb coherence was stronger than inter-limb coherence, in accordance with the idea of a functional organization of muscle activation. Since high-pass filtering and inter-limb synchronization (i.e. between the legs) excluded the possibility of movement artifacts and simple volume conduction, respectively, the coherences found in the two frequency bands were, in all likelihood, caused by MU synchronization[6]. Note that a recent simulation study indicated that other factors, such as excitation level, muscle size and mean motor unit conduction velocity, can affect the cross-correlation between surface EMGs (Keenan et al., 2006). Thus, one may argue that the increase in 6-11 Hz synchronization could have been caused by a fatigue-related change in these factors. However, the increase in 6-11 Hz synchronization with fatigue augments results by Christou and colleagues (2006), who showed that a higher MU discharge rate, putatively caused by a

[6] In general, the here applied coherence analysis between surface EMGs differs from cross-correlation between individual MUs as measured with needle electrodes. Because surface EMG is a coarse-grained measure of MU activity, coherence between surface EMG provides only an indirect measure of synchronization of individual MUs. However, as was already indicated in the introduction, the estimation of MU synchronization by means of both methods are to a large degree compatible (cf. Grosse et al., 2002). That is, the amplitude of the surface EMG is related to the net MU activity and can thus be used as an index input level to the MU pool (e.g., Farina et al., 2004). The amplitude modulation of surface EMG is caused by rhythmically grouped discharges of individual MU spike trains (Elble and Randall, 1976) and coherence between surface EMGs can thus be seen as measure of the synchronization of the net activity of different MU pools pointing at common rhythmic input to both MU pools (cf. McAuley et al., 1997, Grosse et al., 2002, Boonstra et al., 2007a).

larger descending drive onto the motor neuron pool, was accompanied by an increase in 8-13 Hz synchronization of different MUs as measured with needle electrodes. Indeed, these results confirm ours even though Christou and colleagues used needle electrodes and thus underscore the correspondence between both techniques. Hence, we submit that the here-reported increase in 6-11 Hz coherence between surface EMGs was most likely caused by increased MU synchronization.

Both experimental protocols appeared rather effective in inducing differential levels of fatigue as demonstrated by changes in EMG amplitude and median frequency. We did not measure the decrease in force generating capacity of the muscles, but the effect on EMG activity closely corresponded to those of other studies on muscle fatigue (cf. Introduction). That is, EMG amplitude increased during each trial and increased stronger at higher force levels and the median frequency of the EMGs tended to decrease in both experiments. The increase in muscle fatigue was associated with an increase of the 6-11 Hz inter-limb coherence, i.e. 6-11 Hz inter-limb coherence increased over time and more strongly so at higher force levels. In contrast, an ambiguous pattern in the 13-18 Hz band was found: while in the first experiment 13-18 Hz coherence was stronger at large knee angles (low force levels), it was stronger at higher force levels but remained unaffected by fatigue in the second experiment. Evidently, this discrepancy excluded a direct relation between force level or muscle fatigue with coherence around 13-18 Hz.

MU synchronization and tremor activity

Coherence in both frequency bands was accompanied by pronounced peaks in the EMGs' power spectra as well as in the power spectra of the force sensors in Experiment 2. In all likelihood, these peaks in the spectra reflected tremor activity, which has been studied extensively, especially in the 6-11 Hz frequency band (e.g., McAuley and Marsden, 2000). Tremor around 10 Hz is well-documented and typically referred to as physiological or central tremor, be it when limbs are outstretched yielding postural tremor (Halliday and Redfearn, 1956; Elble and Randall, 1976; Hagbarth and Young, 1979) or during isometric contractions (Allum et al., 1978; McAuley et al., 1997). In view of the diversity of tremor manifestations, it is not surprising that various mechanisms have been proposed to account for 10 Hz oscillations. As it stands, physiological tremor appears multifactorial in origin (McAuley and Marsden, 2000). To isolate some of the possible sources it is particularly interesting that physiological tremor is affected by muscle fatigue in that the tremor strength increases during isometric contractions at high force levels (Loscher et al.,

1996; Cresswell and Loscher, 2000; Ebenbichler et al., 2000). Importantly, the presently observed changes in the 6-11 Hz frequency band are entirely consistent with these findings as the strength of the oscillations increased with increasing muscle fatigue and are likely related to physiological tremor.

Compared to the 10 Hz region, oscillatory activity in the 13-18 Hz frequency band seems far less common. However, various studies have reported EMG-EMG coherence in the beta band (15-30 Hz), either between different hand muscles using needle electrodes (Farmer et al., 1993) or between rectified surface EMGs (Kilner et al., 1999). The motor cortex is most likely involved in the generation of this synchronized beta activity as EMG activity is also coherent with local field potentials in monkeys (Baker et al., 1997) and with MEG activity in humans (Conway et al., 1995; Salenius et al., 1997; Kilner et al., 2000; Mima et al., 2000). Although the 13-18 Hz interval is part of the lower beta band, the observed synchrony appears quite different from beta band coherence. First, beta band coherence is typically most pronounced around 20-25 Hz, instead of 13-18 Hz. Second, beta band coherence is usually broadband, i.e. it is not as sharp-peaked as the coherence spectra found in the present experiments. Third, 13-18 Hz coherence in a few participants reached values up to 0.8, which is much larger than typically reported for the beta band. Hence, it seems that the 13-18 Hz found in both experiments differs for the typically reported coherence in the beta band.

In a similar experiment on bilateral MU synchronization between muscles of the upper arm, we found a fatigue-related synchronization increase in the 8-12 Hz frequency similar to the present findings (Boonstra et al., 2007a). In contrast, however, synchronization between 13-18 Hz was absence in the upper arm implying that 13-18 Hz MU synchronization is specific for leg muscles. Interestingly, a pronounced 16 Hz synchronized bilateral oscillations have been reported in healthy participants during improper balance (Sharott et al., 2003). The relationship between balance control and 16 Hz activity is consistent with the results of Experiment 1 showing that the 16 Hz coherence was strongest at large knee angles, i.e. in a position close to upright stance. It remains an open question, however, why the strength of the 16 Hz rhythms differed strongly between participants and what caused the change in strength and the shift in peak frequency in both experiments.

Bilateral neural coupling

Although physiological tremor may have many causes (McAuley and Marsden, 2000), the fatigue-related increase in 6-11 Hz bilateral synchronization found in both experiments is more likely to have a central origin. In particular, the increase of inter-limb coherence signifies an increase in common input to both MU pools and afferent fibers have no direct effect on MUs of the homologous muscle, but act by modulating the excitability of interneurons (Harrison and Zytnicki, 1984; Arya et al., 1991; McCrea, 2001). Hence, while afferent feedback might modulate oscillatory activity, it seems unlikely that afferent feedback serves as a coupling mechanism causing MU synchronization between quadriceps muscles of both legs. However, because inter-limb coherence at 6-11 Hz was rather weak in both experiments, a single global oscillatory source causing tremor activity in different body segments appears unlikely (cf. Hurtado et al., 2000). Indeed, Marsden and coworkers (1969) already showed that physiological tremor activity was not synchronized between hands. Bilaterally independent tremor activity was also shown for enhanced physiological, essential, and Parkinsonian tremor (Lauk et al., 1999; Hurtado et al., 2000). All in all, it seems that there are at least two neural oscillators that are normally uncoupled, but can synchronize under specific conditions, such as fatigue.

What caused the increase in 6-11 Hz bilateral coupling during fatiguing contractions? As already mentioned in the Introduction, there is a marked relationship between mirror movements and fatigue, as evidenced by an increase of bilateral co-activation during unilateral contractions at high force levels, referred to as motor irradiation or motor overflow (e.g., Zijdewind and Kernell, 2001; Aranyi and Rosler, 2002). Motor overflow parallels the increase in 6-11 Hz inter-limb coherence observed in both experiments in that both phenomena signify increased bilateral coupling during fatiguing contractions. Interestingly, bilateral, coherent tremor activity around 10 Hz has been found in patients with persistent mirror movements (Köster et al., 1998; O'Sullivan et al., 2002). However, no specific neural mechanisms have yet been identified, although the alleged cortical origin of this motor overflow has been extensively investigated (see Hoy et al., 2004, for a review). Unfortunately, most studies on motor irradiation did not examine the overlap in spectral content between EMGs. Nevertheless, the here-reported increase of inter-limb coherence at 6-11 Hz reflects the increase in motor overflow during fatiguing contractions. Further studies are needed to substantiate this interpretation and pinpoint the neural mechanism underlying this phenomenon.

2.5 Conclusions

The fatigue-related increase in 6-11 Hz inter-limb coherence signifies an increase in common bilateral input and resembles physiological tremor in terms of its frequency content and its fatigue-related increase in strength. The weak coherence between EMGs of homologous muscles agrees with previous studies on physiological tremor. The increase in bilateral synchronization mimics the increase of motor overflow during fatiguing unimanual contractions and both suggest increased bilateral coupling during fatiguing contractions. Although the neural mechanisms underlying these phenomena remain to be identified, it seems likely that fatigue-related changes in excitability along the neural axis, such as the increase or spread of cortical excitability, might facilitate the coupling of neural oscillators (cf. Glass, 2001). The 13-18 Hz synchronization, in contrast, did not correlate with fatigue. Given its frequency content and the strong synchronization between different MU pools, the 13-18 Hz synchronization hints at a physiological subsystem involved in balance-related postural responses (cf. Sharott et al., 2003).

3.

Bilateral motor unit synchronization
is functionally organized

Abstract

In the previous chapter, two experiments were reported that revealed synchronization between homologous muscles in two distinct frequency bands indicating common rhythmic input. This chapter reports a similar experiment that was designed to compare the results for muscles of different extremities and further examine the relation between bilateral MU synchronization and motor overflow. The bilateral coupling between homologous arm muscles was compared during fatiguing elbow flexion and extension contractions. Similar to the results of Chapter 2, MU synchronization was found in the 8-12 Hz frequency band, more strongly so when fatigued. This fatigue-related increase in bilateral MU synchronization was stronger between extensor than between flexor muscles, which appeared consistent with the literature on mirror movements and supported the alleged link between mirror movements and fatigue-related motor overflow. In contrast to the study on leg muscles in Chapter 2, the arm muscles did not exhibit MU synchronization in the 13-18 Hz frequency band, which seemed consistent with the hypothesis that MU synchronization in the higher frequency band, as described in Chapter 2, was linked to balance maintenance. The results are discussed in terms of common bilateral input and substantiate the idea that common input is functionally organized.

Published as: T.W. Boonstra, A. Daffertshofer, E. van As, S. van der Vlugt and P.J. Beek (2007). Bilateral motor unit synchronization is functionally organized. *Experimental Brain Research 178*, 79-88.

3.1 Introduction

During bilateral movements the participating limbs do not move independently but influence each other (e.g., Treffner and Turvey, 1996). Such mutual influences have been extensively investigated in bimanual rhythmic tasks involving finger oscillations and manual circle drawing (see, e.g., Kelso, 1995, for an overview). Interlimb coordination is governed by interactions between limbs arising from various constraints residing at different levels of the motor system (Carson and Kelso, 2004) and several studies have been carried out to pinpoint the neural structures involved (see Carson, 2005, for a review). Recently, evidence has been presented that bilateral coupling primarily stems from shared efferent information (Ridderikhoff et al., 2005b; Spencer et al., 2005) and that afferent processes only play an ancillary role. For instance, muscles that are normally coactivated may share a common drive arising from branched presynaptic fibers or from presynaptic synchronization of last-order inputs (Carr et al., 1994). Similarly, bilateral coupling may arise from cortical neural crosstalk between bilateral motor areas through the corpus callosum (e.g., Franz et al., 1996; de Oliveira et al., 2001; Daffertshofer et al., 2005).

To examine the interactions and processes underlying bimanual coordination, bilateral coupling has been probed by manipulating various parameters, including movement tempo and amplitude (Peper et al., 1995a; Post et al., 2000a; Post et al., 2000b), amount of torque applied (Peper and Carson, 1999), handedness (Treffner and Turvey, 1996), attention (Swinnen et al., 1996; Amazeen et al., 1997), and more. Remarkably, muscle fatigue has hardly been investigated in this context, even though it appears a particularly expedient vehicle to gain insight into the interactions governing interlimb coordination. The reason is that during unilateral fatiguing contractions there is an increase of contralateral coactivation of homologous muscles termed motor irradiation of motor overflow (Zijdewind and Kernell, 2001; Aranyi and Rosler, 2002), indicating increased bilateral coupling during fatigue and/or high effort contractions. In line with those findings, we observed in a previous study an increase in 6-11 Hz MU synchronization between homologous quadriceps muscles during fatiguing contractions (Boonstra et al., 2007b). Based on this result, we hypothesized that increased bilateral MU synchronization and increased motor overflow are different manifestations of the same underlying increase in bilateral coupling during fatiguing contractions.

MU synchronization at a certain frequency band implies a common, rhythmic input (McAuley et al., 1997) that can be quantified via conventional coherence analyses between surface EMGs (cf. Miller and Sigvardt, 1998). MU synchronization as indexed by coherence analyses differs from short-term synchronization as indexed by cross-correlation analyses, which typically result in a narrow central peak in the cross-correlation histogram signifying synchronous discharge times of two MUs caused by common presynaptic input from branched axons (Sears and Stagg, 1976; Kirkwood and Sears, 1978). That is, while cross-correlation analyses estimate the strength of the common input to two MUs, coherence analyses reveal details of the frequency of the common input (Farmer et al., 1993; Semmler, 2002). In the latter case, MU synchronization reflects periodicities in the firing of common presynaptic input to MUs that modulates the EMG amplitude and is likely caused by presynaptic synchronization (Kirkwood et al., 1982). Although rhythmically synchronized input to MUs may arise from various levels of the nervous system (see McAuley and Marsden, 2000, for a review), most researchers seem to agree that it arises at a supraspinal level (Farmer et al., 1993; McAuley et al., 1997; Grosse et al., 2002; Semmler, 2002). As such, MU synchronization might be functionally organized and may act as a binding mechanism integrating spatially distributed, neural activity. In short, it may serve as a neural control mechanism (Farmer, 1998; Singer, 1999; Varela et al., 2001).

To investigate the functional organization of bilateral coupling between homologous muscles, we investigated the difference in increase of MU synchronization during fatiguing elbow flexion and extension. In a recent study on mirror movements, bilateral coupling was stronger between extensor muscles than between flexor muscles (Ridderikhoff et al., 2005a). Similarly, we expected MU synchronization to increase more strongly for extensor than for flexor muscles. We further sought to determine whether earlier results regarding the synchronization between leg muscles (Boonstra et al., 2007b) also hold for arm muscles. In that previous study we did not only find bilateral MU synchronization around 10 Hz, but also around 16 Hz, which was not affected by fatigue. We hypothesized that the latter MU synchronization was related to balance maintenance (cf. Sharott et al., 2003), and thus did not expect to find it in homologous arm muscles. As in the leg muscles, however, we expected to find an increase in fatigue-related 10 Hz interlimb synchronization in the arm muscles. As mentioned before, in light of the study of Ridderikhoff and colleagues (2005a), a stronger increase in 10 Hz synchronization was expected for extensor than for flexor muscles. Such distinct effects on MU synchronization could indeed support the alleged link between fatigue-related

MU synchronization and mirror movements, as both forms of bilateral coupling are affected by fatigue and differ for extensor and flexor muscles.

3.2 Methods and Materials

PARTICIPANTS Eleven healthy students (nine males and two females) from the VU University Amsterdam participated in the experiment (mean age 23 years; range 22-27 years). All participants signed an informed consent after having been informed about the nature of the experiment. The Ethical Committee of the Faculty of Human Movement Sciences of the VU University Amsterdam had approved the experimental protocol before the experiment was conducted.

PROCEDURE Participants were seated in an adjustable chair in upright position and securely strapped in place by two belts to minimize the number of mechanical degrees of freedom that could be recruited in performing the experimental task, which was an isometric force production task (Fig. 3.1). For every participant the chair was adjusted such that both hip and knee joints were flexed at approximately 90°. Participants could exert isometric force, either by elbow flexion or extension, against a metal bar that was placed in front of the participants such that the upper arm was in vertical position and the lower arm in horizontal position with an elbow angle of approximately 90°. At both ends of the metal bar, a force transducer (STS Metric, capacity 200 kg, accuracy class C1) was attached to record the exerted force. Note that the use of the solid bar might have caused 'cross-talk' between the two force sensors potentially yielding finite synchronization values between the force signals. In the present study, however, force signals were only used to control the level of force exerted and synchronization was based solely on EMG recordings.

Because the metal bar had to be adjusted for flexion and extension force production individually, the experiment was divided into two trial sets (flexion and extension), the order of which was counterbalanced across participants. Prior to the experimental trials, the maximum voluntary contraction (MVC) was determined based on two consecutive 10 s recordings, during which participants were instructed to gradually build up force and verbally reinforced to exert maximal force. The maximum force of both recordings was used as MVC reference. Subsequently, participants were asked to produce forces at 20% or 40% MVC to induce different levels of fatigue. Both the required and produced forces were displayed as horizontal lines on a computer screen

placed in front of the participants, who were instructed to tune their force output to the desired force level. In order to encourage and help participants to perform elbow flexions or extensions of both arms as a functional unit, the exerted force of both force sensors were summed and displayed as a single line.

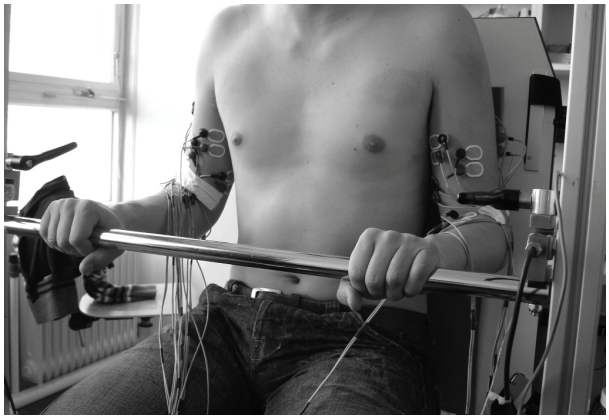

Figure 3.1 *Experimental setup. Participants were sitting in an adjustable chair with a metal bar in front them with force sensors on both ends for recording the exerted force.*

Each participant conducted 2 (flexion/extension) × 2 (force level) × 3 (repetitions) = 12 trials lasting 90 s each. All participants were able to maintain the required force level for the duration of the trial and participants rested for three minutes between trials. The order of force levels and trials was randomized across participants. By performing isometric contractions at different force levels, the effect of fatigue on MU synchronization could be examined when comparing the change of MU synchronization over time in the different force level conditions.

DATA ACQUISITION Surface EMG was recorded from m. biceps brachii caput longum (BL), m. biceps brachii caput breve (BB), m. brachioradialis (BR), m. brachialis (B), m. triceps brachii caput longum (TLo), m. triceps brachii caput laterale (TLa), and m. triceps brachii caput mediale (TM) of both arms. For the purpose of the present study only data from BL, BB, TLo, TLa and TM were analyzed. The electrodes (Ambu® Blue Sensor N) were placed in a bipolar montage with an interelectrode distance of about 2 cm with locations following SENIAM guidelines (Hermens et al., 2000). Data were amplified, band-pass filtered, digitized, and stored on disk (5-1000 Hz, 22-bit sampling depth, 2 kHz sampling rate, Porti 5-16/ASD, TMS International, Enschede, The Netherlands).

DATA ANALYSIS EMG data were filtered off-line using a second-order bidirectional Butterworth high-pass filter (cutoff frequency 20 Hz) to

eliminate movement artifacts. EMG signals were further full-wave rectified using the Hilbert transform (cf. Myers et al., 2003) and normalized relative to the MVC as determined at the beginning of the experiment. Each trial was divided into six consecutive intervals (I, II, …, VI) of 15 s each. Per interval, mean power and median frequency of the EMGs were computed. The median frequency was calculated from the non-rectified EMG using Welch's periodogram method with Hamming windows of 1024 samples length and overlapping 768 samples. The spectral power estimate per interval (I, II, …, VI) was thus based on 114 overlapping data segments with a frequency resolution of 0.98 Hz.

We used identical settings when estimating the power spectral densities and coherence spectra of the EMG. In contrast to the calculation of the median frequency, these two analyses were based on the rectified EMG (the dc-value of each 1024 samples data window was removed before computing the Fourier transform). The resulting power spectral densities were log-transformed (Halliday et al., 1995) and Fisher's transform was applied to the coherence spectra before conducting statistical tests (Amjad et al., 1997). Both rescaling procedures 'stabilize' the variances of the underlying distributions and were used before testing spectral estimates for statistical differences (Rosenberg et al., 1989; Farmer et al., 1993; Gerloff et al., 1998a).

STATISTICAL ANALYSIS Power and coherence spectra were submitted to a PCA to identify spectral components common across participants, conditions, and muscles. PCA was exploited in its capacity to reduce the dimensionality of the data by extracting major frequency components or modes and to quantify the strength of these frequency components in different conditions and muscles. The quality of the data reduction can be evaluated via the eigenvalues representing the contribution of the components extracted by the PCA to the total variance, while conditions can be compared in terms of the corresponding coefficients of the eigenvector (see Boonstra et al., 2005b; Boonstra et al., 2007b, for similar applications). The advantage of such a combined analysis is that the effects of fatigue that are present in this high-dimensional signal vector can be examined in a concise and readily interpretable manner (even if the effects are small or the data are noisy). Hence, the spectra of all participants and conditions were combined into a single signal vector yielding three different high-dimensional signal vectors: a vector for the power spectra of the EMGs with 11 (participants) × 2 (tasks) × 2 (force levels) × 6 (intervals) × 10 (muscles) = 2640 signals, a vector for interlimb coherence during flexion trials with 11 × 2 × 2 × 6 × 2 (BL_{left}-BL_{right}, BB_{left}-BB_{right}) = 528 signals, and a vector

for the interlimb coherence during extension trials with 11 × 2 × 2 × 6 × 3 (TLo_{left}-TLo_{right}, TLa_{left}-TLa_{right}, TM_{left}-TM_{right}) = 792 signals.

To allow comparison with more conventional statistical approaches, we also analyzed the effects of fatigue on the amplitude, median frequency, and coherence by performing a four-way ANOVA (2 × 2 × 2 × 2; *task* × *muscle* × *force level* × *interval*) with repeated measures on the first and last intervals per trial (Boonstra et al., 2007b). This design was used to evaluate whether changes in amplitude, median frequency, or coherence were different between tasks (flexion, extension) or muscle groups (biceps, triceps). To keep the design compact, however, we averaged over the various biceps and triceps muscles (or combinations in the case of coherence) so that the factor *muscle* had two levels (biceps and triceps) – note that such averaging was not necessary for the PCA. The design was completely balanced with equal record lengths for all conditions. Coherence was evaluated in 8-12 Hz frequency bands; this choice was based on the PCA results (see Results). To facilitate the interpretation of significant results obtained with the ANOVAs, effect sizes (f) were calculated in terms of partial η^2 (Cohen, 1988).

3.3 Results

The maximal combined force exerted on both force sensors was 396 ± 112 N for elbow flexion and 341 ± 80 N for elbow extension. EMG_{max} during elbow flexion was 8.57 ± 2.89 mV and 0.80 ± 0.18 mV for the biceps and triceps muscles, respectively, and EMG_{max} during elbow extension was 0.84 ± 0.31 mV (biceps) and 6.91 ± 3.43 mV (triceps). Coactivation was 10.3 ± 3.9% during flexion MVC and 13.9 ± 7.1% during extension MVC.

Both EMG amplitude and median frequency showed marked effects of muscle fatigue (Fig. 3.2). The EMG amplitude of all muscles increased significantly in time ($F(1,10) = 68.4$; $p < 0.001$; $f = 0.87$). The increase of EMG amplitude was significantly greater at a 40% MVC force level compared to the 20% force condition as revealed by a significant force by interval interaction ($F(1,10) = 32.4$; $p < 0.001$; $f = 0.76$). There was no significant difference between the EMG amplitude of the biceps and triceps muscles, whereas the amplitude was slightly larger during flexion than during extension ($F(1,10) = 9.40$; $p = 0.012$; $f = 0.48$). As could be expected, the EMG amplitudes were larger in the 40% force condition. Interestingly, the effects of fatigue were similar for the agonist and antagonist muscles. Median frequencies of the

EMGs of all muscles decreased significantly in time ($F(1,10) = 90.6$; $p < 0.001$; $f = 0.90$) and this decrease was greater in the 40% force condition ($F(1,10) = 62.5$; $p < 0.001$; $f = 0.86$). The EMGs' median frequency showed significant main effects of muscle ($F(1,10) = 9.60$; $p = 0.011$; $f = 0.49$), task ($F(1,10) = 28.1$; $p < 0.001$; $f = 0.74$), and force level ($F(1,10) = 12.2$; $p = 0.006$; $f = 0.55$) indicating that the median frequency was higher for the biceps during extension and at the low force condition, respectively. Again, the effect of fatigue on the EMGs' median frequency was similar for agonist and antagonist muscles (Fig. 3.2). The decrease was even greater for the antagonist than for the agonist muscles ($F(1,10) = 35.8$; $p < 0.001$; $f = 0.78$; decrease in median frequency: biceps flexion, 7.9 Hz; biceps extension, 13.1 Hz; triceps flexion, 11.3 Hz; triceps extension, 9.1 Hz).

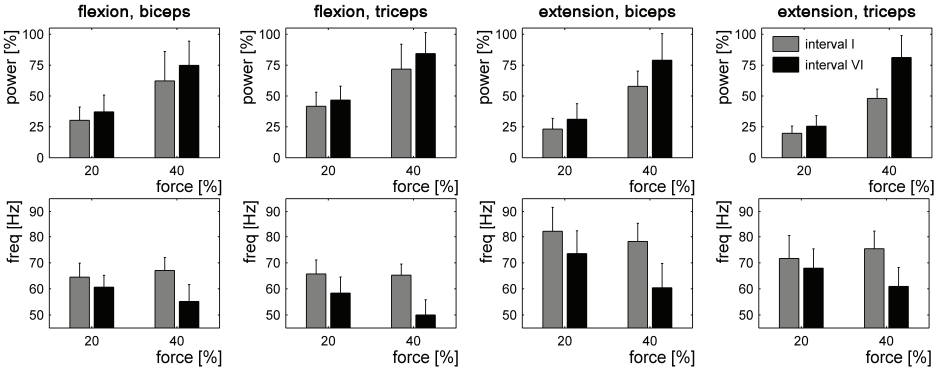

Figure 3.2 *Top panels: power as percentage MVC in the first and last 15 s interval for both tasks (flexion and extension) and averaged over different heads of the biceps and triceps; lower panels: idem, but for median frequency of the unrectified EMG.*

The power spectra of both force sensors revealed that the low-frequency range around 2 Hz contained most power with a second, smaller peak around 10 Hz. The mean normalized power averaged over both force sensors in the 8-12 Hz frequency band was larger in the high force condition and increased in time (flexion: interval I low force, 1.23 ± 0.88%; interval VI low force, 3.43 ± 2.45%, interval I high force, 3.27 ± 2.53%, interval VI high force, 4.43 ± 2.65%; and for extension: interval I low force, 1.45 ± 0.60%; interval VI low force, 2.77 ± 1.49%, interval I high force, 2.34 ± 1.41%, interval VI high force, 5.25 ± 2.81%). The power of the rectified EMGs revealed a peak at a slightly higher frequency, i.e. between 10 and 20 Hz (Fig. 3.3). The first mode of the PCA of the power spectra of the EMG explained 83% (biceps) and 81%

(triceps) of the total variance and represented the spectral distribution common to all muscles irrespective of condition. It displayed a fairly broad spectral peak that was maximal around 15 Hz. The second mode (about 8% of the total variance) had a peak around 18 Hz and its strength decreased in time, particularly in the high force condition, as revealed by the coefficients of the corresponding eigenvector[7]. The third mode displayed a modulation of the peak frequency of the first mode: adding the third mode to the first caused a shift of the 15 Hz peak towards lower frequencies (subtracting it thus yielded a shift towards higher frequencies). For both biceps and triceps muscles, the strength of the third mode increased in time implying that the peak of the first mode shifted towards lower frequencies in the course of a trial. Although PCA did not extract the 8-12 Hz band as a separate frequency component, 8-12 Hz EMG power was higher in the high force condition and increased in time during each trial (Fig. 3.5).

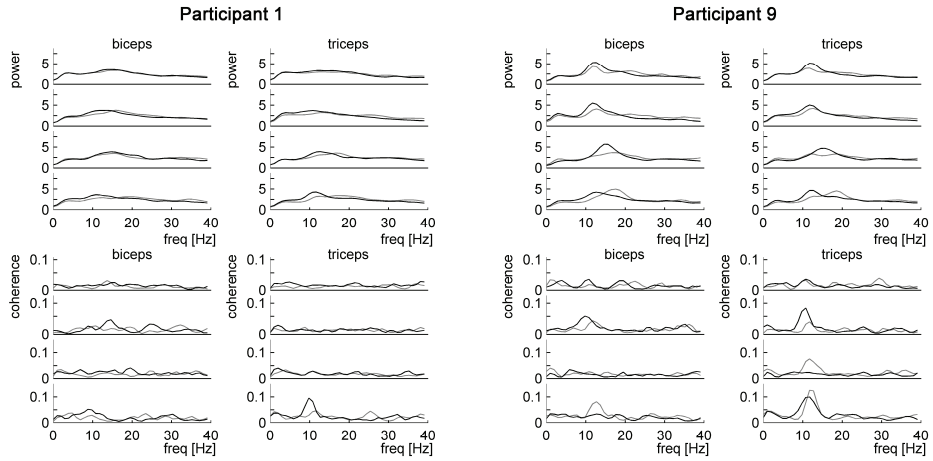

Figure 3.3 *Power and coherence spectra for two participants. Top panels: the normalized power spectra of the rectified EMG for biceps and triceps (averaged over different heads of both arms) in four different conditions (from top to bottom: flexion low force, flexion high force, extension low force, extension high force) for the first (gray line) and last interval (black line). Lower panels: idem, but now for the interlimb coherence spectra.*

Coherence between EMGs of both arms displayed a clear peak around 10 Hz, particularly in the high force condition, and appeared stronger for the

[7] Recall that PCA modes yield eigenvector coefficients that signify the strength of these frequency components in the original spectra of different condition and thus allow for a comparison between conditions.

triceps muscles (Fig. 3.3). PCA of the interlimb coherence spectra yielded a first mode that covered 13% (biceps) and 23% (triceps) of the total variance (Fig. 3.4). For both muscle combinations, the first mode revealed a peak around 10 Hz that was indeed stronger for the triceps than for the biceps[8]. The interlimb coherence between the triceps was strongest during extension at high force and in this condition it increased over time. The structure of the eigenvector coefficients of the first mode of the interlimb coherence between the biceps was less clear-cut but coherence seemed to increase over time both during the high force flexion and extension contractions. The second mode represented a modulation of the frequency of the peak of the first mode similar to the third on the first mode of the power spectra (i.e. adding the second mode to the first caused a shift of the 10 Hz peak towards lower frequencies, whereas subtracting it yielded a shift towards higher frequencies). Again, the structure of eigenvector coefficients was most obvious for the triceps: during extension at high force, the strength of the mode increased considerably in time. This indicates that the peak frequency of the 10 Hz coherence decreased in frequency over time during extension at high force.

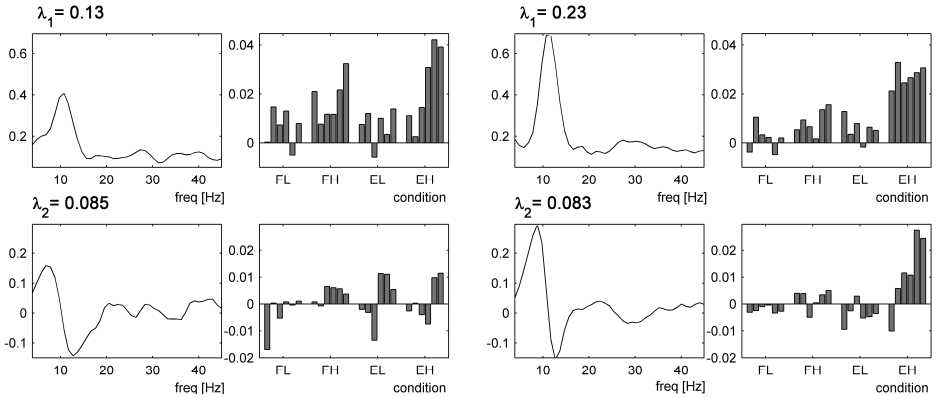

Figure 3.4 *First two PCA modes of interlimb coherence between biceps (left two columns) and triceps muscles (right two columns). First column: first two principal coherence spectra (eigenvalues 13%, 9%) of the biceps muscles; second column: mean coefficients for corresponding eigenvectors for flexion low force (FL), flexion high force (FH), extension low force (EL), and extension high force (EH) at the six intervals; column 3 and 4: idem, but now for the PCA of the interlimb coherence between the triceps muscles.*

[8] The original coherence spectra can be reconstructed by multiplying the projection of each mode with the coefficients of the eigenvector, cf. Appendix A.

By and large, the results of the ANOVA on the coherence spectra were in agreement with the PCA results. The 8-12 Hz intralimb coherence was significantly higher during the high force condition ($F(1,10) = 8.90$, $p = 0.014$, $f = 0.47$; mean coherence: 20% MVC, 0.018 ± 0.004; 40% MVC, 0.025 ± 0.010) and increased in time ($F(1,10) = 5.55$, $p = 0.040$, $f = 0.36$; mean coherence: interval I, 0.020 ± 0.006; interval VI, 0.023 ± 0.008). The force by interval interaction was almost significant ($F(1,10) = 4.73$, $p = 0.055$, $f = 0.32$), reflecting a stronger increase in coherence in the high force condition (Fig. 3.5). Further, there was a main effect of task ($F(1,10) = 5.43$, $p = 0.042$, $f = 0.35$; mean coherence: flexion, 0.020 ± 0.006; extension, 0.023 ± 0.007), but no main effect of muscle ($p > 0.05$), indicating that coherence was similar for biceps and triceps. Finally, there was a significant task by muscle interaction ($F(1,10) = 4.97$, $p = 0.050$, $f = 0.33$), which revealed that coherence between triceps muscles was higher during extension.

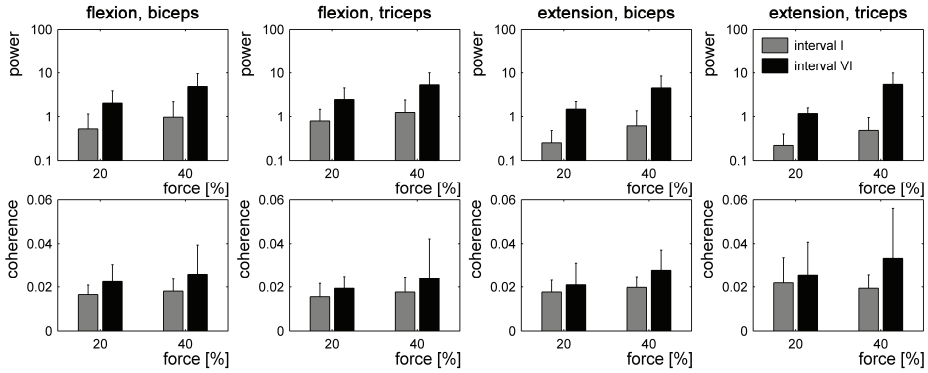

Figure 3.5 *Mean power and interlimb coherence in the 8-12 Hz frequency band. Upper panels: the grand average of the EMG power in the 8-12 Hz frequency band of the first and last interval in the four different conditions. Data are plotted on a log scale and the error bars indicate the between-subject standard deviation. Lower panels: idem, but now for the interlimb coherence in the 8-12 Hz frequency band.*

3.4 Discussion

PCA revealed fatigue-related 8-12 Hz interlimb coherence for both the biceps and triceps muscles. As expected, 8-12 Hz synchronization was stronger during the high force condition and increased significantly over time. The increase in interlimb synchronization was particularly strong between the triceps muscles during high force extension. Interlimb synchronization was

associated with fatigue in that EMG amplitude increased and median frequency decreased as fatigue increased and these changes were stronger in the high force condition. However, although there were significant differences in interlimb coherence, absolute coherence levels were rather low and PCA converged only slowly, indicating that bilateral MU activity remained largely uncoupled (i.e. MU synchronization was weak). The 8-12 Hz interlimb coherence was accompanied by a similar peak in the power spectra of the force sensor showing tremor activity at 8-12 Hz. The 10 Hz peak in the coherence spectra shifted towards lower frequencies over time, particularly during flexion at high force. This changeover was accompanied by a similar shift towards lower frequencies in the power spectra of the rectified EMG. Given that participants were holding the bar with both hands, the increase in 8-12 Hz interlimb coherence with fatigue might have been related to an increase in 8-12 Hz power in the force exerted on the bar via a common afferent feedback that, in principle, could have simultaneously influenced MU discharges in both limbs. The increase in 8-12 Hz synchronization, however, agreed with the results of an earlier study (Boonstra et al., 2007b) in which bilateral force was exerting against mechanically independent force sensors. That is, it seemed unlikely that mechanical cross-talk (in combination with afferent feedback) caused the here-observed coherence. In contrast to our previous study, no synchronized activity was found around 16 Hz, which is consistent with our hypothesis that 16 Hz activity is related to balance maintenance (cf. Sharott et al., 2003).

We quantified muscle fatigue in terms of changes in EMG amplitude and median frequency. In all likelihood, fatigue-related increase in EMG amplitude is caused by the recruitment of additional MUs and the increase in firing frequency that are invoked to compensate for reduced muscle contractility (Lippold et al., 1960; Viitasalo and Komi, 1977; Bigland-Ritchie et al., 1986). A decreasing median frequency, on the other hand, is thought to be related to the progressive slowing of the conduction velocity of action potentials along the muscle fiber resulting from an increase in extracellular metabolites (Mortimer et al., 1970; Lindstrom et al., 1977). However, because the relative decrease of the median frequency often exceeds the relative decrease of conduction velocity, other researchers have pointed at additional factors such as synchronization of MU firing (Bigland-Ritchie et al., 1981; Krogh-Lund and Jorgensen, 1993). Noteworthy in this regard is the here reported increase in EMG amplitude and decrease in median frequency of the antagonist muscles matching the change of the agonist muscles. It is unlikely that this decrease in median frequency of the antagonist muscles was caused by increased

extracellular metabolites because the cocontraction level was only about 10% of the agonist activity and peripheral fatigue was therefore not to be expected. Indeed, several studies have shown that the force generating capacity of the antagonist muscles remained equal after fatiguing contractions of the agonist muscles (e.g., Levenez et al., 2005). Although the effects on the EMG amplitude and median frequency of the antagonist muscle could, in principle, result from cross-talk, it is typically interpreted as an effect of a common drive to the agonist-antagonist couple (Psek and Cafarelli, 1993; Ebenbichler et al., 1998; Mullany et al., 2002; Levenez et al., 2005). In support of this interpretation, an increase in amplitude and a decrease in median frequency have been found in the contralateral homologous muscle after unilateral muscle fatigue (Morrison et al., 2005). Note that common drive refers to a homogeneous input to MU pools (De Luca et al., 1982; De Luca and Erim, 1994) and that antagonist cocontraction could be instrumental in maintaining joint stability (Solomonow et al., 1988).

Similar to the 6-11 Hz interlimb synchronization between quadriceps muscles found in our previous study (Boonstra et al., 2007b), the increase in 8-12 Hz interlimb coherence found in the present experiment seems related to physiological tremor. Most obviously, the 8-12 Hz MU rhythm resembles physiological tremor in its frequency content (see McAuley and Marsden, 2000, for an overview). The relation between bilateral 8-12 Hz MU synchronization and physiological tremor is supported further by a contralateral increase in physiological tremor after unilateral muscle fatigue (Morrison et al., 2005). Similarly, the decrease in peak frequency of the 8-12 Hz interlimb coherence over the course of a trial resembles the decrease in peak frequency of the acceleration in tremor activity during fatiguing contractions (Vaillancourt and Newell, 2000). As described in the introduction, MU synchronization at a certain frequency points at a common rhythmic input (cf. McAuley et al., 1997). That is, rhythmic MU synchronization, e.g., underlying tremor activity, reflects in-phase MU rhythms that are additional to those at the MU intrinsic firing rates (cf. Christakos et al., 2006). Put differently, there is not necessarily an entrapment of the firing rates of individual MUs into the 8-12 Hz rhythm, but MU synchronization, as measured by surface EMG, reflects rhythmic modulation of the total EMG amplitude and suggests rhythmic input. Note, however, that the amount of common bilateral input remained fairly small throughout the experiment in agreement with previous findings of bilateral independent tremor activity (Marsden et al., 1969; Lauk et al., 1999; Marsden et al., 1999; Hurtado et al., 2000). There, MU synchronization was examined primarily between bilateral

hand muscles, whereas in the present experiment the increase in 8-12 Hz bilateral synchronization was found between upper-arm muscles. As such, our results support a distal-axial difference in bilateral synchronization, revealing synchronization in different frequency bands for different muscle groups (Marsden et al., 1999).

The stronger increase in bilateral 8-12 Hz synchronization between extensor muscles compared to flexor muscles agrees with the stronger bilateral coupling found in a recent study on mirror movements from our research group (Ridderikhoff et al., 2005a). It thus strengthens the alleged link between 8-12 Hz interlimb coherence and fatigue-related increase in motor overflow (Boonstra et al., 2007b). That is, there seems to be a fatigue-related increase in common bilateral input, which may be reflected either in increased 8-12 Hz MU synchronization or increased mirror movements (or both). As described in the Introduction, there are several neural pathways via which the fatigue-related increase in bilateral coupling could come about, but several findings point at a supraspinal origin (cf. Carson, 2005). For instance, afferent fibers have no direct, crossed effect on MUs of homologous muscle but only modulate the excitability of interneurons (Harrison and Zytnicki, 1984; Arya et al., 1991; McCrea, 2001). Furthermore, behavioral data showed that afferent information plays only an ancillary role in bilateral coupling (Ridderikhoff et al., 2005b; Spencer et al., 2005). It was shown for both maximal and submaximal contractions that there is a common drive to homologous muscles that might be instigated by interneuronal connectivity between both motor areas (Oda, 1997).

Interestingly, 8-12 Hz MU synchronization as well as mirror movements were stronger for extensor muscles than for flexors muscles, consistent with a functional organization of common drive. Put differently, most precisely controlled unimanual movements are made by using flexor muscles and it is therefore to be expected that flexor muscles are controlled more independently than extensor muscles (cf. Carson and Riek, 2001). This line of argument supports the idea that movements are, in principle, controlled bimanually and in order to achieve unimanual movements the contralateral side is inhibited (Daffertshofer et al., 2005). Such a control structure would imply that contralateral inhibition is less developed for extensors than for flexors as extensors appear to be hardly used in isolation. A decrease in the functional coupling between cortical motor areas was found during bimanual skill acquisition (Andres et al., 1999) and, in view of the present results, it would be rather interesting to investigate whether such changes in bilateral coupling differ between flexor and extensor movement.

4.

Effects of sleep deprivation on event-related fields and alpha activity during rhythmic force production

Abstract

In the last two chapters neural synchronization was investigated between EMGs of different muscles. In the following, an experiment is reported in which MEG and EMG signals were recorded during acoustically paced rhythmic force production. To manipulate neural synchronization both central and muscle fatigue were induced. The effects of force level on cortical activity are reported elsewhere (Daffertshofer et al., 2007); in this chapter the effects of sleep deprivation (SD) on cortical brain activity are reported. Effects of SD on brain activity were examined via spatial distribution of spectral power over the scalp at different frequency bands and via auditory- and motor-evoked fields. For the latter, principal component analysis revealed that auditory- and motor-evoked fields were attenuated after SD. Furthermore, an anterior shift of alpha power towards more frontal channels was found. At the behavioral level, SD resulted in a reduction of the lag (negative asynchrony) between produced forces and acoustic stimuli at higher movement tempos. Conjointly, these results are interpreted in terms of a change of central processing of afferent sensory input due to SD. Apart from the effect of cortical synchronization, no consistent synchronization was found between cortical and spinal activity (Boonstra et al., 2004).

Published as: T.W. Boonstra, A. Daffertshofer and P.J. Beek (2005). Effects of sleep deprivation on event-related fields and alpha activity during rhythmic force production. *Neuroscience Letters 388*, 27-32 .

4.1 Introduction

The effects of central fatigue on EEG activity have been studied extensively in the context of the sleep-wake cycle. During the transition from wakefulness to sleep EEG activity changes considerably across frequencies, particularly in the alpha band (Cantero et al., 2002). Near sleep onset, a posterior-anterior shift of alpha power occurs that corresponds with a decrease of alpha power above occipital areas and an increase above more frontal areas (Cantero et al., 1999; De Gennaro et al., 2001). To date, however, changes in alpha power lack a more functional interpretation, although they readily point at a link with attention (Suffczynski et al., 2001; Yamagishi et al., 2003).

Apart from relations with fatigue or attention, oscillatory EEG activity in the alpha band (mu-rhythm) is thought to play an important role in motor tasks (Pfurtscheller and Aranibar, 1978; Mima et al., 1999). The mu-rhythm seems to reflect an information processing loop between motor cortices and sub-cortical structures, which entails reverberating activity in thalamo-cortical and cortical-cortical circuits (Lopes da Silva et al., 1980; Cantero et al., 2002).

To uncover the role of alpha activity in motor functioning, we examined the effects of SD on the performance of a simple motor task and the accompanying MEG activity. In this task, participants had to produce isometric forces either in synchrony with auditory stimuli (synchronization) or in-between successive stimuli (syncopation). In a similar experimental setup, transitions from syncopation to synchronization occurred when the inter-response interval was shortened (Kelso, 1984; Kelso et al., 1992; Daffertshofer et al., 2000a). Based on previous results obtained in experiments on the influence of attention on interlimb coordination (Monno et al., 2000), we expected SD to affect the (critical) frequency of these transitions. With regard to brain activity, SD was expected to have an effect on the motor-related mu activity. Since the transition from wakefulness to sleep is also known to alter the N1-P2 component of the auditory ERP (Campbell and Colrain, 2002; Ferrara et al., 2002), SD was further expected to affect event-related activity.

4.2 Methods and Materials

PARTICIPANTS Four male participants (between 25 and 45 years of age) participated in the experiment that was conducted in accordance with the Declaration of Helsinki and the guidelines of the Medical Ethical Committee

of the VU medical center. All participants were self-proclaimed right-handers and signed an informed consent prior to participation.

PROCEDURE Neuromagnetic activity was recorded using a whole-head MEG (CTF Systems Inc., Vancouver, Canada). Participants were lying on a bed in a comfortable position to avoid artifacts due to head motion or involuntary contractions of head and shoulder muscles. Participants were instructed to produce isometric forces by adducting their thumb against a MEG-compatible force sensor (Boonstra et al., 2005a; Appendix B) that was fixed on the bed allowing for almost maximal arm extension. Adduction forces had to be produced either simultaneously with or in-between the acoustic stimuli that were delivered binaurally using EARTone 3A Insert Earphones (Cabot Safety Corporation). Stimulus trains consisted of 100 tones (pitch 400 Hz; 50 ms duration each) that were presented with decreasing inter-stimulus intervals (ISIs: ranging from 1000 to 357 ms over ten plateaus), i.e. with increasing tempo from 1 Hz to 2.8 Hz in steps of 0.2 Hz (Kelso et al., 1992; Daffertshofer et al., 2000a). Each trial lasted about one minute.

Every participant participated in two experimental sessions at consecutive days, roughly starting at the same time of day. During those days participants had to abstain from drinking alcohol and coffee. On the second day, the participants were sleep deprived, as they had been kept awake for 24 hours under the supervision of one of the experimenters. The recordings of the first day served as control condition. On both days, participants performed $2 \times 12 = 24$ trials; total duration about 24 minutes per day. Synchronization and syncopation trials were randomized over participants. The produced force was monitored on-line and visually fed back by projecting it on the ceiling (feedback signals were low-pass filtered to eliminate oscillatory components; 4^{th} order Butterworth filter, cut-off 0.33 Hz). Participants were instructed to maintain the force level within a certain range indicated by two reference lines (2.5% and 7.5% of the maximum voluntary contraction, which was determined at the beginning of the experiment). To minimize eye movements, participants were further asked to fixate their gaze at a small cross that was displayed in the middle of the force-feedback region.

DATA ACQUISITION The MEG comprised of 151 SQuID sensors (3^{rd}-order gradiometers) distributed homogeneously across the helmet surface. Two channels were not operational so that, effectively, 149 MEG signals were recorded. The voltages of force sensor and acoustic stimuli were sampled simultaneously with the MEG using two additional analogue-digital channels.

All signals were low-pass filtered at 415 Hz before digitization at a sampling rate of 1250 Hz.

DATA PROCESSING To quantify the effects of SD on motor performance, the relative phase between tone and force signals was determined via the Hilbert transform of the band-pass filtered signals (e.g., Rosenblum et al., 1996). Per movement tempo, we computed the mean relative phase (Mardia, 1972) and, for the syncopation trials, transition points were established as center of a sigmoid function that was determined by a least squares fit.

Further, we estimated the frequency spectra of the MEG signals using Welch's periodogram method providing a frequency resolution of 1 Hz (window size: 1250 samples; overlap: 625 samples). For all four conditions (synchronization vs. syncopation; fatigued vs. control), the log-power spectral densities were averaged on a sensor level over trials and participants for each movement tempo. Differences in frequency spectra between fatigued and control conditions were examined using PCA. For this sake, the frequency spectra at the ten movement tempos were concatenated for each MEG channel in both fatigued and control conditions, resulting in a set of 2×149 signals (for both the fatigued and control condition) of 10×60 frequency bins (0-60 Hz with resolution of 1 Hz).

Principal components were calculated (Kelso et al., 1992; Daffertshofer et al., 2000a) and studied by analyzing the resulting eigenvalue distributions, the spatial modes (per condition) and the corresponding frequency spectra. Note that by concatenating frequency spectra we focused on persistent spatial activity patterns irrespective of movement tempo. Note further that, in this particular application, the PCA served as an unbiased multivariate clustering measure, classifying conditions similar to a (time-resolved) multivariate analysis of variance.

Subsequently, both auditory- and motor-related fields were calculated using tone onsets and maxima of the force cycles, respectively, as event-defining indices. Before averaging over events, MEG data were band-pass filtered (4^{th}-order Butterworth: 0.5-60 Hz). For the auditory-evoked fields (AEFs), epochs were individually averaged for each movement tempo (1.0 … 2.8 Hz) and condition over an interval from -100 to 300 ms (with 0 ms referring to the moment of tone onset). Similarly, motor-evoked fields (MEFs) were calculated by averaging over a -150 to 250 ms interval (with 0 ms referring to the moment of maximal force production for each cycle). Artifact-contaminated epochs were excluded from averaging. Magnetic field distortions (e.g., elicited by eye movements and blinks) were marked as artifacts if the

amplitude of a MEG channel was larger than eight times the standard deviation for the entire trial. In total, 6.5% of the epochs were removed, leaving at least 350 epochs for averaging for each movement tempo. To examine whether the event-related fields were different in the fatigued condition, PCA was used equivalently to the analysis of the frequency spectra. Both AEFs and MEFs were averaged over participants and concatenated for every MEG channel in each condition, resulting in a matrix of 2 × 149 channels by 10 × 400 ms duration for both the synchronization and the syncopation condition. Notice that given the consistency of the here reported features of the ERFs, we used grand averages to focus on the inter-subject commonalities.

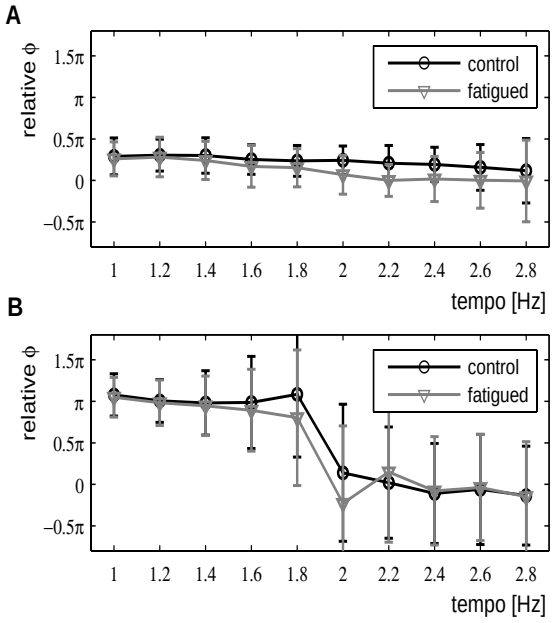

Figure 4.1 *A) Mean relative Hilbert phase (Φ) between force and tone for all 10 plateaus in the synchronization condition (0 and 2π represent in-phase force production). Error bars display the circular standard deviation of mean phases over trials and participants.* ***B)*** *Idem, but now for the syncopation condition.*

4.3 Results

The relative Hilbert phase between produced forces and tones disclosed that, in the synchronization condition, the former anticipated the latter, that is, peak forces occurred prior to tone onsets (negative asynchrony). A 10 × 2 (*tempo* × *fatigue*) ANOVA of the relative Hilbert phase revealed that this anticipation was reduced at higher movement tempos ($F(9,27) = 3.8$, $p < 0.005$) and that this reduction was stronger in the fatigued than in the control condition ($F(9,27) = 3.0$, $p < 0.05$; Fig. 4.1A). In the syncopation condition, a clear transition from syncopation to synchronization was found around a movement tempo of 2 Hz

(Fig. 4.1B). No significant effect of SD on the transition frequency was found: in the fatigued condition the transition occurred on average after 35.6 ± 10.0 s compared to 35.8 ± 12.0 s in the control condition (the end of the 1.8 Hz plateau).

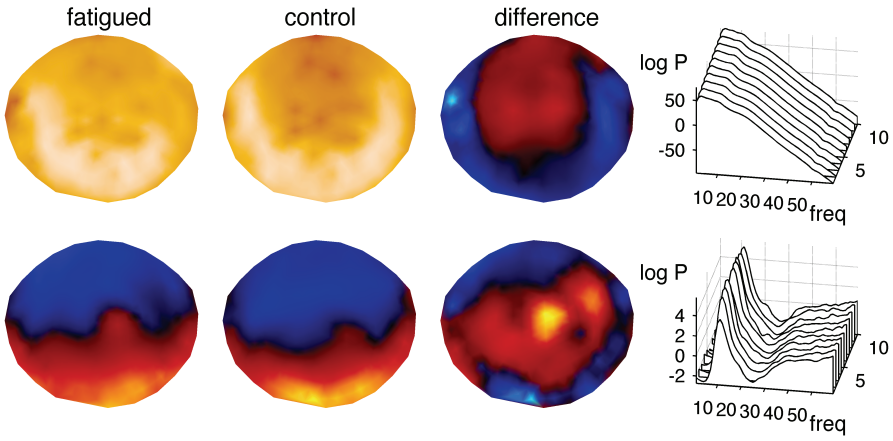

Figure 4.2 *The first two modes of the PCA of the power spectral densities. From left to right: the part of the eigenvectors belonging to the fatigued condition and plotted on a 2D scalp* ***(fatigued)****; the part of the eigenvectors belonging to the control condition* ***(control)****; the difference between both parts of the eigenvector showing the difference between conditions* ***(difference)****; PCA projections; the frequency spectra belonging to the first two modes sliced in parts corresponding to the different frequency plateaus. Top panels: first mode; lower panels: second mode*

PCA of the frequency spectra yielded a drastic reduction of the data as the first principal mode of the power spectral densities already covered more than 99% of the data's spread, with the parts of the eigenvector corresponding to the fatigued and the control conditions being rather similar. The power spectra corresponding to the first mode turned out to be almost identical for every movement tempo. In other words, there was a dominant spectral distribution reflecting the consistency of the frequency content during the experiment. Interestingly, the spatial distribution of the power differed after SD (Fig. 4.2) in that the power was decreased at occipital and temporal channels (maximal at channel MLT32: -13% for synchronization and -11% for syncopation) and increased at frontal and central channels (maximal at channel LC31: +5.8% for synchronization and RC31: +7.8% for syncopation). The second principal mode (about 0.1% of the data's spread) reflected the commonly reported concentration of alpha power around occipital channels.

This spatial pattern, however, was less pronounced after SD because of an anterior shift of alpha activity. The increase was maximal at channel RC41 in the synchronization condition and at channel RC42 in the syncopation condition. The frequency band extracted by mode two was roughly bounded between 9 and 13 Hz peaking at 11 Hz for all movement tempos.

By and large, three principal modes sufficed to describe AEFs and MEFs (eigenvalues for AEFs: 0.53 + 0.18 + 0.08 = 0.79 for synchronization and 0.59 + 0.08 + 0.08 = 0.75 for syncopation; similarly for MEFs: 0.6 + 0.21 + 0.05 = 0.86 and 0.59 + 0.14 + 0.05 = 0.78). Importantly, AEF modes appeared to be permutated MEF modes (modes one and two were swapped, Fig. 4.3, first two rows). The first mode in the AEFs displayed two bipolar activity patterns (bilateral auditory cortices), whereas the first mode in the MEFs reflected a bipolar field above the left contralateral motor area. The observed averages always contained fields that originated from both auditory- and motor-related processes, although the auditory-related fields were clearly stronger in the auditory-related average due to better alignment and vice versa. The left/right symmetric mode three was similar in both averages but appeared more event-locked in the case of AEFs (cf. sharp peak around t = 100 ms in Fig. 4.3).

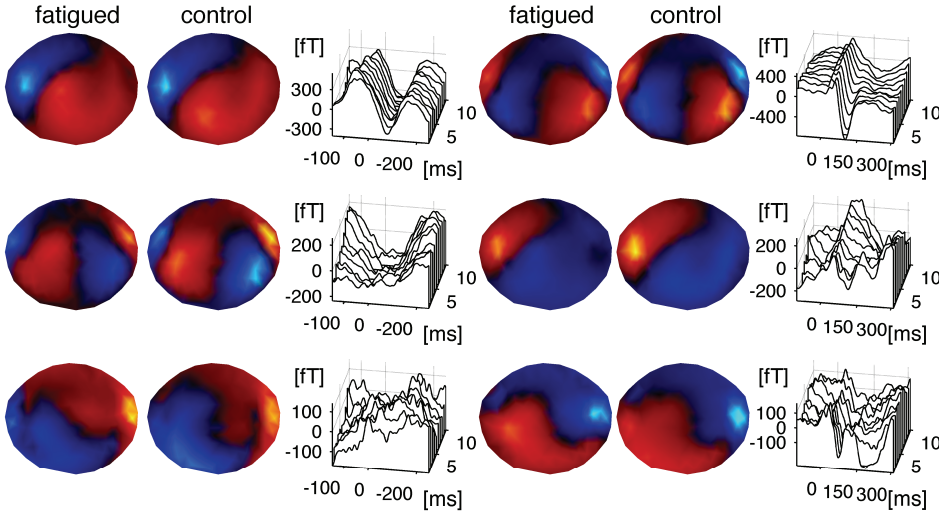

Figure 4.3 *The first three PCA modes of the ERFs. Left panels: The parts of the eigenvectors belonging to the fatigued and control condition and the corresponding time-series (projections) of the MEFs. Right panels: Idem, but now for the PCA for the AEFs.*

The spatial distribution of the evoked fields was almost identical for synchronization and syncopation and did not change due to SD. In contrast,

the modes' strengths differed significantly between the fatigued and control condition: the part of the eigenvector corresponding to the fatigued conditions was, in general, smaller than the part of the eigenvector corresponding to the control condition. A more detailed look at Figure 4.3 revealed that the eigenvector of the first mode of the AEFs had a maximal strength at a right temporal channel (RT32) and the MEFs were maximal at a left temporal channel (LT13) in all four conditions. At channel RT32 the strength of the eigenvector for the AEFs was 19% and 11% smaller in the fatigued compared to the control condition for synchronization and syncopation, respectively. In the synchronization condition, for instance, this decrease corresponded to an amplitude reduction of the N1 from 161 fT to 139 fT at an ISI of 1 s. Similarly, for the MEFs the strength at channel LT13 was 9% (synchronization) and 19% (syncopation) weaker when sleep deprived. In the second modes, an even more pronounced decrease of amplitude was found in the fatigued condition. To investigate the difference in amplitude reductions in the fatigued condition between synchronization and syncopation, the ERFs of all four conditions were analyzed concurrently after concatenating ERFs of all four conditions into a '4 × 149 channels by 10 × 400 ms duration' array. The resulting eigenvalues were rather similar (AEFs: 0.57 + 0.11 + 0.07 = 0.75; MEFs: 0.59 + 0.16 + 0.06 = 0.81). Again, the first eigenvector was maximal at channel RT32 for the AEFs and at channel LT13 for the MEFs across conditions. Interestingly, at these channels the first principal mode was almost identical to the original ERFs, that is, the reduction to a single PCA mode did preserve the primary structure of the ERFs (Fig. 4.4). The explained variance at this channel (covariance of PCA reconstruction and original data divided by the variance of the original data) was always above 86%, both for AEFs and MEFs. The reduction of the amplitude of ERFs after SD is shown in Figure 4.4 (left panels): both for synchronization and syncopation, amplitudes are reduced in the fatigued condition. Furthermore, there is a reduction of amplitude for syncopation compared to synchronization, for the AEFs only in the fatigued condition and for the MEFs only in the control condition.

In addition to the amplitude reduction of the ERFs, the principal modes also revealed changes of ERFs related to movement tempo. While for different ISIs the MEFs did not alter, the AEFs changed considerably. The amplitude of the N1m decreased strongly with decreasing ISIs to disappear almost entirely at an ISI of 500 ms where it converged onto a later component peaking at 180 ms after tone onset. The decreasing strength of the part of the first AEFs' eigenvector corresponding to the fatigued condition might have been caused solely by the decrease of the N1m amplitude in the first five plateaus. To test

this, we finally examined whether the effect of SD on the AEF was indeed only present at long ISIs. For this purpose, two separate PCAs were conducted by dividing the data in subsets containing plateau 1 to 5 and plateau 6 to 10. If the effect of SD was restricted to the N1m component, one would expect the difference due to SD to be only present in the PCA of plateau 1 to 5. Instead, however, the effect was more pronounced in the first principal mode of the subset of plateau 6 to 10.

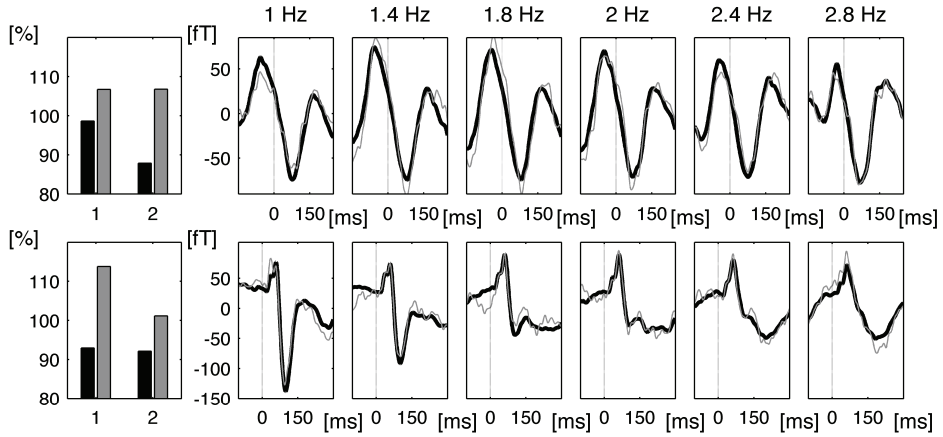

Figure 4.4 *Results of the PCA for the ERFs over all four conditions. Left panels: The strength of the eigenvector in all four conditions at the channels at which the ERFs were maximal (MEF: LT13; AEF: RT32) (1: synchronization; 2: syncopation; black: fatigued; grey: control). Differences between conditions are displayed as percentage change relative to the mean over all four conditions (100%). Right panels: the reconstruction of the first mode in the synchronization, non-fatigued condition at channel LT13 en RT32. Thin line displays the original ERFs. Upper panels: MEFs; lower panels: AEFs.*

4.4 Discussion

In the present study, we examined the effects of SD on MEG activity during performance of an acoustically paced rhythmic force production task. Participants were instructed to either produce adduction forces at the tones (synchronization) or in-between the tones (syncopation). For synchronization, SD resulted in a stronger reduction of the negative asynchrony between the produced forces and the tones at higher movement tempos. Recently, Doumas and coworkers (2005) found a similar reduction of the negative asynchrony in a tapping task after rTMS stimulation of the motor cortex. In line with the suggestion that negative asynchrony reflects a difference in processing times of

somatosensory and auditory information (Aschersleben and Prinz, 1995), they hypothesized that the observed reduction was caused by altered processing of somatosensory input from each tap. Similarly, the present reduction of the negative asynchrony might imply that SD affected the processing of somatosensory information. Contrary to our expectation, SD did not lead to a change in the transition frequency in the syncopation condition. Perhaps, in the present experiment, the difficult syncopation task led to an increase of attention to compensate the detrimental effects of SD, whereas in the aforementioned study of Monno and colleagues (2000) attention was forced away from the coordination task by means of a second dual task.

The effects of SD on MEG activity were twofold and consistent with our expectations. First, across all movement tempos the distribution of MEG power changed markedly. The overall power decreased at occipital and temporal channels and increased at central and frontal channels (cf. Drake et al., 2004), while the alpha band revealed an anterior shift of power towards central channels. This anterior shift might reflect an increase of motor-related mu-rhythm activity above central channels, because the mu-rhythm and occipital alpha activity have similar frequencies (Andrew and Pfurtscheller, 1997). Since desynchronization of mu-rhythm has been associated with a functional alerting of motor areas (Babiloni et al., 1999), the observed anterior shift of alpha power could imply a reduction of this functional alerting of motor areas. An alternative interpretation of the observed changes in MEG activity along the anterior-posterior axis is that the effects of SD are local and pertain mostly to (pre-)frontal areas as these areas are most vulnerable to SD (Horne, 1993). SD is known to reduce the activity specially in the prefrontal cortex (e.g., Drummond et al., 1999) and previously reported sleep-related effects on EEG imaged brain activity have also been interpreted as a result of deactivation of frontal areas (Werth et al., 1996; Atienza et al., 2001; De Gennaro et al., 2001).

Second, the amplitudes of both AEFs and MEFs were attenuated after SD. The decrease of AEF amplitude confirms previous studies (Atienza et al., 2001; Ferrara et al., 2002), although, in contrast to the more traditional focus on the N1-P2 complex, we analyzed the AEF as a whole. N1 is typically related to timing aspects or to onset information of the auditory stimulus (Näätänen and Winkler, 1999), which agrees with the participants' self-reported difficulties in evaluating their performance when sleep deprived. Interestingly, the drop of AEF amplitude was also found at short ISIs for which the typical N1m was no longer present. Apparently, the effects of SD were not restricted to a reduction of the N1m component but also reduced

later AEF components found at shorter ISIs. In addition, we found a decrease in MEF amplitude. In general, motor-related fields observed in motor tasks reflect both motor outflow processes and sensory feedback, but several research groups have shown that the largest MEF component (MEF1) signifies sensory feedback from the periphery (Cheyne et al., 1997; Woldag et al., 2003; Oishi et al., 2004). Amplitude decreases after SD, similar to the ones seen here in AEFs and MEFs, have also been reported for event-related potentials in the visual cortex (Corsi-Cabrera et al., 1999) rendering the fatigue-related drop in amplitude canonical and suggesting that SD might be related with a change of central processing of sensory input.

Besides effects of SD we also found effects of stimulus presentation. The N1m component of the AEF had the largest amplitude at long ISIs and decreased progressively with decreasing ISIs to transform into a later component at an ISI of 500 ms. This effect has been studied in depth and is thought to display the slow refractoriness of the neuronal population producing the N1 responses (Näätänen and Winkler, 1999). Although the separation of MEFs and AEFs appears quite successful, we cannot doubtlessly determine whether the reduction of the N1 amplitude is caused either by attenuation of the underlying neural activity or by a change in timing-related morphology of this component. Indeed, it has recently been shown that the N1 amplitude also depends on motor-related activity (Praamstra et al., 2003), which may have also affected the here reported reduction of N1m amplitude.

In sum, the present experimental findings converge on the interpretation that SD causes a reduced 'responsiveness' of sensory areas to peripheral input. However, to examine the specifics of this general conclusion, future studies are needed that involve larger groups of participants. Such studies may help to uncover the neuronal mechanism(s) that link deactivation of frontal (or other) brain areas with the attenuation of ERF components.

۵.

Amplitude and phase dynamics associated with acoustically-paced finger tapping

Abstract

In this chapter the event-related brain activity associated with the performance of an acoustically paced synchronization task is further examined. The data are from a previously conducted experiment on polyrhythmic performance of drummers (Daffertshofer et al., 2000). To gain insight into the neural dynamics causing the auditory- and motor-related activity, the amplitude and phase dynamics inherent in MEG signals were analyzed across frequency bands. By comparing amplitude and phase dynamics, a distinction was made between so-called evoked and induced responses. Again, PCA was used, this time, however, to compare amplitude and phase changes during mere listening, paced and unpaced tapping. Using PCA allowed for a separation of brain activity related to motor and auditory processes, respectively. Motor performance was accompanied by phasic amplitude changes and increased phase locking in the beta band. Auditory processing of acoustic stimuli resulted in a simultaneous increase of amplitude and phase locking in the theta and alpha band. The temporal overlap of auditory-related amplitude changes and phase locking indicated an evoked response, in accordance with previous studies on auditory perception. The temporal difference of movement-related amplitude and phase dynamics in the beta band, on the other hand, suggested a change in ongoing brain activity, i.e. an induced response supporting previous results on motor-related brain dynamics in the beta band.

Published as: T.W. Boonstra, A. Daffertshofer, C.E. Peper and P.J. Beek (2006). Amplitude and phase dynamics associated with acoustically-paced finger tapping. *Brain Research 109*, 60-69.

5.1 Introduction

To investigate how the nervous system processes information to subserve human functioning, various techniques have been developed to study brain activity. Owing to its good temporal resolution and non-invasive nature, encephalography (EEG and MEG) is a suitable tool for studying information processing sequences in the human brain (Näätänen et al., 1994). By averaging encephalographic signals with respect to an event, brain activity related to cortical processing can be extracted with high signal-to-noise ratio. Recently, further progress has been made in identifying the neural processes associated with event-related activity (e.g., Cheyne et al., 2006; Serrien et al., 2006). In particular, it has become evident that differentiating between amplitude and phase changes allows for a distinction between evoked and induced changes (see Penny et al., 2002, for a review). The primary question governing this line of research is whether event-related components result from a stimulus-evoked activation that is superimposed on the ongoing background activity (evoked response), or whether the ongoing activity is altered by means of changes in amplitude and/or phase (induced response). The latter possibility is of particular interest, as it signifies interactions between response and ongoing brain activity, that is, genuine information processing (David et al., 2005).

Similarly, encephalographic studies on motor behavior showed a shift in focus over the years (cf. Pollok et al., 2006, for a review). Early studies on the neural dynamics underlying action control focused on event-related potentials during motor tasks. A negative potential, the readiness potential, was measured above supplementary motor area prior to movement execution, which was followed by various reafferent potentials (Kornhuber and Deecke, 1965; Cheyne and Weinberg, 1989). More recently, event-related desynchronization (ERD) was found during motor performance (e.g., Pfurtscheller, 1981; Gerloff et al., 1998a) followed by event-related synchronization (ERS) after movement termination (Pfurtscheller et al., 1996), both reflecting other aspects of cortical activation than the readiness potential (Feige et al., 1996). ERD and ERS appear primarily in the beta band (15-30 Hz) and increase with task difficulty (Gross et al., 2005). Motor performance is also accompanied by ERD/ERS in the alpha band (Pfurtscheller and Aranibar, 1979), although the specific temporal and spatial properties of alpha and beta rhythms differ (Crone et al., 1998b; Pfurtscheller and Lopes da Silva, 1999). In fact, induced changes in activity are neither restricted to alpha and beta oscillations nor to motor performance, but have been found across frequency regimes and could be

linked to various functional processes. For instance, gamma activity has often been related to attention (Tiitinen et al., 1993; Fries et al., 2001; Schoffelen et al., 2005).

The rapidly accumulating evidence regarding the functional role of oscillatory activity suggests that different brain processes occur simultaneously in different frequency bands. However, since these activities intermingle continuously and share frequency components, one has to look for additional parameters such as amplitude enhancement, time locking, phase locking, and so on, to further identify the function of specific (oscillatory) brain activities (Basar, 1998; Makeig et al., 2004). Phase locking to stimuli was already demonstrated for auditory responses several decades ago (Sayers and Beagley, 1974; Sayers et al., 1974), but regained interest when it became apparent that differences in event-related amplitude enhancement and (time-) locking of phases may help to discriminate between evoked and induced responses (Makeig et al., 2002; Penny et al., 2002; Fell et al., 2004; Hertrich et al., 2004; Klimesch et al., 2004; Mäkinen et al., 2005). Evoked responses generate simultaneous increases of amplitude and phase locking as they are superimposed on ongoing brain activity. Put differently, evoked responses are simply added onto ongoing brain activity so that the recorded event-related activity just displays the amplitude and phase of the response (apart from the background 'noise'). Because these event-related responses occur at the same instance and with the same phase, they yield simultaneous increases of amplitude and phase locking. In contrast, whenever event-related activities induce separate changes in amplitude and phase locking (i.e. concurrent increases are absent), one can conclude that these activities do not reflect simple evoked responses but a change of ongoing brain activity (induced responses) (Klimesch et al., 2004). Note that we abandon the notion that all phase-locked responses are evoked responses (e.g., Tallon-Baudry and Bertrand, 1999) by differentiating between evoked responses and 'pure' phase resetting, which reflects different underlying neural processes (see above; Penny et al., 2002; Fell et al., 2004; Klimesch et al., 2004; Makeig et al., 2004).

Against this background, we examined the phase and amplitude dynamics in brain activity associated with the performance of an acoustically-paced synchronization task by reanalyzing data collected in an experiment on polyrhythmic tapping involving paced and unpaced unimanual fast repetitive finger movements as control conditions (Daffertshofer et al., 2000b). The primary objective of the study was to differentiate between auditory and motor-related processes by examining the phase and amplitude dynamics in the recorded MEG signals and to classify them in terms of evoked or induced

responses. To this end, we compared phase and amplitude dynamics in various frequency bands. In general, fast repetitive finger movements are accompanied by distinct and thus discernible movement-related fields: a motor field and a post-movement field similar to the cortical fields recorded during single movements (Gerloff et al., 1997; Gerloff et al., 1998b; Mayville et al., 2001; Pollok et al., 2003). Hence, we examined whether finger tapping was also associated with phasic changes in the beta band related with ERS/ERD during single movements. Because metronome pacing might interfere with movement-related activity, particularly due to the sensitivity of MEG to tangential generators (Gerloff et al., 1998b), we first tried to differentiate between brain activity related to auditory and motor processes by means of PCA (Kelso et al., 1992; Daffertshofer et al., 2000a; Mayville et al., 2001; Boonstra et al., 2005b). In view of the aforementioned studies, we expected that motor responses would be predominantly manifested as an integral modification of beta brain activity (i.e. induced responses), whereas auditory responses would be superimposed on ongoing brain activity (evoked responses).

5.2 Methods and Materials

Since the experiment has already been reported elsewhere (Daffertshofer et al., 2000b), we here briefly summarize the most important features instead of providing a full description.

PARTICIPANTS Three right-handed male drummers (between 29 and 34 years of age) participated in the experiment. The experiment was conducted in full compliance with the guidelines of the Medical Ethical Committee of the VU medical center. All participants signed an informed consent form prior to participation.

PROCEDURE Neuromagnetic activity was recorded using whole-head MEG. Participants were seated in a comfortable position (head in helmet, eyes closed) and were instructed to tap with the index finger on the piezoelectric sensors mounted on the armrests. Participants performed three different tasks: listening to an acoustic pacing signal without making any movements, tapping in synchrony with the pacing signal, and tapping without pacing. The two tapping conditions were administered in compound trials, involving a synchronization part (with pacing) and a continuation part (without pacing), as

in the so-called continuation paradigm (Wing and Kristofferson, 1973; Kato and Konishi, 2006). Participants performed the tapping tasks with either the left or the right index finger (during the synchronization part the participants tapped along with auditory stimuli presented on the left or right ear, respectively). The auditory stimuli (duration: 50 ms; pitch: 200Hz left or 400Hz right) were presented at different pacing frequencies (left: 1.2, 1.33, and 2Hz; right: 2 and 3 Hz). Seven trials were recorded per condition; the trials lasted 35 s for listening only and $2 \times 35 = 70$ s for the tapping trials (35 s paced and 35 s unpaced tapping).

DATA ACQUISITION Brain activity was recorded using a 151-channel MEG (CTF Systems Inc., Vancouver, Canada) with 3rd order synthetic gradiometers. Two piezoelectric sensors (∅ 2 cm) were mounted on the armrests to record moments of tap onset simultaneously with acoustic stimuli and MEG. Prior to digitization at a sampling rate of 312.5 Hz, the data were on-line filtered using a 4th order Butterworth low-pass filter at 100 Hz and notch filters at $k \times 50$ Hz.

DATA PROCESSING Auditory- and movement-related fields (ARFs and MRFs) were calculated using tone and tap onsets, respectively, as event-defining indices. This design yielded in total four event-related fields for the three experimental conditions, since in the paced tapping condition both ARFs and MRFs could be defined. Before averaging, MEG data were high-pass filtered (second order Butterworth; cut-off frequency 0.33 Hz). For ARFs and MRFs, epochs were averaged individually for each movement tempo (1.2, 1.33, and 2 Hz for the left index finger and 2 and 3 Hz for the right index finger) and condition (left vs. right; ARFs: listening vs. paced tapping; MRFs: paced vs. unpaced tapping) in an interval from -330 to 330 ms around tone or tap onset. Artifact-contaminated epochs were excluded from averaging. Magnetic field distortions (e.g., elicited by eye movements and blinks) were marked as artifacts if the amplitude of an MEG channel was larger than eight times its standard deviation for the entire trial.

To examine the event-related changes in different frequency bands that might be hidden in event-related fields (cf. Tass, 2004), MEG data (single trials) were band-pass filtered in 10 different frequency bands (band width 6 Hz; overlap 3 Hz) in a range from 0 to 33 Hz. Amplitude and phase changes were examined separately via the analytical signal based on the Hilbert transform (Pikovsky et al., 2001; Bruns, 2004). First, amplitudes of the band-pass filtered data were averaged with respect to tone and tap onsets per movement tempo

and condition (grand average over participants, trials, and epochs) yielding event-related fields, i.e. $\mathrm{amp}(t) \rightarrow \langle \mathrm{amp}(t) \rangle$, where $\langle \cdots \rangle$ denotes the average over epochs. Then, for every frequency band we defined the event-related amplitude (ERF_{amp}, i.e. ARF_{amp} and MRF_{amp}) as the relative deviation of the mean amplitude $\overline{\mathrm{amp}} = {}^{1}\!/_{T} \int^{T} \mathrm{amp}(t)\,dt$, that is, we defined $\mathrm{ERF}_{\mathrm{amp}}(t) = \left\langle \mathrm{amp}(t) - \overline{\mathrm{amp}} \right\rangle / \overline{\mathrm{amp}}$ (the $\overline{\cdots}$ notation indicates an average over time). With this definition we analyzed amplitude changes from the mean amplitude rather than differences from a baseline reflecting a resting state, enabling us to focus on the dynamics within a movement cycle. The resulting values may thus differ slightly from those reported in traditional ERS/ERD studies. Second, to quantify synchrony with respect to the tone or tap onsets, we determined the event-related phase uniformity (ERF_{ph}, i.e. ARF_{ph} and MRF_{ph}) over all events relative to the tone and tap onsets. The phase uniformity, or $\text{circular variance} = 1 - \left| \left\langle e^{i\phi} \right\rangle \right|$ (Mardia, 1972; Fisher, 1993), quantifies to what extent the phase at each time point is similar over different epochs. To obtain large values for narrow phase distributions we used $(1 - \text{circular variance}) = \left| \left\langle e^{i\phi} \right\rangle \right|$ (Mardia, 1972), which is identical to the more recently discussed phase coherence (e.g., Mormann et al., 2000) and formally equivalent to the phase locking index used by Klimesch and colleagues (2004).

In order to differentiate between components related to auditory processes and components related to movement execution or afferent feedback, the $ERFs_{amp}$ and the $ERFs_{ph}$ were analyzed in terms of their principal components (cf. Chapman and McCrary, 1995; Daffertshofer et al., 2000a, Bernat et al., 2005; Boonstra et al., 2005b). PCA[9] can be used for a 'blind source separation' of spatially fixed components from recorded (multivariate) encephalographic data, without the need for a direct specification of the sources' locations (Makeig et al., 1997; Makeig et al., 1999; Hyvärinen et al., 2001; Kayser and Tenke, 2005). For this purpose, we first concatenated the grand averages of different movement tempos yielding time series of $2 \times 207 = 414$ and $3 \times 207 = 621$ samples (the interval from -330 to 330 ms contained 207 samples) for right and left performance, respectively, for every MEG channel. Recall that for every channel we had calculated ERFs after filtering at ten

[9] Here we chose PCA over ICA because PCA results can be easily ranked in terms of the explained variance. However, ICA yielded similar results.

different frequency bands that were combined into a 10-dimensional signal vector. Furthermore, the three different conditions were combined for which we had computed a total of four different event-related fields (two with respect to tone and two with respect to tap onsets). Per channel we thus obtained 4 × 10 time series yielding sets of 151 × 10 × 4 = 6040 ERF-signals. Principal components were calculated separately for left and right side condition $ERFs_{amp}$ and $ERFs_{ph}$ (i.e. a total of four PCAs) and investigated by analyzing the resulting eigenvalue distributions, the spatial modes, and the projected time series. Notice that, due to the aforementioned combination of the four ERFs into a large multivariate signal vector, we addressed both auditory- and motor-related components per single PCA. The discrimination between auditory and motor activity can therefore be made by comparing the parts of the eigenvector belonging to the different conditions, i.e. the presence/absence of specific activity in either the listening or unpaced tapping will suffice to identify the activity as auditory- or motor-related (see Boonstra et al., 2005b, for a similar application of PCA). Hence, for the purpose of identifying such components and illustrating the applicability of the methods, no further statistical analyses are needed (cf. Makeig et al., 1997; Makeig et al., 1999).

Besides studying condition and frequency effects on $ERFs_{amp}$ and $ERFs_{ph}$, we looked for possible (temporal) relations between amplitude and phase uniformity modulations. For this sake, the cross-covariance function between the original $ERFs_{amp}$ and $ERFs_{ph}$ was examined. Recall that the absence of a match between amplitude and phase changes, i.e. an instantaneous covariance at lag zero, renders evoked responses unlikely and thus point to the presence of induced responses (Klimesch et al., 2004).

5.3 Results

In the unpaced tapping condition, participants were able to continue to tap at the required frequency. On average, the tapping frequencies in the unpaced tapping condition were 1.18, 1.33, and 1.99 Hz (left) and 2.00 and 3.07 Hz (right), compared to 1.20, 1.33, and 2.00 Hz (left) and 2.00 and 3.00 Hz (right) in the paced tapping condition. In the paced tapping condition, participants anticipated the stimuli in that tap onsets preceded tone onsets (negative asynchrony; left 1.2 Hz, -17 ms; left 1.3 Hz, -15 ms; left 2 Hz, -14 ms; right 2 Hz, -15 ms; right 3 Hz, -17 ms; note that the anticipation is typically well-pronounced in musically trained participants (cf. Lang et al., 1990; Aschersleben, 2002).

The ARFs in the listening and paced tapping condition yielded comparable fields. The N1-P2 amplitude was reduced at higher pacing frequencies (Fig. 5.1A). Simultaneous with the N1-P2 component, there was an increase in the $ARFs_{amp}$ and $ARFs_{ph}$ in various frequency bands peaking roughly 100 ms after tone onset. The changes were present in a frequency range from 3-15 Hz and were most pronounced in the 3-9 Hz frequency band. At higher pacing frequencies, the increase of the $ARFs_{amp}$ and $ARFs_{ph}$ around 100 ms was reduced, corresponding to the reduced N1-P2 amplitude observed at these frequencies. In contrast, the MRFs were similar across tapping frequencies irrespective of condition (paced and unpaced). These effects of pacing frequency and movement tempo on the ERF amplitudes were consistent with the results of previous studies (Mayville et al., 2001; Boonstra et al., 2005b).

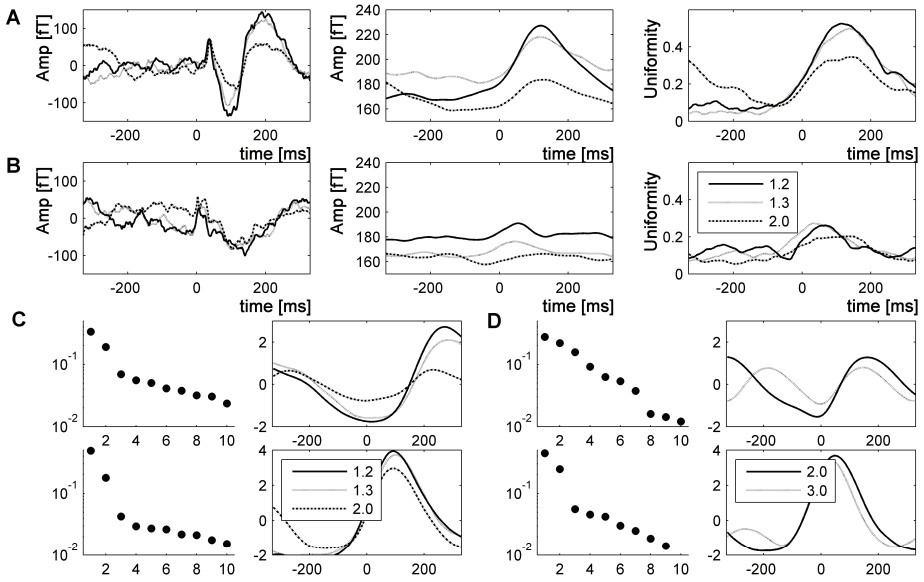

Figure 5.1 *Grand averages of event-related fields: **A**) Grand averages of different types of ARFs for three different tempos in the left listening condition for channel RT22 located above right auditory cortex (left: normal ARF; middle: ARF_{amp} in the 3-9 Hz frequency band (not normalized); right: ARF_{ph} in the 3-9 Hz frequency band). Note that standard CTF channel names are used (cf. Stam et al., 2002, for location of different channels); **B**) Grand averages of MRFs, as for the ARFs, but now for unpaced tapping; **C**) The first 10 eigenvalues and the projections of the first mode for the left side conditions (upper panels: amplitudes; lower panels: phases); **D**) Idem, but now for the right side condition.*

PCA of the ERF_{amp} and ERF_{ph} yielded a substantial reduction of the data to a few major principal modes (Figs. 5.1C and 5.1D): the first two eigenvalues combined always explained more than 50% of the variance. The data reduction was more effective for the ERF_{ph} than for the ERF_{amp} and more effective for the left than for the right side. The projections of the first mode revealed a cyclical change of ERF_{amp} with a minimum around the tap/tone onset and a maximum after about 200 ms (Figs. 5.1C and 5.1D). The projections of the first mode of the ERF_{ph} followed a different pattern showing a decrease in phase variance, which reached a peak between 50-100 ms after tap/tone onset. The projections were rather similar for the left and right condition and across movement tempos, although the cyclical changes of ERF_{amp} were attenuated at higher movement tempos.

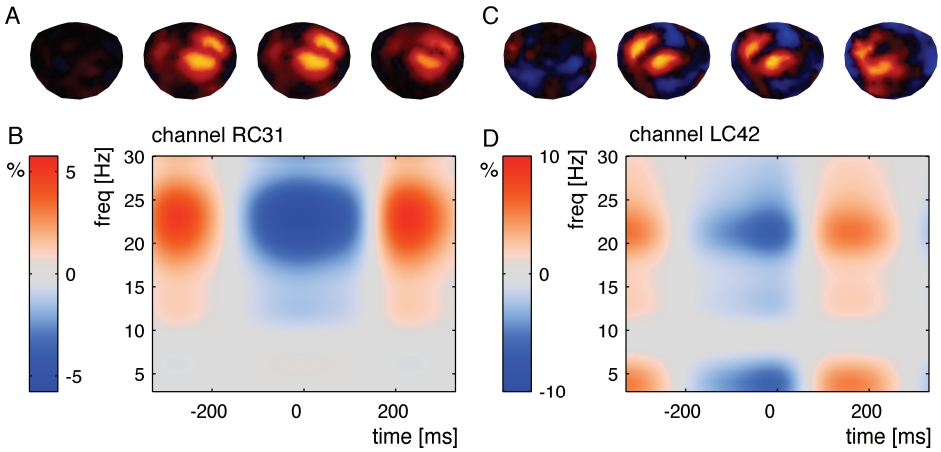

Figure 5.2 *Reconstruction of the first mode of the ERF_{amp}: **A**) Distribution of power in the 18-24 Hz frequency band at 220 ms after tap/tone onset (left side; tempo: 2 Hz; from left to right: listening, paced tapping averaged to tone onset, paced tapping averaged to tap onset and unpaced tapping; yellow, positive coefficients; blue, negative coefficients); **B**) Time-frequency plot of channel RC31 located above right motor cortex (at which the field was maximal) in the paced tapping condition averaged with respect to tap onset; **C-D**) Idem, but now for the right side condition at 2 Hz.*

To further assess the described changes, the first mode was reconstructed by multiplying projections with the first eigenvector. By dividing the resulting matrix precisely as it was concatenated, the different time series belonging to the different frequency bands, channels, and conditions were reconstructed. Figure 5.2 shows the reconstruction of the first mode of the ERF_{amp}, revealing a modulation that was largely confined to the beta band. This modulation of

ERF_{amp} was only present in the paced and unpaced tapping condition and had a dipolar distribution above the contralateral motor area, which indicated that the beta modulation was related to motor performance. The overlap of spatial distributions of beta power (Figs. 5.2A and 5.2C) for paced and unpaced tapping (both averaged with respect to tap onset) was 92% for left and 83% for right condition, whereas the overlap for listening and paced tapping (both averaged with respect to tone onset) was 1% for left and 4% for right condition. Because this pattern was almost identical in the paced and unpaced tapping task, the involvement of auditory processes can be excluded. Despite the large overlap of the spatial distributions between paced and unpaced tapping, the beta modulation was stronger in the paced than in the unpaced tapping condition as revealed by the length of the corresponding part of the eigenvector: 23% (left) and 9% (right) stronger in the paced tapping condition – note that such left/right asymmetries have been reported previously (Pollok et al., 2005).

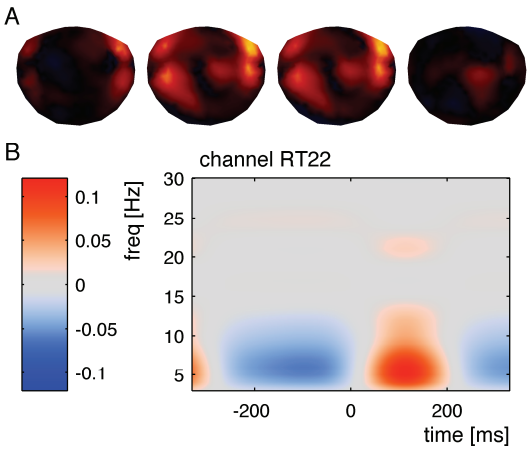

Figure 5.3 *Reconstruction of second mode of ERF_{amp}: **A**) Distribution of power in the frequency band 3-9 Hz at t = 112 ms for left side conditions (tempo: 2 Hz; from left to right: listening; paced tapping averaged to tone onsets, paced tapping averaged to tap onsets and unpaced tapping; yellow, positive coefficients; blue, negative coefficients); **B**) Reconstruction of channel RT22 located above right auditory cortex (at which the field was maximal) in the paced tapping condition.*

As described in the preceding, the ERF_{amp} was minimal at the time of tap/tone onset and peaked after about 200 ms. The strength of the amplitude change was dependent on movement tempo and was stronger at lower movement tempos. The maximal decrease of amplitude in the 21-17 Hz frequency band was -14%, -13%, -5% (paced tapping left; 1.2, 1.3, and 2 Hz, respectively), and -5%, -3% (paced tapping right; 2 and 3 Hz, respectively), compared to -16%, -13%, -5% (left) and -5%, -3% (right) for the unpaced tapping conditions. The maximal increase of amplitude, i.e. around 200 ms

after the tap onset, was 19%, 14%, 5% (paced tapping left; 1.2, 1.3, and 2 Hz, respectively) and 6%, 3% (paced tapping right; 2 and 3 Hz, respectively), compared to 15%, 13%, 5% (left) and 5%, 3% (right) in the unpaced tapping condition (cf. Fig. 5.1C). In the left side condition, the second mode of the ERF_{amp} revealed an amplitude change that occurred mainly in the theta and alpha band. The amplitude peaked 110 ms after the tone or tap onset and displayed two dipolar distributions above the auditory cortices in the listening and paced tapping condition (Figs. 5.3A and 5.3B). The overlap of the spatial distributions of power in the listening and paced tapping condition (both averaged with respect to tone onset) was 71%. Consistent with previous findings (Virtanen et al., 1998; Woldorff et al., 1999), binaural activation patterns were present although acoustic pacing was presented monaurally. The separation of auditory-related fields was less clear in the right side condition where both auditory- and motor-related fields were mixed in mode two and three.

The reconstruction of the first mode of the ERF_{ph} revealed combined effects related to auditory and motor processes. The increase of the ERF_{ph} in the lower frequency bands (3-15 Hz), peaking around 80-100 ms after tone/tap onset, was found only in the auditory-related fields (listening and paced tapping condition averaged with respect to tone onset; overlap of spatial distributions was 94%). This increase in ERF_{ph} had a dipolar pattern above the bilateral auditory areas (Fig. 5.4), which further pointed to a relation with auditory processes. Maximal phase locking values in the 3-9 Hz frequency band were 0.50, 0.47, 0.42 (listening left: 1.2, 1.3, and 2 Hz, respectively) and 0.25, 0.24 (listening left: 2 and 3 Hz, respectively) compared to 0.55, 0.53, 0.48 (left) and 0.40, 0.28 (right) for the paced tapping condition. Thus, auditory-related phase locking appeared to decrease with increasing stimulation rates (cf. Figs. 5.1C and 5.1D). Recall that phase locking values are bounded between 0 (no locking) and 1 (complete phase locking). Simultaneously, a smaller increase of the ERF_{ph} was found in the beta band above the contralateral motor area that was only present in the motor-related fields (paced and unpaced tapping condition averaged with respect to tap onset; overlap of spatial distributions was 92%), indicating a relation with motor performance instead of auditory processing. Maximal phase locking values in the 21-27 Hz frequency band were 0.24, 0.22, 0.20 (paced tapping left: 1.2, 1.3, and 2 Hz, respectively) and 0.30, 0.29 (paced tapping right: 2 and 3 Hz, respectively) compared to 0.22, 0.21, 0.20 (left) and 0.33, 0.28 (right) for the unpaced tapping condition.

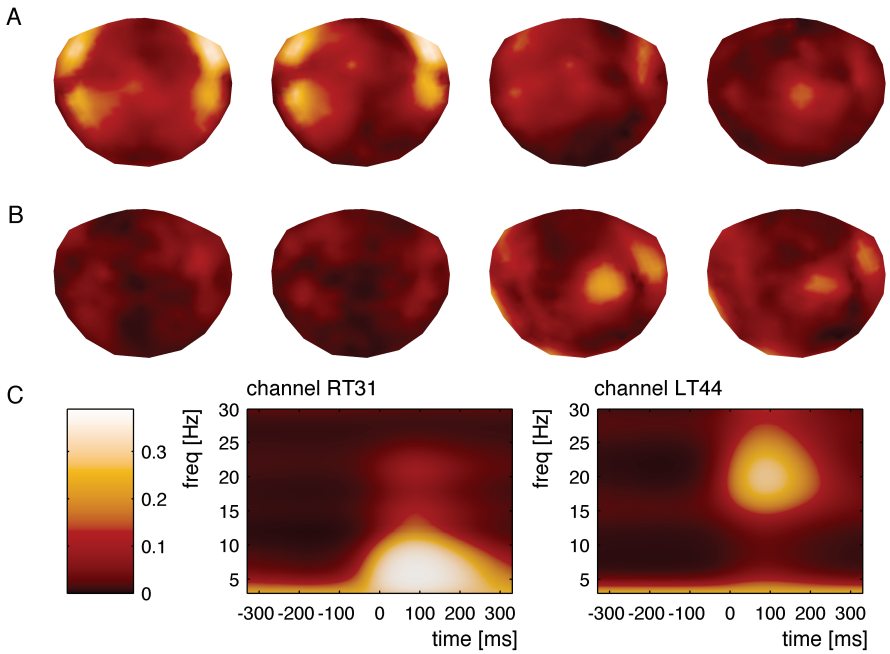

Figure 5.4 *Reconstruction of the first mode of the ERF_{ph}: **A)** Distribution of phase variance for the frequency band 6-12 Hz at 83 ms (from left to right: listening, paced tapping averaged to tone onsets, paced tapping averaged to tap onsets, unpaced tapping); **B)** Idem, but now for the frequency band 21-27 Hz; **C)** time-frequency plot of the channel at which the field was maximal in the paced tapping condition (left: 6-12 Hz, right: 21-27 Hz).*

The cross-covariance between ERF_{amp} and ERF_{ph} showed maxima in two frequency bands in the paced tapping condition (Figs. 5.5B and 5.5D). In the 3-9 Hz frequency band, ERF_{amp} and ERF_{ph} changed concurrently, i.e. the cross-covariance was maximal at a time shift of 0 ms. That peak appeared to be associated with auditory processing because it was solely present in the listening and paced tapping condition and because it was localized above bilateral auditory areas (Fig. 5.5A). It was mainly visible in the 3-9 Hz frequency band and was reduced at higher (alpha) frequencies in which auditory-related changes of ERF_{ph} were also found. Another cross-covariance peak, found in the 21-27 Hz frequency band, was most likely related to motor processing because it was only present in the paced and unpaced tapping condition with a dipolar structure above the contralateral motor area (Fig. 5.5C). This peak, however, was found at a time lag of about 200 ms implying that the increase of the ERF_{amp} followed the ERF_{ph}, i.e. the cross-covariance

was maximal when the ERF_{amp} was shifted 200 ms relative to the ERF_{ph}. Results were similar for different movement tempos and the left and right condition.

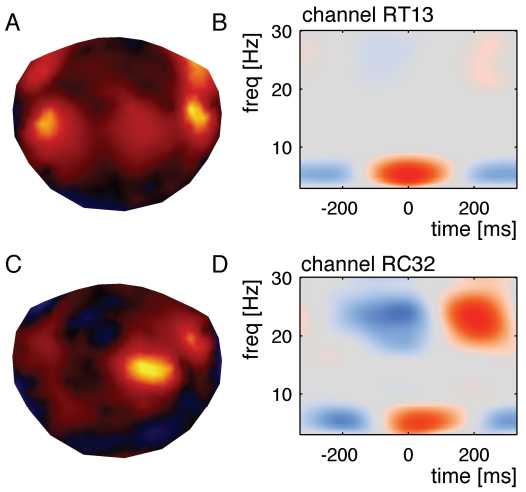

Figure 5.5 *Cross-covariance between ERF_{amp} and ERF_{ph} in the paced tapping condition with the left hand at a tempo of 2 Hz. The time axis refers to the shift in time of amplitude relative to the phase changes. Positive covariance at a positive shift of time therefore implies that the amplitude change followed the phase change in time.* ***A)*** *Distribution of covariance in the frequency band 3-9 Hz at time t = 0;* ***B)*** *Time-frequency plot of covariance at the channel above right auditory cortex at which the field was maximal (red, positive covariance; blue, negative covariance);* ***C)*** *Distribution of covariance in the frequency band 21-27 Hz at time t = 0.19 s;* ***D)*** *Time-frequency plot of covariance at channel RC31 located above right motor cortex at which the field was maximal.*

5.4 Discussion

By analyzing the amplitude and phase dynamics in distinct frequency bands we were able to separate auditory- and motor-related activity during paced tapping and to classify the activity in question as either evoked or induced responses. The simultaneous change in amplitude and phase locking in the theta/alpha band related to auditory performance indicates an evoked response (Klimesch et al., 2004). The temporal difference of movement-related amplitude and phase dynamics in the beta band, on the other hand, suggests a change in ongoing brain activity, i.e. an induced response.

As expected, motor-related activity was mainly manifested in the beta band as a change of event-related amplitude. PCA revealed that, whenever participants tapped (paced or unpaced), dipolar beta activity was clearly present above contralateral motor areas. This dipolar pattern was absent when participants only listened to acoustic stimuli. Hence, we concluded that this

activity was related exclusively to motor performance. The more detailed temporal features of these fields revealed that amplitudes were maximally decreased at the moment of tap onset and then increased rapidly to peak roughly after 200 ms. These findings support current interpretations of ERS and ERD during motor performance as summarized in the introduction (e.g., Pfurtscheller, 1981; Gerloff et al., 1998a), with the proviso that in the present experiment participants moved continuously (i.e. cyclically) and ERS and ERD were related to different phases of movement execution. As such, the continuous change of beta amplitude within a movement cycle contradicts the recent suggestion that event-related beta synchronization would be exclusively linked to the end of a (complex) motor process rather than to the end of (simple) tasks like the production of taps with a single finger (Alegre et al., 2004). Instead, the continuous alteration of beta amplitude seems to suggest that ERD and ERS are not just reflections of movement initiation and termination but subserve distinct functional purposes. Interestingly, Feige et al. (1996) hypothesized that ERD and ERS are independent processes and that ERS may serve to tune (a part of) the network into a different mode of operation.

Next to amplitude effects, we also found changes in phase variance. Rhythmic movements were accompanied by cortical beta activity that was phase-locked with the tap onsets. The corresponding spatial distribution again displayed dipolar activity patterns above contralateral motor areas during both paced and unpaced tapping. The latency for maximal phase locking was about 80 ms after tap onset. Time-resolved covariance analysis revealed that phase locking preceded the amplitude changes in time. Similar temporal differences between amplitude changes and phase locking have been reported before in a study on conscious perception of threshold-intensity somatosensory stimuli[10] (Palva et al., 2005), as well as in a study on late ERP components in a visual oddball paradigm (Fell et al., 2004).

Motor performance was also accompanied with conventional motor-related fields. Although both slow motor-related fields and changes in the beta band could be related to motor performance, they appeared to reflect distinct aspects of cortical activation in accordance with previous results (e.g., Feige et al., 1996; Nagamine et al., 1996). That is, slow components of motor-related fields were invariant against changes in movement tempo as was reported

[10] In this study the increase in phase locking with stimuli was followed by a decrease in amplitude (mainly in the alpha band) that coincided with a motor response suggesting a movement-related desynchronization.

before (Mayville et al., 2001; Boonstra et al., 2005b), whereas amplitude changes in the beta band decreased with increasing movement tempo. The slow motor-related field components reflected activity around the movement frequency and were probably related to efferent and (re-)afferent activity (Gerloff et al., 1997; Gerloff et al., 1998b), whereas the temporal difference between amplitude changes and phase locking in the beta band pointed at induced changes, i.e. changes of ongoing brain activity (Klimesch et al., 2004). Put differently, the delayed covariance ruled out a simple evoked response (see Introduction) and points at non-trivial interactions between input and ongoing brain activity, probably reflecting motor-related information processing, e.g., sensorimotor integration.

Acoustic stimulation resulted in changes in both amplitude and phase dynamics. Event-related amplitude increased in the 3-15 Hz frequency band, i.e. the slow-wave components (Pantev et al., 1991), reaching a maximum around 100 ms after tone onset (cf. Mäkinen et al., 2004) and was accompanied by a similar decrease in phase variance (cf. Sayers and Beagley, 1974; Sayers et al., 1974). Both effects displayed a dipolar pattern above auditory cortices and were only present in the listening and paced tapping conditions. The covariance analysis revealed that the increase of event-related amplitude occurred simultaneously with the decrease of phase variance, reflecting an evoked response (Klimesch et al., 2004). Similarly, Mäkinen and colleagues (2005) showed that the auditory event-related activity underlying the N1m response was generated independently of ongoing brain activity, reflecting an evoked response. The decrease in amplitude changes and phase locking at higher pacing tempos (or shorter inter-stimulus intervals) further matched the decrease in the auditory- related fields (cf. Mayville et al., 2001; Boonstra et al., 2005b). Note that, apart from the here discussed slow-wave components, auditory perception may also be accompanied by gamma band responses, which have been related to cognitive processing of auditory stimuli (Pantev et al., 1991; Joliot et al., 1994; Tallon-Baudry and Bertrand, 1999).

In sum, using event-related frequency analyses we succeeded in pinpointing amplitude and phase effects within a movement cycle. PCA enabled us to discriminate between different conditions, that is, to separate auditory- and movement-related activity. While the power of auditory-related activity was primarily present at lower frequencies and located above auditory cortices, movement-related activity was found above motor areas with maximal amplitude changes in the beta band. The subsequent analyses of the corresponding phase distributions enabled us to distinguish between evoked and induced responses supporting earlier findings: the simultaneous changes

related with auditory processing suggest an evoked response, whereas the temporal difference in amplitude and phase changes related to motor performance points at a change of ongoing brain activity, i.e. an induced response. As described in the introduction, evoked and induced responses correspond to rather different forms of brain dynamics, as the former reflect activity added onto ongoing brain activity whereas the latter reflects a change of ongoing brain activity.

In this regard, we would like to remark that the motor-related phase resetting in the beta band is particularly interesting as it may provide an additional mode for information processing and communication using oscillatory brain activity by means of frequency modulated and phase-locked interactions (e.g., Salinas and Sejnowski, 2001; Foffani et al., 2005). If two or more neural clusters are considered as self-sustaining oscillations that are weakly coupled, information can be exchanged via phase modulations (Hoppensteadt and Izhikevich, 1998; Breakspear et al., 2003; Tass, 2004). From this perspective, one might speculate that motor-related phase resetting in the beta band might relate to an information exchange between cortical and subcortical brain areas (Riecker et al., 2003). In fact, pyramidal tract stimulation has been shown to cause cortical phase resetting in the beta band (Jackson et al., 2002). Although a unique neural source of beta phase resetting has proven difficult to find (if it exists at all), its functional role for the control of motor behavior can be investigated by varying task parameters. The present study pursued this idea and showed that the modulation strength of beta amplitude seemed to decrease with increasing movement tempo. However, future studies are needed to address this issue in more detail.

6.

Multivariate time-frequency analysis of electromagnetic brain activity during bimanual motor learning

Abstract

The analysis method presented in the previous chapter is used further to examine the changes in neural synchronization during motor learning. To this end, MEG and EMG activity was recorded while participants learned to perform a 3:5 polyrhythm. As this task involved bimanual rhythmic activity at distinct movement tempos, it was expected to elicit neural activity in bilateral motor cortices that could be readily disentangled. Building on the results of Chapter 5 regarding motor-related fields, synthetic aperture magnetometry (SAM) analysis was used to focuse on the beta band to separate bilateral activity in both motor cortices. On a behavioral level, performance converged onto the to-be-learned 3:5 polyrhythm in the course of the experiment. The SAM-based reconstruction of the activity of the motor cortices revealed phasic changes in beta activity related to force production of the contralateral finger. The degree of beta modulation increased during the experiment and was positively correlated with motor performance, in particular for the motor cortex contralateral to the slow hand. These findings support the view that activity in motor cortex co-varies closely with behavioral changes in the course of learning.

Published as: T. W. Boonstra, A. Daffertshofer, M. Breakspear, P. J. Beek (2007). Multivariate time-frequency analysis of electromagnetic brain activity during bimanual motor learning. *NeuroImage 36*, 370-377.

6.1 Introduction

Motor performance typically improves with repetition and practice. One would expect that the proficiency in a motor task requires a modulation of cortical motor output to accommodate the newly acquired ability. For the modulation of cortex output, the plasticity of the brain appears vital as it enables the neural system to reorganize and adapt to improve motor control. Indeed, skill acquisition is accompanied by changes in metabolism using functional imaging techniques (Schlaug et al., 1994; Karni et al., 1998; Toni et al., 1998), primarily indicating a reorganization of motor areas. Although the reorganization of cortical structures is generally thought to depend on, or to be caused by, changes in electromagnetic neural activity, relatively little is known about specific changes in neural activity during motor learning.

Locally synchronized behavior of neural assemblies yields fluctuations in local field potentials that can be measured using EEG and MEG (Lopes da Silva, 1991; Nunez, 1995). Using these techniques, motor performance is usually found to be accompanied by beta activity, i.e. oscillatory encephalographic activity in a frequency range of about 15 to 30 Hz. Above contralateral motor areas the amplitude of this beta activity decreases during motor performance and increases after movement termination, referred to as event-related desynchronization (ERD) and synchronization (ERS), respectively[11] (Pfurtscheller, 1981; Feige et al., 1996; Pfurtscheller et al., 1996; Crone et al., 1998b; Gerloff et al., 1998a; Pfurtscheller et al., 1998; Doyle et al., 2005). The significance of beta activity in motor performance has been further underscored by studies on cortico-muscular synchronization in the beta band recorded during constant force production (Conway et al., 1995; Salenius et al., 1997; Gross et al., 2000; Kilner et al., 2000; Mima et al., 2000). Apart from submitting a central role of beta activity per se, these results suggest that beta (de-)synchronization can serve as an effective mechanism of motor control, or in the least provides a direct index of such a mechanism (cf. Farmer, 1998).

In the present study we examined changes in cortical activity during the acquisition of a new, demanding motor skill: a bimanual 3:5 polyrhythm. Polyrhythmic or multi-frequency performances are particularly useful for studying motor learning as the degree of difficulty can be easily manipulated

[11] There is an inference concerning the coherence of neurons which we do not measure here. We are aware of this, but prefer to follow convention for the purpose of relating the findings to the established literature.

by altering task demands (Peters, 1985; Summers et al., 1993a; Peper et al., 1995b; Monno et al., 2000). When examining the accompanying brain activity, polyrhythmic performance allows for an immediate separation of activity originating from the bilateral motor cortices due to the obvious difference in movement frequency between fingers or hands (Daffertshofer et al., 2000b). As with motor performance in general, rhythmic movements are also accompanied by changes in cortical beta amplitude (Toma et al., 2002; Boonstra et al., 2006; Daffertshofer et al., 2007). Hence we used this amplitude modulation to localize sources and reconstruct their time-dependent signals using synthetic aperture magnetometry (SAM) (cf. Cheyne et al., 2006; Houweling et al., 2007). SAM is a so-called beamformer technique that stresses signals originating from a certain region while suppressing residual activity from all other locations. In the present study SAM enhanced our focus on motor-related activity by suppressing activity related to other processes, e.g., activity caused by auditory pacing. The resulting signals were further studied via their event-related power (Boonstra et al., 2006) in order to identify learning-specific spectral changes in cortical activity. To achieve this, we employed PCA in the form of partial least squares (PLS) (McIntosh and Lobaugh, 2004) to quantify the co-variation between cortical activity and motor performance during motor learning

6.2 Methods and Materials

Nine participants (mean age: 28.5 years, range: 23-44, 7 male, 2 female) with no previous musical education took part in the experiment. Eight participants were self-reported right-handers. The experiment was conducted in full compliance with the guidelines of the medical ethical committee of the VU University medical center. All participants signed an informed consent form prior to participation.

Participants were instructed to produce isometric forces by flexing left and right index fingers at a frequency ratio of 3:5 (cf. Fig. 6.1). To assist this difficult, bimanual performance, both hands were paced by auditory stimuli presented ipsilaterally using earphones (50 ms duration; pitch: 600 Hz fast finger, 400 Hz slow finger; EARTone 3A, Cabot Safety Corporation). The inter-stimulus interval of the pacing signal was 900 ms for the fast and 1500 ms for the slow finger (or 1.11 and 0.67 Hz, respectively). Participants performed two blocks of six trials each: in one block the right finger produced the fast and

the left finger the slow frequency and in the other block frequencies were swapped from left to right. The order of blocks was counterbalanced over participants. To optimize performance, a block always started with a trial in which participants were only required to listen passively to the rhythm. This was followed by five trials in which they were instructed to perform the polyrhythm to the best of their ability. Each trial lasted 45 s and consisted of ten complete rhythmical cycles, yielding a total of 50 and 30 stimuli for the fast and slow finger, respectively. Trials were interspersed by 15 s breaks during which participants received visual feedback about their performance. To achieve this, the produced force pattern averaged over the ten cycles was displayed in combination with the auditory pacing signal.

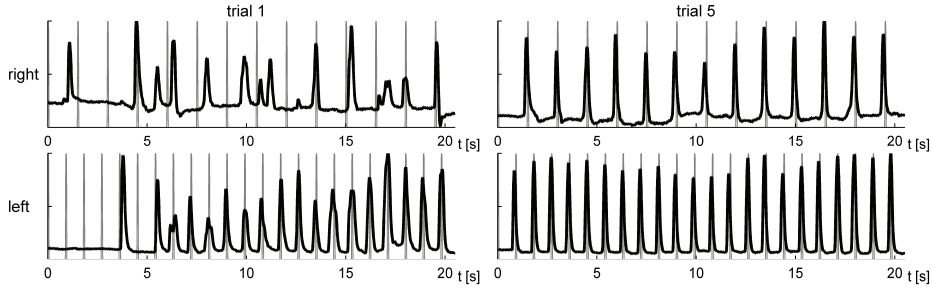

Figure 6.1 *Force traces of a single participant performing the 3:5 polyrhythm with the fast rhythm on the left side. Left panels show the first 20 seconds of the first trial, i.e. the first encounter with the 3:5 polyrhythm. The upper panel shows the force of the right finger (black line) and the auditory pacing signal (grey line); lower panel is identical but displays the left side. Clearly this participant did not perform the proper polyrhythm during trial 1 (see the slow, right hand). Right panels show the first 20 seconds of trial 5 after the participant had successfully learned the polyrhythmic performance.*

Brain activity was recorded using a 151-channel MEG (CTF Systems Inc., Vancouver, Canada) with 3rd-order synthetic gradiometers. One channel was not operational so that, effectively, 150 MEG signals were analyzed. The surface EMG was recorded from the flexor digitorum superficialis of both arms; electrodes (Ag-AgCl; ∅ 1 cm) were placed in a bipolar montage with an inter-electrode distance of approximately 1 cm. The voltages of both MEG-compatible force transducers (Boonstra et al., 2005a; Appendix B) and acoustic stimuli were simultaneously sampled. All signals were low-pass filtered at 415 Hz prior to digitization at a rate of 1250 Hz.

Motor performance was assessed by the frequency relationship between the force productions of both fingers. For this sake we determined the power spectra of the force signals using Welch's periodogram method with Hamming windows of 13.5 s, i.e. the first cycle of each trial was omitted to eliminate transient behavior and the next nine cycles were divided into three consecutive segments of three movement cycles. The frequency relationship was determined using a rescaled cross-spectral overlap (Daffertshofer et al., 2000b) measuring the common spectral characteristics of fast and slow fingers after rescaling the frequency axis of the slow finger. More specifically, the overlap of the power spectra at a scaling factor of 3 : 5 = 0.6 was used to quantify the extent to which participants were performing the proper polyrhythm. The rescaled cross-spectral overlap was computed for each individual segment for scaling factors ranging from 0.1 to 2 in steps of 0.003.

EMG signals were high-pass filtered using a second order Butterworth filter to eliminate movement artifacts (cut-off frequency, 20 Hz) and normalized to unit variance to correct for individual differences in signal strength. Next, EMGs were further full-wave rectified using the Hilbert transform (Myers et al., 2003).

Sources of cortical activity were defined from the MEG data by means of SAM, which defines a spatial filtering technique based on a nonlinearly constrained minimum-variance beamformer (Vrba and Robinson, 2001; Gaetz and Cheyne, 2006). Volumetric source images were generated by applying SAM to each voxel in the region of interest (5 mm voxel resolution) defined via an average MRI (International Consortium of Brain Mapping, ICBM). Focusing on beta ERS/ERD, we filtered the signals (band-pass frequency, 15-30 Hz) prior to computing covariance matrices (cf. Taniguchi et al., 2000). The SAM analysis was based on a comparison of beta activity between active and control states. Because cortical beta activity decreases during force production and increases afterwards, the active state was defined as time interval intervals of -200 to 200 ms relative to maximally produced force and the control state as the interval of 200 to 600 ms. Using the pseudo-T differences, a statistical parametric image was computed and single-trial time series (virtual sensors) were reconstructed for the peak location of activity in these images, enabling analysis of source activity as a function of time. Event-related power of these reconstructed source data and the EMG data were determined using a continuous wavelet transform that was applied to single trials. We used

complex Morlet wavelets[12] at 1 Hz intervals in the 5 to 45 Hz range (cf. Duzel et al., 2003). The SAM source data were normalized to unit variance. The wavelet transform yielded complex wavelet coefficients whose squared modulus specified the signals' time-dependent power at distinct frequencies. Power values were averaged with respect to the motor output, i.e. force maxima, separately for different data segments, trials, participants and sides, resulting in 3 × 5 × 9 × 2 = 270 time-resolved power spectra for each of the four channels (2 × EMG and 2 × MEG).

Statistical analyses of the frequency coupling of motor output and time-frequency decompositions of EMG and MEG data were realized with PCA in its capacity to extract major components from multivariate signals (see Appendix A). Notice that PCA can be seen as the basis of several other multivariate data analysis methods such as PLS (McIntosh et al., 1996; Lobaugh et al., 2001), whereby it is restricted to the brain-behavior covariate matrix. In these terms, our application of PCA matched McIntosh and Lobaugh's spatiotemporal task PLS with mean centering (McIntosh and Lobaugh, 2004). In detail, we combined data of different conditions into a single matrix with (*number of observations* × *number of conditions*) rows and (*number of signals* × *number of samples*) columns. In all analyses, the number of observations was 3 (consecutive segments) and the number of conditions was *trials* × *side* × *participants* = 5 × 2 × 9 = 90. The performance-related signals of the fast and slow hands were pair-wise combined in order to compare the time-frequency signals of both left and right conditions. The number of elements and samples differed across analyses: for the rescaled cross-spectra there were 634 samples and 1 element, whereas for the wavelet spectra there were 1876 samples (1.5 s at 1250 Hz) and 41 elements (frequencies). Singular values of all seven matrices (2 × EMG, 2 × MEG, 3 × cross-spectra) were computed, yielding 90 eigenvalues with corresponding eigenvectors for each matrix. Apart from the first eigenvector all other eigenvalues were rather small so that we could restrict the subsequent analyses to the first mode in all PCAs. We further projected the data onto the first eigenvector to determine the time-frequency changes that were covered by the

[12] Similar to the more common Gabor transform, a complex Morlet wavelet includes a sliding Gaussian window of width a, which defines time scales or a certain frequency band around a central frequency f_o. It reads

$$w(t,a) = \sqrt{\frac{1}{\pi a}} \exp\left\{-\frac{t^2}{a}\right\} e^{2\pi i f_o t}$$

in which t is time and i denotes the complex unit.

first principal mode. Finally, multiplying these projections with the data yielded a matrix of so-called *brain scores* that were used to indicate the variation of task effects across observations, conditions, and participants (McIntosh and Lobaugh, 2004).

For the subsequent statistical assessment of the so obtained principal modes we used a repeated measure ANOVA. Instead of testing for significance of principal modes against a null distribution with, e.g., permutation testing, jackknife, or bootstrapping estimates, we tested whether the variance of test effects was significantly different ($p < 0.05$) between conditions. In other words, we compared eigenvector coefficients of the first modes by performing a two-way ANOVA (*trial* × *side* = 5 × 2) with repeated measures. To address possible transfer effects of learning between sides, we added a between-subject variable *order* denoting whether a participant started the experiment either in the right or left side condition. Finally, to test whether changes in motor performance were directly related to changes in event-related power, we compared the *brain scores* of the frequency coupling of the force signals with those of the time-frequency power of the SAM channels by means of conventional Pearson correlations for individual participants. For subsequent group analysis, the correlation coefficients were Fisher-transformed and tested for significance using a one-sample T-test.

6.3 Results

Analysis of motor behavior

Participants clearly learned the desired motor task (cf. Fig. 6.1). Their performance improved as signified by the convergence of the frequency locking between the force productions of both fingers towards the 3:5 polyrhythm. PLS analysis of rescaled cross-spectral overlaps extracted the 3:5 frequency locking in the first mode, which represented 88% of the variance (Fig. 6.2A, left panel). Apart from a peak at $3 : 5 = 0.6$, the analysis also revealed small peaks at 0.3 (= 3 : 10) and 1.2 (= 6 : 5), i.e. at a higher harmonic and a subharmonic, presumably because the signals were not perfectly sinusoidal. As is evident from the right panels of Fig. 6.2A, the coefficients of the first eigenvector showed a significant increase in 3:5 frequency locking strength over trials ($F(4,28) = 11.9$, $p < 0.001$). The coefficients further revealed that participants who initiated the protocol with the fast frequency on the right side displayed a weaker frequency locking during that condition (Fig. 6.2A, most right panel), which was confirmed by a significant effect of *side* ($F(1,7) =$

9.96, $p = 0.016$) and a significant *side* × *order* interaction ($F(1,7) = 44.1$, $p < 0.001$). In that condition, the improvement in performance over *trials* was stronger than in the other conditions ($F(4,28) = 3.90$, $p = 0.012$). The improvement in performance was mainly due to improved timing of the slow finger, that is, the fast hand followed the fast pacing signal almost correctly from the start of the experiment (cf. Fig. 6.1 and Summers et al., 1993b).

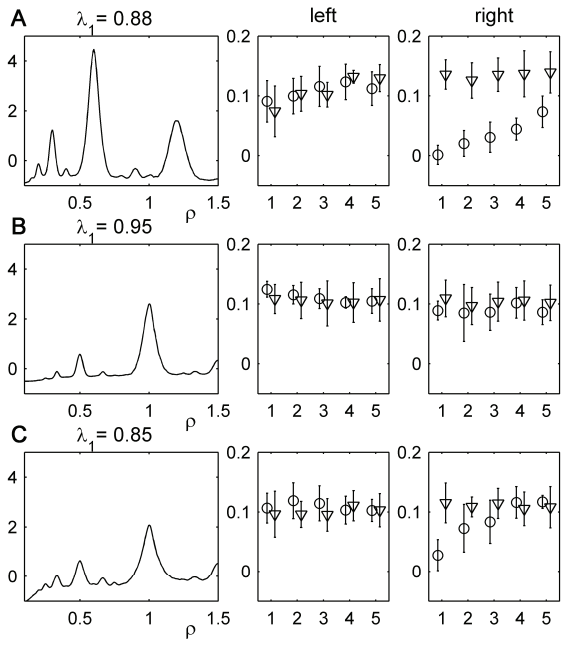

Figure 6.2 *Projections and eigenvectors of the first mode of PLS analyses of the frequency locking spectra: **A**) First PLS mode of frequency locking between the force production of the left and right side. Left panel: projection of the first mode revealing a peak in the frequency locking at 0.6 (3:5); the first mode explained 88% of the total variance. Right panels: eigenvector coefficients for trial 1 to 5 in both conditions (left: fast rhythm on left side; right: fast rhythm on right side). Circles refer to participants that started with the fast frequency on the right hand and triangles to participants that started with the fast frequency on the left side (error bars indicate the between-subject standard deviation); **B**) First PLS mode of frequency-locking between force production of the fast hand and the fast pacing signal explaining 95% of the variance; **C**) First PLS mode of frequency-locking between force production of the slow hand and the slow pacing signal explaining 85% of the variance.*

The frequency locking between the fast finger and the fast pacing signal revealed a 1:1 frequency locking (Fig. 6.2B, left panel), and the strength of this frequency locking remained by and large constant during the experiment (see eigenvector coefficients in Fig. 6.2B, right panels). The steady performance of the fast finger was also underscored by the absence of any significant effect in the ANOVA. The slow finger, on the other hand, showed an obvious change in performance over trials as revealed by the frequency locking strength with

the slow pacing signal: frequencies were locked at a 1:1 ratio throughout the experiment, but the locking strength increased over trials (Fig. 6.2C). The ANOVA of the corresponding eigenvector coefficients showed a significant effect of *trial* ($F(4,28) = 3.15$, $p = 0.029$) and a significant *trial* × *order* interaction ($F(4,28) = 2.92$, $p = 0.039$), implying a stronger increase over trials for participants starting with the right finger at the fast frequency. Finally, a significant three-way interaction between *trial*, *side*, and *order* ($F(4,28) = 6.24$, $p = 0.001$) demonstrated that the strongest increase in performance occurred in the right side condition of participants that started with the fast frequency for the right side (cf. Fig 6.2C, right panel, circles).

Analysis of brain data

SAM analysis revealed a clear event-related decrease in beta power originating from the contralateral motor cortex. The maximal pseudo-T values averaged over participants were 10.6 and 11.1 for the left and right motor cortex, respectively (Fig. 6.3).

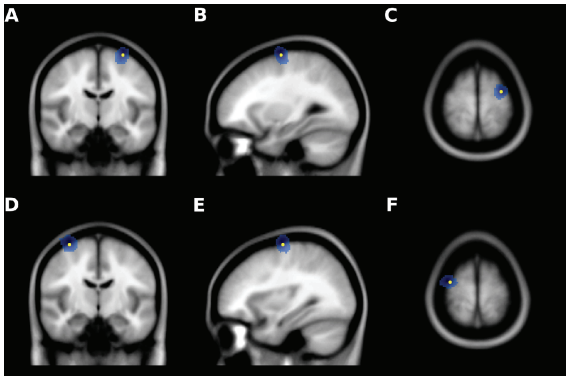

Figure 6.3 *Results of the SAM analysis: upper panels show the most prominent virtual channel (average pseudo-T, 11.1) when participants produced forces with their left index finger in coronal image **A**, sagittal image **B**, and axial image **C**; lower panels display the same information for the right index finger (average pseudo-T, 10.6). Coronal and axial views show left on left.*

As displayed in the time-frequency plots of Figures 6.4C and 6.4D, the wavelet power of the rectified EMG showed a broadband increase peaking about 100 ms before the maximum force output. Neither the force trajectories nor the change in EMG power changed across conditions as revealed by the corresponding eigenvector coefficients (Figs. 6.4A-6.4D, right panels). The event-related wavelet power of the reconstructed source data of both motor cortices revealed a clear modulation of power in the beta band with the maximum increase between 20 and 25 Hz (Figs. 6.4E & 6.4F). The beta power was inversely related to the produced force in that it was minimal during maximum force production and increased when the force decreased again.

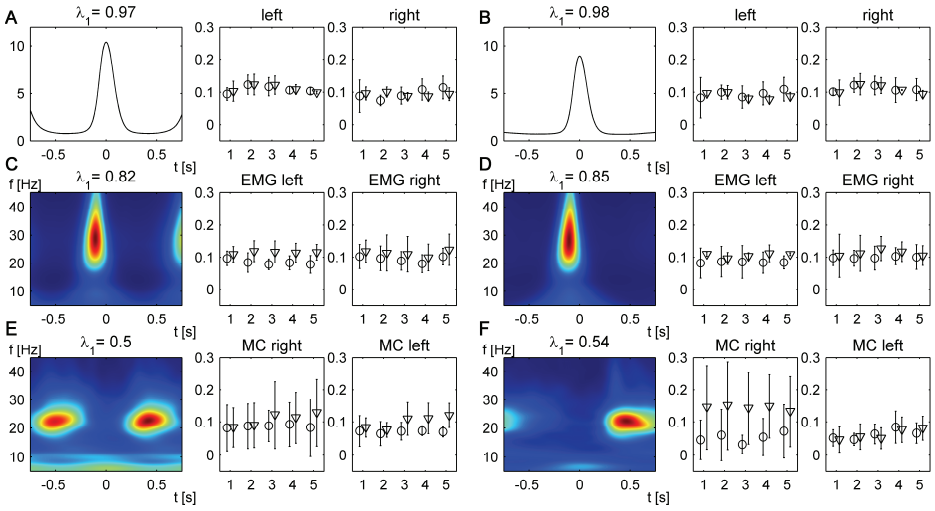

Figure 6.4 *Projections and eigenvectors of PLS analyses: **A**) First mode of PLS of the force trajectories of the fast hand averaged with respect to the force maxima explaining 97% of the variance. Left panel shows the projection and the right panels show the eigenvector coefficients of the corresponding conditions. Circles refer to participants that started with the fast frequency on the right hand and triangles to participants that started with the fast frequency on the left side (error bars indicate the between-subject standard deviation; x-axis, time in second; y-axis, force output); **B**) First PLS mode of the force trajectories of the slow hand explaining 98% of the variance; **C**) First PLS mode of the event-related wavelet power of the EMG of the fast hand explaining 82% of the variance. Left panel shows the time-frequency plot corresponding with the projection (red: increase in power, blue: decrease in power; x-axis, time in seconds; y-axis, frequency in Hz) and the right panels show the corresponding eigenvector coefficients; **D**) First PLS mode of the event-related wavelet power of the EMG of the slow hand explaining 85% of the variance; **E**) First PLS mode of the event-related wavelet power of the reconstructed source data of the contralateral motor cortex of the fast hand explaining 50% of the variance; **F**) First PLS mode of the event-related wavelet power of the reconstructed source data of the contralateral motor cortex of the slow hand explaining 54% of the variance.*

In the motor cortex contralateral to the fast finger the increase in beta power peaked around 400 ms after the force maximum (Fig. 6.4E), while in the motor cortex contralateral to the slow finger the increase occurred slightly later, at about 500 ms (Fig. 6.4F). The modulation of beta power was noticeably related to the force production of the contralateral hand as the event-related power

revealed no evident pattern when averaged with respect to the force maxima of the ipsilateral hand (results not shown here).

Analysis of brain-behavior covariates during motor learning
The eigenvector coefficients revealed a significant increase of the modulation of event-related beta power over trials both for the motor cortex contralateral to the fast ($F(4,28) = 5.17$, $p = 0.003$) and the slow finger ($F(4,28) = 4.17$, $p = 0.009$), suggesting a relationship with motor performance (Figs. 6.4E and 6.4F, right panels). The ANOVA revealed no other significant effects. The direct comparison with the bimanual performance score, i.e. the Pearson correlation between brain scores of frequency locking in individual data segments and brain scores of event-related power in the motor cortices, showed that beta modulation was indeed positively correlated with motor performance. For the motor cortex contralateral to the fast finger the correlation was significant for two out of the nine participants (mean correlation: 0.13 ± 0.23), but grouped over all participants the correlations coefficients did not differ significantly from null ($T(8) = 1.70$, $p = 0.127$). For the motor cortex contralateral to the slow finger the correlation was significant for four out of the nine participants (mean correlation: 0.29 ± 0.30) and grouped over all participants the correlations differed significantly from null ($T(8) = 2.91$, $p = 0.019$).

6.4 Discussion

We studied learning-related changes in cortical activity during isometric, bimanual force production, coordinated as a 3:5 polyrhythm. Motor learning was evidenced as improved performance of the polyrhythm with practice, as quantified via the strength of frequency locking between the fingers' force trajectories that increased at the 3:5 target ratio. The degree of beta modulation was directly correlated with the behavioral outcome, especially for the motor cortex contralateral to the finger performing the slow component of the polyrhythm. Put differently, our results clearly indicated that when participants learned to perform the bimanual polyrhythm, the accompanying event-related beta modulation was enhanced, in particular in the contralateral motor cortex of the more-difficult-to-adjust end-effector, here, the slow finger. Hence, these data suggest that motor learning was associated with a change in neural activity in cortical motor areas that differed across hemispheres. This suggestion is consistent with the insight gleaned from behavioral data that

learning a polyrhythm is achieved by interleaving the timing of the slow hand into that of the fast hand (Summers et al., 1993a).

When moving voluntarily, neurons in the motor area have been proposed to shift from an activated state (~ERD) to a resting state (~ERS) following movement termination, or from a processing to an idling mode (Pfurtscheller et al., 1996). We have shown that this idea finds principal support during rhythmic motor production, as was also reported before (Toma et al., 2002; Boonstra et al., 2006). That is, beta amplitude was relatively lower during individual motor events and increased in between such movements (Fig. 6.4). Importantly, however, rhythmic movement lacks movement termination as participants are in a continuously active motor state. Hence, we here submit that event-related beta synchronization is probably unrelated to movement termination. To strengthen that argument we note that post-movement beta rebound often exceeds the level of beta activity during rest and decreases back to base level 1 s after movement termination (Jurkiewicz et al., 2006). This suggests that event-related beta synchronization does not just reflect a passive shift back to a resting state, but is likely to have a more active role, such as active immobilization or inhibition of cortical networks (Salmelin et al., 1995; Cassim et al., 2001; Pfurtscheller et al., 2005).

We analyzed the interdependence of brain and behavior via PLS, i.e. using the statistical co-variation between signals. Using this measure the causality in the relation between brain and behavior cannot be determined. To do so, we examined phase synchronization between MEG and EMG but failed to pinpoint a statistically significant coupling. Indeed, the absence of cortico-muscular synchronization is in line with other studies reporting vanishing synchronization during dynamical movements (Kilner et al., 2000). Likewise, the presence of enhanced beta modulation during motor learning that we report is compatible with other studies on altered cortical activity during motor skill acquisition (Recanzone et al., 1992; Pascual-Leone et al., 1994; Sanes and Donoghue, 2000). Our results also complement reports on enhanced event-related alpha desynchronization during (implicit) motor learning (Zhuang et al., 1997), increased cortico-spinal beta synchronization following visuo-motor skill learning (Perez et al., 2006) and increased interhemispheric synchronization during the early stage of bilateral learning (Andres et al., 1999). Taken together, these findings suggest that the change in beta modulation reflects a reorganization of neural activity in the motor cortex during skill acquisition. Interestingly, one finds a general consensus that event-related beta synchronization is, at least primarily, generated in the contralateral motor area located anterior to the central sulcus (Salmelin et al., 1995;

Jurkiewicz et al., 2006) or near the postcentral sulcus (Parkes et al., 2006). Notice that our focus on activity in the primary motor cortex was not meant to imply that activity in other brain areas was not altered in the course of motor learning. Several studies showed various changes in, for instance, supplementary motor areas, premotor cortex, and singulate motor cortex (Sadato et al., 1997; Debaere et al., 2001; Schaefer et al., 2005). Here we simply have to conclude that these areas did not display significant changes in the frequency regimes under study. That is, concentrating on the beta band primarily extracts activity in primary motor areas.

7.

Epilogue

7.1 Neural synchronization in human action control

What insights did we gain from the present series of experiments into the neural implementation of motor control? Or, more specifically, which dynamical characteristics along the neural axis appeared relevant for proper motor functioning and how were these affected by physiological and cognitive factors? Before answering these questions, it is useful to first recapitulate the theoretical framework that was introduced in Chapter 1, allowing me to discuss more general features of the experimental findings within this framework.

In Chapter 1 a searchlight theory was put forward promoting a rigorous focus on change: *panta rhei*. That theory belongs to a longstanding tradition in science in which processes rather than structures are considered fundamental. In neuroscience, 'structure-oriented' translates into network topology and structural anatomy, whereas 'process-oriented' refers to neural dynamics and the functioning of cells and cell networks. Surely, the spatial aspects of neural organization are important for understanding neural motor control, e.g., by pinpointing the neural structures that contribute to specific aspects of motor control. As explained in Chapter 1, the spatial organization also constrains the interacting processes within and between these structures. However, it is the information transfer through these interactions that defines neural functioning. In my thesis I therefore investigated motor-related information processing with a focus on temporal aspects of neural activity. To this end, measurement and analysis techniques were employed that allowed for extracting temporal features of neural activity patterns, as well as changes therein as a function of experimental manipulations. In this manner, dynamical aspects of the neural underpinnings of motor control were uncovered, which are complementary to the insights garnered in more structure-oriented approaches. As the specific outcomes were already discussed in the individual chapters, I only briefly reiterate the main findings and discuss their impact for the understanding of brain dynamics in general.

A first compelling feature of the data is the omnipresence of synchronization in neural dynamics during the execution of motor tasks. In particular, two distinct synchronization patterns stood out across experiments: the 10 Hz synchronization between bilateral EMG reported in Chapters 2 and 3 and the beta modulation above the contralateral motor cortex observed in Chapters 4 to 6, with the proviso that the beta modulation in the experiment of

Chapter 4 was reported elsewhere (Daffertshofer et al., 2007). This ubiquity of synchronized activity was anticipated from the perspective of complex dynamical systems that was put forward in Chapter 1. In general, the brain is considered an open system consisting of a huge number of interacting units. Collectively, these units generate neural activity that, dependent on the dynamical context, is shaped by underlying attractors that may be static, periodic, quasi-periodic or strange. My experimental results support that oscillatory dynamics is a fundamental mode of operation of meso-scale activity during motor performance. By this I mean that oscillatory activity in specific regions of the central nervous system was found across various frequency bands that could be related to distinct aspects of motor control. Moreover, neural synchronization was consistently modulated by various task parameters, in line with the alleged functional role of neural synchronization. For instance, the 10 Hz bilateral MU synchronization increased with fatigue pointing at increased bilateral coupling and cortical beta modulation was affected by movement tempo, force level (Daffertshofer et al., 2007), and learning. Although strictly speaking these findings do not prove a functional role of neural synchronization as only correlations between synchronization and aspects of motor control were reported, they are fully compatible with this notion. Indeed, synchronization appears to be a hallmark of the neural dynamics of motor control and thus an essential ingredient for understanding its temporal aspects.

A second, equally persistent feature of the data is the diminution or absence of beta activity during rhythmic motor performance. On the meso-scale, cortical beta amplitude was modulated over a movement cycle and increased beta activity may be interpreted as a measure of synchronization of groups of neurons into a dynamic cell assembly. Put differently, if individual neurons in the motor cortex synchronize at a beta frequency, beta amplitude of the magnetic field measured with MEG will increase and vice versa. In Chapters 4 to 6, beta amplitude was found to decrease during force production or around tap onsets and to increase between individual motor events. This pattern appeared to be also present at the macro-scale, i.e. in the interaction between cortical and spinal activity. In Chapters 4 and 6 the macro-scale displayed a lack of beta synchronization between the simultaneously recorded MEG and EMG activity, which will be discussed in depth in Section 7.2. At first glance, one may think that these findings contradict the abundance of corticospinal beta synchronization during static contractions as reported in the literature. However, in my experiments performance was not static but entailed the production of rhythmic movements or forces. Apparently, during

rhythmic motor performance the periodic mode, i.e. the beta oscillation, is less stable so that the neural dynamics become more erratic. A reason for this might be that the relaxation time of the corticospinal synchronization dynamics is large compared to the time scale of motor performance. As a result, the network cannot damp out or compensate for possible perturbations and, hence, synchronization patterns cannot come to the fore.

A slow relaxation of the corticospinal dynamics towards or away from synchronous modes may have general implications for the functional role of neural synchronization in motor control. Although for static motor control neural synchronization may be an expedient vehicle for information transfer, its general attenuation during rhythmic motor control renders this interpretation in this context less convincing, at least as overarching mechanism. In my experiments, the desynchronization of beta activity was not accompanied by increased oscillatory activity at other frequencies up to 45 Hz, apart from neural activity around the movement frequency. As explained in Chapter 5, the very low frequency components were most likely caused by evoked activity and hence determined by task characteristics rather than by intrinsic neural dynamics. If, during rhythmic motor performance, synchronized neural activity does not serve as a means for motor-related information transfer between cortical and spinal areas, then what kind of dynamics are present during these desynchronized periods and what causes the desynchronization of corticospinal activity? As said, the adopted complex systems perspective suggests a reduced stability of the underlying, here periodic, dynamics. The eventual disappearance of stable oscillations may either yield complete instability or announce the emergence of other stable states. Before discussing this issue in greater length, I first present additional results of corticospinal synchronization as examined during bilateral motor learning. By relating these preliminary results with extant literature, I will draw new directions for further research and evaluate the merits of the theoretical perspective adopted in this thesis.

7.2 Methodological considerations

Throughout my thesis I applied several methods to quantify neural synchronization based on phase locking, i.e. a constant phase difference, at single fixed frequencies or, at least, within narrow bands. In Chapters 2 and 3, I started with conventional coherence analysis, i.e. the normalized cross-

spectrum as frequency domain equivalent of the cross-correlation function (Chatfield, 2004). Since coherence integrates effects of the signals' amplitude and phase variations in a single scalar value, I disentangled amplitude and phase in subsequent chapters using either the classical construction of the analytical signal through the Hilbert transform (Chapter 5) or the complex wavelet transform (Chapter 6) (cf. Rosenblum et al., 1996; Tass et al., 1998; Mormann et al., 2000; Stam et al., 2007). Although the Hilbert transform generally allows for estimating phase independent of frequency and is therefore seen as the most generic approach to study phase locking (Pikovsky et al., 2001), both EMG and MEG were band-pass filtered prior to the Hilbert transform. In doing so, the Hilbert phases were related to distinct frequency bands presupposing that the signals have common frequencies when studying their phase locking characteristics. There are alternative time-frequency analyses like the conventional short-time Fourier transform, but all of them estimate frequency locking between two signals at a fixed, common frequency. Indeed, all these measures turn out to be both formally and effectively equivalent (Le Van Quyen et al., 2001; Bruns, 2004). The assumption of a fixed frequency readily allows for subsequent statistics of the degree of phase locking between the two signals, which can be realized by several means like circular variation (Mardia, 1972), Shannon entropy (Tass et al., 1998), or average mutual information (Palus, 1997). Again, these statistical methods are largely equivalent and the similarity of the listed synchronization measures insures the consistency of results across approaches.

In Chapter 6, I investigated changes in corticospinal synchronization during motor learning. EMG and MEG both showed alterations in terms of changes in their oscillatory activity. Building on these results, I further tested for equivalent effects at a more macroscopic scale, i.e. synchronization between EMG and MEG. To this end, I determined the time- and frequency-dependent phases of both signals by means of the angle of the complex wavelet coefficient, which, as said, is a quantity very comparable to the Hilbert phase exploited in Chapter 5. For every point in time, the synchronization at different frequencies was quantified based on the phase difference between EMG and MEG signals, i.e. as the uniformity of the phase difference over a sliding window of 100 ms. The resulting time-resolved phase uniformity was averaged with respect to motor events (peak forces of the corresponding finger) yielding event-related phase synchronization spectra for each participant, condition, and frequency band. As in Chapter 6, data were subsequently analyzed using partial least squares. The first EMG-MEG phase locking mode is shown in Figure 7.1 in the form of an event-related

modulation of phase locking in the frequencies around 20-40 Hz. This analysis revealed distinct parts in the movement cycle during which both signals synchronized or desynchronized. These results thus seem to support the previously discussed macroscopic synchronization between cortex and spinal cord.

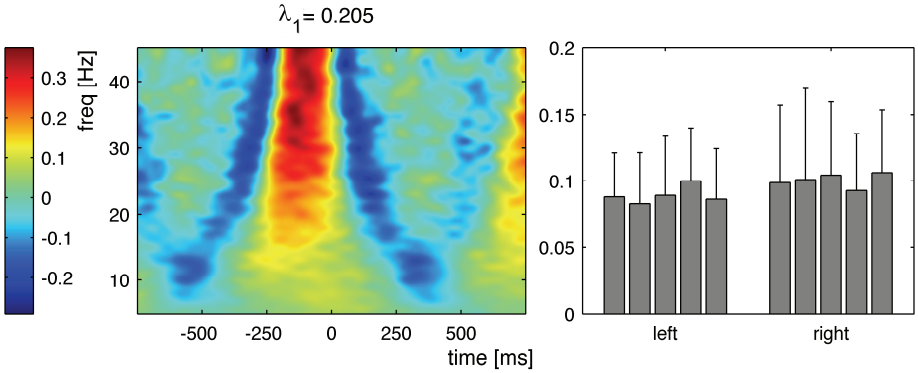

Figure 7.1 *First mode of the PLS analysis of the phase-locking between the rectified EMG and reconstructed MEG data of the contralateral motor cortex. Left panel shows the time-frequency plot corresponding to the projection of the first mode. Phase locking is quantified as the uniformity of the phase difference over a 100 ms window for each frequency separately. Phase-locking values are averaged over different movement cycles by aligning data with respect to the maximal force production of the corresponding finger. Right panel shows the eigenvector coefficients of the first mode. The eigenvectors indicate that the phase-locking pattern shown in the left panel remains stable over trials and for left and right hand condition.*

To test for statistical significance I employed a bootstrapping method and reshuffled the two signals by means of a random translation resulting in two sets of 99 surrogate data for which either the EMG or the MEG was shifted in time prior to computing their relative phase uniformity. Phase synchronization was considered significant if the original uniformity was either smaller or larger than that of 98% of the surrogates (data were assigned the values -1 and +1, respectively). Non-significant uniformities were assigned the value 0 yielding two sets of phase synchronization data with values of -1, 0, and 1, which were subsequently analyzed as described before. The results of the reshuffled EMG signals (Fig. 7.2, upper panels) revealed that the phase-locking pattern displayed in Figure 7.1 was significant when tested against the distribution of the surrogates. The significance of the phase-locking pattern implies that the original data differed significantly from the surrogates, i.e.

misaligning the EMG data destroyed the phase-locking pattern between EMG and MEG signals. In contrast, when comparing the original data with the phase randomized MEG data, the phase-locking pattern did not differ significantly from the distribution of the surrogate data as no significant phase-locking pattern was present (Fig. 7.2, lower panels). Misaligning the MEG data did not disrupt the phase-locking pattern and it can therefore be concluded that the proper alignment of the MEG data was not necessary to reveal the phase-locking pattern shown in Figure 7.1. That is, most likely the phase-locking pattern in question was not caused by a genuine interaction between EMG and MEG activity but simply by local changes in the EMG signal. Notice that the phase-locking pattern closely matched the change in EMG power (Figs. 6.4C and 6.4D) and the apparent synchronization pattern might be caused by the dynamical changes of the EMG signals, i.e. there was a strong change in amplitude and frequency content of the EMGs within each epoch that might have rendered the phase estimation ambiguous (cf. Chavez et al., 2006; Rudrauf et al., 2006).

The absence of frequency-fixed synchronization between EMG and MEG activity during rhythmic movements does not necessarily imply that temporal correlations were completely absent. As was already discussed in Chapter 1, interacting subsystems may display various dynamical features depending on their coupling and intrinsic dynamics. Over the years various methods have been developed that capitalize on the concept of synchronization in order to quantify other forms of interaction dynamics (Pradhan and Dutt, 1993; Jansen, 1996; Stam, 2005). For instance, to quantify interactions between oscillators with different frequencies, existing synchronization measures have been generalized to capture the coupling between oscillators with a specific frequency ratio, e.g., bicoherence (Schanze and Eckhorn, 1997) and n:m phase coupling (Tass et al., 1998). The frequency ratio can be determined via cross-spectral estimates (Daffertshofer et al., 2000b) and the so-called generalized relative phase (accounting for the n:m ratio) can be treated by the same statistics as mentioned above. As said, the unfiltered Hilbert phase can also be used to determine more general synchronization dynamics, even when frequencies change at any rate (Pikovsky et al., 2001). However, the poor signal-to-noise ratio of neural data can be problematic when estimating the phase of a signal. To overcome these problems for signals with continuously varying frequencies, many alternatives are currently discussed like the so-called frequency flow analysis (Rudrauf et al., 2006), synchronization likelihood (Stam and van Dijk, 2002), and non-linear interdependence (Breakspear and Terry, 2002).

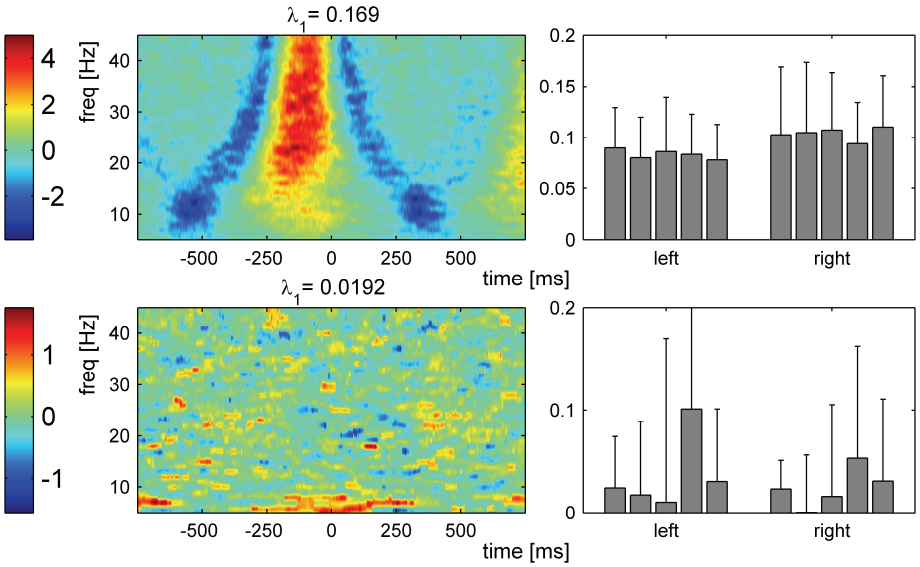

Figure 7.2 *First modes of the PLS analysis of the surrogate data of phase locking between the rectified EMG and reconstructed MEG data. Upper panels: a set of 99 surrogate data was constructed by shifting the EMG signal randomly in time before recomputing the uniformity of the phase difference. Original data points are assigned 1 if the uniformity was higher than 97 of the 99 surrogate data, -1 if it was lower than 97 of the 99 surrogate data, and 0 if otherwise. The lower panels show the results of a similar analysis, but with the MEG signal shifted in time. As in Figure 7.1, left panels show the time-frequency plot corresponding to the projection and right panels show the mean eigenvector coefficients of the first mode.*

In sum, the analyses employed in this thesis failed to show the presence of fixed-frequency synchronization, i.e. conventional synchronization, between spinal and cortical activity during rhythmic motor tasks. However, the absence of synchronization does not imply that all interdependencies were absent as different forms of synchronization might have been present, i.e. generalized synchronization (cf. Stam and van Dijk, 2002).

7.3 Conceptual considerations

There seems to be an essential difference between static and dynamic tasks, as bilateral MU synchronization was present during static isometric contractions (shown in Chapters 2 and 3), whereas macroscopic synchronization between EMG and MEG was largely absent during dynamic force production. These

results are consistent with other findings reported in the literature, e.g., cortical beta amplitude decreased during motor performance (ERD) and increased after motor termination (ERS) (Pfurtscheller and Lopes da Silva, 1999). Similarly, corticomuscular synchronization was absent during dynamic motor control (Kilner et al., 2000) and increased after termination of a phasic voluntary contraction (Feige et al., 2000), i.e. a rebound in corticospinal beta synchronization analogous to the rebound in cortical beta power. The similarity in the decrease of cortical beta activity and corticospinal beta synchronization suggests that both phenomena are not completely independent (cf. Kristeva et al., 2007). The difference between them can be explained if it is assumed that corticospinal phase entrainment has a longer relaxation time and therefore requires more time to reestablish in-between subsequent motor events. If beta synchronization is prominent during periods of static contractions and related with, for instance, the stabilization of an existing motor state, then how is cortical motor control established during phasic motor control and how is it manifested in the coupling between cortical and spinal activity? In the dynamic tasks discussed in this thesis it seems inevitable that cortical activity influenced spinal activity as neural information at the cortical level is used for motor control, e.g., to synchronize motor output with auditory pacing signals. Some kind of relationship between cortical and spinal activity is therefore to be expected. As already discussed, various forms of dynamics are possible and the coupling between cortical and spinal activity may change and cause a switch from a periodic to other dynamical modes during rhythmic motor control.

A first possibility is that motor-related beta desynchronization coincides with increased synchronization in other frequency bands. For instance, Crone and colleagues (1998a) reported an increase in cortical gamma power during motor performance in conjunction with a decrease in alpha and beta power. Similarly, a shift from beta to gamma synchronization has been found between cortical and spinal activity during motor preparation (Schoffelen et al., 2005) as well as during periodically modulated dynamic isometric force output (Omlor et al., 2007). Such results can been interpreted as evidence for a functional segregation between frequency bands with a specific functional role of gamma synchronization in establishing effective neural communication (e.g., Munk et al., 1996; Fries, 2005; Schoffelen et al., 2005). The central role of gamma synchronization in cortical motor control has not received extensive empirical support yet, which may be partly due to the frequency range that has been examined most, i.e. from 0 to 45 Hz (e.g., Kilner et al., 2000, and Section 7.2). Nevertheless, the shift towards higher frequencies with increasing processing

demands seems to be a general phenomenon in brain functioning as similar shifts in frequency content are present, for instance during sleep-wake transitions (see, e.g., Boonstra et al., 2007c, for a review) and in various pathologies (e.g., Stam et al., 2002). Likewise, most low-frequency synchronization patterns during motor control are related to pathologies such as tremors, as discussed in Chapter 2.

Alternatively, a transition to synchronization between different frequencies may occur during dynamic motor tasks. For instance, it has been proposed that functional integration of neuronal systems may proceed at the level of transient dynamics (Friston, 1997). In transient coding the incoming activity from one population exerts a modulatory influence not on the activity of units in the second population but on the interactions among these units to change the population's intrinsic dynamics. In that case, the prevalence of certain frequency components in one cortical area will be associated with the expression of different frequencies in another area (Friston, 1997). Finally, a transition from periodic to erratic dynamics has been studied extensively in the field of complex systems. As described in Chapter 1, the coupling between interacting dynamical systems determines the overall dynamics. If control parameters are scaled beyond critical points, the entire system may undergo a phase transition resulting in a qualitative change in the macroscopic dynamics and reveal, for instance, erratic behavior. Systems on the edge of regular and chaotic behavior have been claimed to have features related to an optimal state of information processing (Tononi et al., 1998; Stam, 2004). For example, the neural system may be organized as scale-free networks displaying power-law scaling behavior of spontaneous oscillations that allows for quick reorganization during processing demands (Linkenkaer-Hansen et al., 2001). The balance between excitatory and inhibitory input appears crucial for the formation of scale-free dynamics (Shin and Kim, 2006). Interestingly, an experimental study by Berg and coworkers (2007) showed that the synaptic excitation and inhibition of motoneurons varies in phase during rhythmic scratch-like activity in turtles. That is, inhibition and excitation peak together during the depolarizing waves of scratch episodes, hampering regular firing by increasing membrane conductance and promoting irregular firing.

In sum, consistent changes in neural synchronization were found in various experimental settings substantiating the theoretical framework that was put forward in Chapter 1. Specifically, beta activity desynchronized during rhythmic movements both within the motor cortex (meso-scale) and between cortex and spinal cord (macro-scale). These findings pose a challenge to theories that consider neural synchronization, as measured by fixed-frequency

phase locking, essential for achieving effective motor control. The transition from a synchronized to a desynchronized state might be due to different types of reorganization of neural dynamics. The different scenarios discussed above all point at a transition to a new state in which there are still temporal correlations between neural activities at different levels of the motor system, but which cannot be adequately quantified with the methods used in this thesis. As such, they are consistent with the general focus on change, and the dynamical system approach in particular, from which the work reported in this thesis was motivated. Only when the relation between cortical and spinal activity is robbed from all temporal correlations, i.e. as in the case of pure rate coding, this focus turned out to be misguided.

7.4 Future directions

In this thesis, I adopted a focus on change to uncover how the nervous system exerts control over the muscles. From this general framework a more specific prediction was derived, namely that neural synchronization plays a functional role in motor control. In particular, by forming macroscopic synchronization patterns appropriate motor control signals may be assembled and spinal activity may be entrained by cortical activity to achieve effective motor control. To investigate the plausibility of this scheme, various experiments were conducted in which neural synchronization was manipulated by varying task parameters. Neural synchronization was found in different frequency bands and the level of synchronization was affected by various task parameters consistent with the alleged functional role of neural synchronization. However, during rhythmic motor performance corticospinal synchronization could not be determined. The data presented in this thesis therefore renders the hypothesis that fixed-frequency phase locking between cortical and spinal activity serves as a general mechanism for achieving effective motor control unlikely. From the perspective of complex systems different macroscopic dynamics can be expected that may serve as means of corticospinal interaction and several methods have been discussed that may be able to quantify these instances of generalized synchronization. These possible extensions assume different temporal correlations between neural activities along the spinal tract during dynamic motor performance and are therefore in agreement with the core commitment of this paradigm or research program.

This research program appears therefore progressive and requires further support to evolve to a mature state resembling realism. According to Lakatos (1978) the appraisal of a research program is based on its recent performance in terms of empirical and theoretical progress and choices between programs are made based on this progress, not on the basis of a single critical experiment. Laudan (1977) posited that the preferable theory is one that maximizes empirical successes while minimizing conceptual liabilities. According to both philosophers, experimental evidence plays a crucial role in theory appraisal, and similar to Kuhn (1962), contradicting evidence does not lead to a rejection of a research program, but to modifications of the ontology and methodology common in the successive theories. In a similar vein, the experimental findings of this thesis, i.e. the absence of corticospinal synchronization during rhythmic movement, should not result in the abandonment of this paradigm, but to the formulation of new extensions of the theory. The adjustment of specific predictions to incorporate new experimental results indeed appears to be the natural course of scientific development (cf. Laudan, 1977; Lakatos, 1978). In particular, research programs are suggested to evolve from an initial state resembling instrumentalism to a mature state resembling realism (Lakatos, 1978)[13].

If these ideas are applied to the research program embarked upon in the present thesis, it is evident that it is still largely in an instrumentalistic stage. The experimental findings that were obtained in the form of task-dependent changes in neural synchronization are consistent with other literature on neural synchronization as stipulated in the individual discussions. As such, scientists of different theoretical persuasions agree how to measure synchronization and the resulting outcomes are generally in accordance with each other. However, a consensus remains to be established on the underlying neural process that brings about these patterns of synchronization. Neural synchronization may be referred to as functional connectivity (Gerstein et al., 1978; Friston, 1994; Tononi et al., 1998; Sporns et al., 2000), i.e. patterns of temporal correlations between distributed activity related to cognitive or behavioral functioning (cf. Cabeza and Kingstone, 2001). To establish a realistic, as opposed to an instrumental, understanding of neural

[13] These ideas closely resemble Popper's ideas on the searchlight theory (1972): "If in this way we look out for new observations with the intention of probing into the truth of our myths, we need not be astonished if we find that myths handled in this rough manner change their character, and that in time they become what one might call more realistic or that they agree better with observable facts."

synchronization, the data on functional connectivity should be linked to other data on the neural organization of motor control. In particular, the integration of the different levels of observation, or organization, i.e. the micro-, meso-, and macro-scale, seems to be a prerequisite for a comprehensive description of neural dynamics (cf. Haken, 1996). The interaction between different levels can be rigorously investigated in the immediate vicinity of phase transitions. There, the system's subcomponents partition into order parameters and enslaved modes and in most cases the dynamics of the order parameters are low dimensional compared to the entire high-dimensional system. Phase transitions can thus be used to identify a system's macroscopic and microscopic dynamics. In this manner, the interaction between scales of organization can be captured to understand how meso-scale dynamics result in the formation and annihilation of corticospinal synchronization during motor performance.

Based on the findings of this thesis, the neural dynamics along the corticospinal tract during dynamic motor tasks appear to be the prime candidate for future research. The transition between different motor states, such as static holding, readiness to respond and dynamic motor performance, seems to be a suitable experimental protocol to investigate the change in temporal correlations between spinal and cortical activity. These motor states are associated with distinct effects on the frequency content of neuronal activity and it is expected that a transition in motor state will be accompanied by qualitative changes in neural dynamics. That is, the switch to dynamic motor performance may be accompanied by a phase transition in the neural dynamics resulting in a qualitative change in macroscopic dynamics, e.g., from a periodic to a strange attractor. Furthermore, new data analysis methods can be applied to examine whether other forms of temporal correlations are present during dynamic motor performance or the total loss of stability. Finally, by gradually decreasing the movement frequency until it resembles static contraction, the frequency at which corticospinal beta synchronization reappears can be established. Similarly, the movement frequency can be gradually increased from very slow movement frequencies to examine whether the corticospinal synchronization disappears again at the same movement frequency or whether hysteresis is present providing further information about the stability of the observed dynamics.

The adopted focus on change in general and neural synchronization in particular has proven to be a successful perspective to investigate neural activity. It has prompted several research questions that have been tested experimentally in this thesis. The resulting data largely agreed with the theory of this research program and deviating findings led to theoretical extensions in

the form of new hypotheses. Promising and exciting new directions were formulated to test the validity of these new hypotheses in future experimental work, which, no doubt, will lead to further theoretical developments, and so on, ad infinitum.

Appendix A

Principal component analysis

To further explain the key feature of the here applied PCA, we denote a finite set of N power or coherence spectra by $\{s_n(f_k)\}$ with n = 1,2,…,N. The arguments f_k (k = 1,2,…,L) represent discrete frequencies resulting from a discrete Fourier transform. We further define a single spectrum's mean over all frequencies as $\langle s_n \rangle = 1/L \sum_{k=1}^{L} s_n(f_k)$. For the sake of simplicity, we omit the f_k dependency whenever possible. As will be explained below, PCA qualifies signal combinations via their contribution to the entire set's variance so that it is convenient to discuss the signals' deviations from their mean rather than the original set. The major goal using PCA can thus be seen as finding a proper approximation of these deviations for all frequencies f_k, which can be formalized as

$$s_n - \langle s_n \rangle \approx \sum_{q=1}^{M} v_{nq} \xi_q \; ; \qquad (1)$$

v_{nq} are scalar factors (or weights), while ξ_q represent M distinct functions of frequency, that is, $\xi_q = \xi_q(f_k)$. Especially in the case of $M < N$, that is, whenever the N-dimensional set $\{s_n(f_k)\}$ is to be reduced to an M-dimensional set $\{\xi_q(f_k)\}$, one may ask how to determine the factors v_{nq}. To answer this question, least squares fits can be used under the constraint that the to-be-determined sets $\{v_{11}, v_{21}, \ldots, v_{N1}\}, \{v_{12}, v_{22}, \ldots, v_{N2}\}, \ldots, \{v_{1M}, v_{2M}, \ldots, v_{NM}\}$ are linearly independent and orthogonal (see below). The fit can be cast in the form

$$error = \sum_{n=1}^{N} \left\langle \left[\left(s_n - \langle s_n \rangle\right) - \sum_{q=1}^{M} v_{nq} \xi_q \right]^2 \right\rangle = \min! \qquad (2)$$

Published as part of: T.W. Boonstra, A. Daffertshofer, J.C. van Ditshuizen, M.R.C. van den Heuvel, C. Hofman, N.W. Willigenburg and P.J. Beek (2007). Fatigue-related changes in motor-unit synchronization of quadriceps muscles within and across legs. *Journal of Electromyography and Kinesiology.* DOI:10.1016/j.jelekin.2007.03. 005.

That is, the sum of all mean (squared) Euclidean distances between signals and approximation is to be minimized. The aforementioned orthogonality reads

$$\sum_{n=1}^{N} v_{np} v_{nq} = \delta_{pq} = \begin{cases} 1 & \text{for } p = q \\ 0 & \text{otherwise} \end{cases}, \tag{3}$$

providing sufficient constraints for a unique solution of (2). Half a century ago (Loève, 1945; Karhunen, 1946; Loève, 1948) showed that the solution of (2) corresponds to eigenvectors of the original signals' covariance matrix with elements $C_{nm} = \left\langle \left(s_n - \langle s_n \rangle\right)\left(s_m - \langle s_m \rangle\right) \right\rangle$. That is, $\{v_{1q}, v_{2q}, \ldots, v_{Nq}\}$ is identical to the q-th eigenvector of $\{C_{nm}\}$ allowing for an algebraic solution of (2) without the need for a time-consuming minimization procedure. Next to the eigenvectors, PCA yields two extra features that, in combination, define the principal modes. First, the eigenvalue, ξ_q, which accompanies the eigenvector $\{v_{1q}, v_{2q}, \ldots, v_{Nq}\}$ may serve as measure of the q-th mode's contribution to the signal set's total variance – we always sorted modes by the size of ξ_q in descending order. Second, the mode's frequency dependency is given by $\xi_q = \xi_q(f_k)$ that can be obtained by projecting the original data $s_i(f_k)$ onto the (orthogonal) eigenvectors like

$$\sum_{n=1}^{N} v_{nq} \left(s_n - \langle s_n \rangle\right) \overset{(1)}{\approx} \sum_{n=1}^{N} v_{nq} \sum_{p=1}^{M} v_{np} \xi_{np} = \sum_{n=1}^{N} \sum_{p=1}^{M} v_{np} v_{nq} \xi_p \overset{(3)}{=} \xi_q . \tag{4}$$

Put differently, for every frequency the different $\xi_q(f_k)$ are 'weighted means' of the original spectra $\{s_n(f_k)\}$ (after subtracting the mean). Examples for these projections are given, e.g., in the left panels of Figures 2.4 and 2.7. In these figures the axis titles show λ_p – we always normalized the spectra to unit variance, that is, the total variance was equal or $\sum_{p=1}^{N} \lambda_p = 1$; the figures' right panels display different combinations of the weights (or eigenvector's coefficients) v_{nq}.

Notice that with equation (1) the original data set $\{s_n\}$ can be approximately reconstructed using the determined weights $\{v_{nq}\}$ and projections $\{\xi_q\}$. The quality of this approximation generally improves with an increasing number of incorporated modes, that is, the larger M, the smaller the error (2) unless the analyzed data are strictly redundant.

Appendix B

MEG-compatible force sensor

Introduction

Over the years, MEG has proven to be a reliable tool in studying electromagnetic activity in the cortex. Despite the weakness of neural sources that generate magnetic fields of only a few hundred fT, superconducting quantum interference devices yield excellent signal-to-noise ratios. Especially when arranged as n^{th} order gradiometers (Weinberg et al., 1984; Vrba et al., 1991), noise levels may become as low as 10 fT×rms/$Hz^{½}$ (Fife et al., 1999; Vrba, 2002). Given the sensitivity of MEG, however, additional hardware is difficult to integrate in experimental settings. In particular, electronic devices need to be shielded as they always generate magnetic fields. Metal in general will cause magnetic inductions when moved, which not only renders the use of metal-based constructions difficult but may also hamper MEG recordings, for instance, in patients with metallic implants. Hence, it seems inevitable to avoid external (moving) metal constructions in MEG. Certain alloys in specific geometrical shapes, however, appear to be MEG-compatible and are used, for instance, to simultaneously record the electro-encephalogram and/or the electromyogram (Weinberg et al., 1990; Virtanen et al., 1996; Grosse et al., 2002).

In MEG studies, the motor system has been a primary focus of many research groups. Most of these studies involve active limb movements, especially finger and hand movements, to investigate corresponding activities in sensorimotor areas. By now, the movements themselves have been monitored by several means that can be classified in two categories: recordings of movement instances, i.e. specific points within the movement versus recordings of movement trajectories (e.g., velocity, force). Paradigmatic for the first category are piezoelectric-crystal based sensors (Benzel et al., 1993) and optical switches (Xiang et al., 1997). Optical switches are commonly used

Published as: T.W. Boonstra, H.E. Clairbois, A. Daffertshofer, J. Verbunt, B.W. van Dijk and P.J. Beek (2004). MEG-compatible force sensor. *Journal of Neuroscience Methods 144*, 193-196.

because they produce the least artifacts and, in principle, allow for non-contact measurements. Realizing the second category, that is, recovering movement trajectories is seemingly more difficult. Presently used techniques range from air-inflated plastic pillows (Kelso et al., 1998) to opto-mechanical constructions (Kilner et al., 2000) that, unfortunately, all suffer from both practical and technical problems. Recording isometric forces with inflated pillows, for instance, (i) restricts the force that can be produced in view of material restrictions; (ii) confines the resolution of force recordings due to the elasticity of the pillow; (iii) causes significant delays due to the subsequent air-pressure transmission with finite velocities. Correcting for the latter requires rather accurate calibration, which might be difficult in the case of pressure-dependent transmission velocities. In any case, due to the delay, inflated pillows cannot be used when an instantaneous feedback of force production is required.

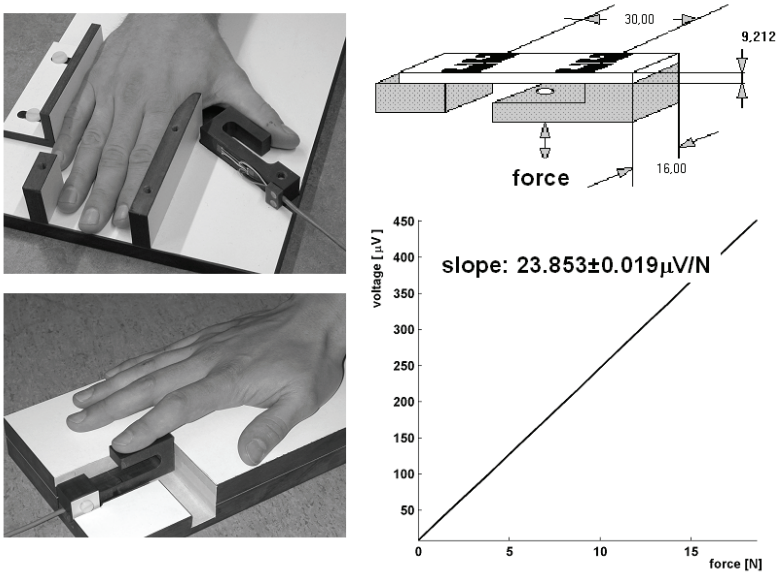

Figure B1 *Left upper panel: Mounted force sensor, here implemented for the recording of isometric thumb adduction. Left lower panel: idem but for the recording of finger tapping. Right upper panel: Blueprint of the force sensor (units mm) developed in T-design software (BLH®, Canton, Mass.). Right lower panel: the force/voltage relation is practically linear (deviation < 1‰).*

We developed a force sensor based on the reversed bending beam principle, as is commonly used in strain gauge based sensors. The special feature of the sensor described here, which makes it compatible with MEG, is the insulating, elastic material of which it is made. The material in question

consists of thermosetting resins, homogeneously reinforced with wood or cellulose fibers, and manufactured under high pressure and at high temperatures (Trespa International B.V. Weert, The Netherlands). Importantly, with this material one can cover a wide range of force strengths (Young's modulus is about 18500 N/mm^2) and it can be flexibly used to construct other kinds and forms of force sensors, such as the double bending beam. Depending on the chosen layout, various types of forces can be easily measured (in the left panels of Fig. B1 we illustrate implementations for the recording of isometric thumb adduction and for finger tapping allowing for forces up to 307 N). The force itself is converted to an electric potential by two strain gauges (BLH®, strain gauge type: FAE2-A6174J-35-S13E, 350 Ω) with sensitivity of 2.199 ± 0.0017 mV/V at 307 N (Hoffmann, 1989).

Methods and Materials

CALIBRATION The force sensor was calibrated and tested for linearity using standard weights ranging from 0.1 to 1.9 kg (step size 0.1 kg) including a null measurement.

PROCEDURE To test for artifacts, the force sensor was mounted on a stool and placed at three different distances (0.6, 0.9, and 1.1 m) from the center of the dewar. A participant sat at about one meter distance and pressed the sensor at a self-paced frequency of about 2 Hz while the magnetic field was recorded. For comparison we added two control conditions. In the first control condition, a participant sat at about one meter distance from the MEG scanner without pressing the force sensor to obtain a baseline in terms of residual noise of the MEG. In the second control condition, the same participant was sitting next to the MEG and pressed the sensor while another, second participant was lying in the MEG with the instruction not to move – this enabled us to determine the strength (or weakness) of the magnetic field induced by the sensor relative to the baseline brain activity. Finally, the usability of the sensor was illustrated by a supplementary MEG recording during which a participant was lying in the MEG pressing at a self-paced tempo of about 2 Hz causing motor-evoked fields (isometric thumb adduction). In all conditions a recording of ~105 s was made (2^{17} samples).

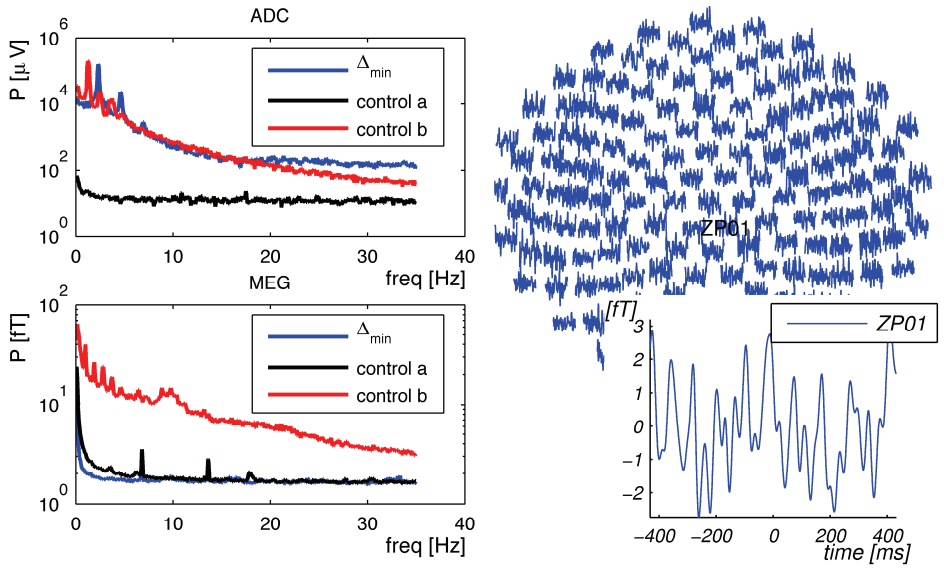

Figure B2 *Left panels: Spectral power P(f) as a function of frequency f computed via Welch's periodogram method (overlapping Hamming windows with a length of 2^{14} samples; square root of normalized power spectral densities) of three conditions: at a distance of Δ_{min} = 0.6 m the sensor was pressed by the participant sitting next to the MEG (blue lines); a participant was located next to the MEG, the sensor was not pressed (first control condition, black lines); the sensor was pressed by the participant sitting next to the MEG while another participant was resting in the MEG (second control condition, red lines). ADC refers to the force sensor's output (upper panel), MEG refers to the mean of all MEG channels (lower panel: peaks in the power spectra with participant in MEG represent the participant's heart beat). Right panel: movement-related averaged fields obtained at a distance of Δ_{min} = 0.6 m. Events were based on the maxima of force sensor's output (N_{events} = 240); absolute values are always below 4 fT; inlet displays data of a single channel.*

DATA ACQUISITION The MEG compatibility of the newly developed device was tested using a 151 whole-head MEG (CTF Systems Inc., Vancouver, Canada) at the VU University medical center in Amsterdam, the Netherlands. We used an excitation of 3.33 V. After pre-amplification (National Instruments, SCXT-1121, gain = 1000) the force sensor's output was recorded using an ADC channel of the MEG amplifier. All signals were on-line low-pass filtered at 415 Hz and digitized at 1250 Hz for off-line analysis.

DATA PROCESSING The effect of the force sensor on the MEG recordings was examined by means of spectral analysis of both signals. No off-line filtering

was performed on the data before computing the normalized power spectral densities via Welch's periodogram method (overlapping Hamming windows with a length of 2^{14} samples). To examine the size of the induced effect, the MEG data were averaged relative to the maximum of the force output of each cycle. Before averaging, linear trends in the data were removed and the data were filtered (4^{th} order Butterworth low pass filter; cut-off frequency 45 Hz) to eliminate artifacts from power line interference and other high frequency noise. Equivalently, the motor-evoked fields in the final condition were calculated demonstrating the usability of the force sensor.

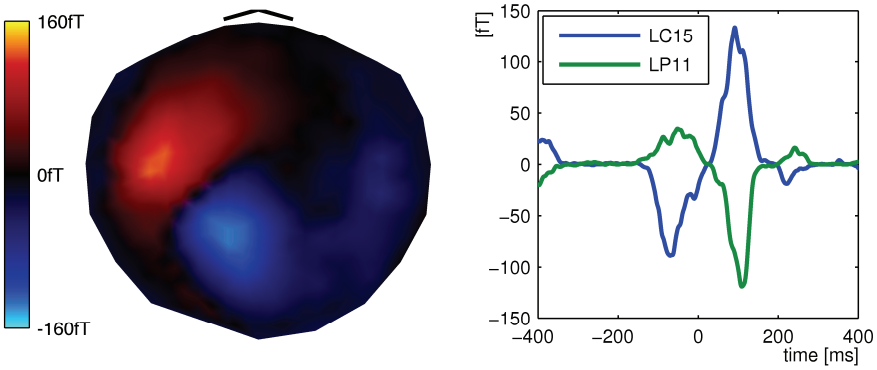

Figure B3 *Motor evoked fields obtained in the final condition (N_{events} = 135). Left panel: dipolar distribution of motor evoked field over the helmet (at t = 0.1 s). Right panel: motor evoked fields (in fT) of two channels as function of time. Channels are located at extrema of the fields shown in the left panel*

Results

The precision and linearity of the force sensors were remarkably high. Measured with 3.33 V excitation and forces smaller than 20 N the non-linearity was about 0.03 N, as is illustrated in Figure B1 (right panel). The average maximal forces of each cycle produced at the three distances were 24, 21, and 20 N, respectively. Since the sensor-related magnetic field was extremely small we only report the results obtained with the sensor positioned at the smallest distance to the MEG dewar (Δ_{min} = 0.6 m). Figure B2 shows the mean power spectra of all MEG channels (lower panel) as well as the movement-related averaged MEG signals (right panel) indicating a maximum magnetic field below 5 fT. Neither the power spectra nor the time series hinted at structured correlations between the force sensor's output (Fig. B2, upper panel ADC) and the recorded magnetic field. The comparison with the control recordings

revealed that the strength of the small magnetic fields was always below the MEG's noise-level. Possible artifacts are therefore expected to be negligible in experimental settings. Indeed, when a participant was lying in the MEG and pressed on the force sensor (final condition), we could not determine any differences to the commonly reported dipolar structures. Figure B3 shows corresponding recordings of the magnetic field above the left motor cortex during isometric adduction with the thumb of the right hand.

Discussion

If at all presents, induced magnetic fields are below magnitude of typical MEG noise levels; the force sensor can therefore be used to record forces in most MEG measurements. Because signal recording and processing are purely electrical, eventual delays can be neglected, unless deliberately created. The sensor can be used to measure force in different directions by mounting it in different ways. Furthermore, the use of the plastic-like material allows for constructing the sensor in different shapes, thus, making it adaptable to use in a variety of experimental settings even if the to be recorded forces are high. In sum, the newly developed device allows for robust force trajectory measurements while recording MEG. The sensor is easily integrated in common MEG settings and can be flexibly utilized in experiments involving different kinds of (isometric) force production even at small distances.

References

Abraham, R.H. and Shaw, C.D., 1984. Dynamics - The geometry of behavior. Aerial Press, Santa Cruz.

Alegre, M., de Gurtubay, I.G., Labarga, A., Iriarte, J., Malanda, A. and Artieda, J., 2004. Alpha and beta oscillatory activity during a sequence of two movements. Clin Neurophysiol 115, 124-130.

Allum, J.H., Dietz, V. and Freund, H.J., 1978. Neuronal mechanisms underlying physiological tremor. J Neurophysiol 41, 557-571.

Amazeen, E.L., Amazeen, P.G. and Treffner, P.J., 1997. Attention and handedness in bimanual coordination dynamics. J Exp Psychol Human 23, 1552-1560.

Amjad, A.M., Halliday, D.M., Rosenberg, J.R. and Conway, B.A., 1997. An extended difference of coherence test for comparing and combining several independent coherence estimates: theory and application to the study of motor units and physiological tremor. J Neurosci Methods 73, 69-79.

Anderson, P.W., 1972. More is different - Broken symmetry and nature of hierarchical structure of science. Science 177, 393-396.

Andres, F.G., Mima, T., Schulman, A.E., Dichgans, J., Hallett, M. and Gerloff, C., 1999. Functional coupling of human cortical sensorimotor areas during bimanual skill acquisition. Brain 122, 855-870.

Andrew, C. and Pfurtscheller, G., 1997. On the existence of different alpha band rhythms in the hand area of man. Neurosci Lett 222, 103-106.

Aranyi, Z. and Rosler, K.M., 2002. Effort-induced mirror movements. A study of transcallosal inhibition in humans. Exp Brain Res 145, 76-82.

Arya, T., Bajwa, S. and Edgley, S.A., 1991. Crossed reflex actions from group II muscle afferents in the lumbar spinal cord of the anaesthetized cat. J Physiol 444, 117-131.

Aschersleben, G., 2002. Temporal control of movements in sensorimotor synchronization. Brain Cogn 48, 66-79.

Aschersleben, G. and Prinz, W., 1995. Synchronizing actions with events: the role of sensory information. Percept Psychophys 57, 305-317.

Atienza, M., Cantero, J. and Escera, C., 2001. Auditory information processing during human sleep as revealed by event-related brain potentials. Clin Neurophysiol 112, 2031-2045.

Babiloni, C., Carducci, F., Cincotti, F., Rossini, P.M., Neuper, C., Pfurtscheller, G. and Babiloni, F., 1999. Human movement-related potentials vs desynchronization of EEG alpha rhythm: a high-resolution EEG study. Neuroimage 10, 658-665.

Baker, S.N., Olivier, E. and Lemon, R.N., 1997. Coherent oscillations in monkey motor cortex and hand muscle EMG show task-dependent modulation. J Physiol 501, 225-241.

Basar, E., 1998. Brain function and oscillations: integrative brain function (Springer Series in Synergetics). Springer-Verlag, Berlin.

Beek, P.J., Peper, C.E. and Stegeman, D.F., 1995. Dynamical models of movement coordination. Hum Mov Sci 14, 573-608.

Benzel, E.C., Lewine, J.D., Bucholz, R.D. and Orrison, W.W., Jr., 1993. Magnetic source imaging: a review of the Magnes system of biomagnetic technologies incorporated. Neurosurg 33, 252-259.

Berg, R.W., Alaburda, A. and Hounsgaard, J., 2007. Balanced inhibition and excitation drive spike activity in spinal half-centers. Science 315, 390-393.

Bernat, E.M., Williams, W.J. and Gehring, W.J., 2005. Decomposing ERP time-frequency energy using PCA. Clin Neurophysiol 116, 1314-1334.

Bernstein, N., 1967. The coordination and regulation of movements. Pergamon, London.

Bigland-Ritchie, B., Cafarelli, E. and Vollestad, N.K., 1986. Fatigue of submaximal static contractions. Acta Physiol Scand Suppl 556, 137-148.

Bigland-Ritchie, B., Donovan, E.F. and Roussos, C.S., 1981. Conduction velocity and EMG power spectrum changes in fatigue of sustained maximal efforts. J Appl Physiol 51, 1300-1305.

Boonstra, T.W., Clairbois, H.E., Daffertshofer, A., Verbunt, J., van Dijk, B.W. and Beek, P.J., 2005a. MEG-compatible force sensor. J Neurosci Methods 144, 193-196.

Boonstra, T.W., Daffertshofer, A. and Beek, P.J., 2005b. Effects of sleep deprivation on event-related fields and alpha activity during rhythmic force production. Neurosci Lett 388, 27-32.

Boonstra, T.W., Daffertshofer, A., Peper, C.E. and Beek, P.J., 2006. Amplitude and phase dynamics associated with acoustically paced finger tapping. Brain Res 1109, 60-69.

Boonstra, T.W., Daffertshofer, A., van As, E., van der Vlugt, S. and Beek, P.J., 2007a. Bilateral motor unit synchronization is functionally organized. Exp Brain Res 178, 79-88.

Boonstra, T.W., Daffertshofer, A., van Ditshuizen, J.C., van den Heuvel, M.R.C., Hofman, C., Willigenburg, N.W. and Beek, P.J., 2007b. Fatigue-related changes in motor-unit synchronization of quadriceps muscles within and across legs. J Electromyogr Kinesiol. DOI:10.1016/j.jelekin.2007.03.005.

Boonstra, T.W., Stins, J.F., Daffertshofer, A. and Beek, P.J., 2007c. Effects of sleep deprivation on neural functioning: an integrative review. Cell Mol Life Sci 64, 934-46.

Breakspear, M. and Terry, J.R., 2002. Detection and description of non-linear interdependence in normal multichannel human EEG data. Clin Neurophysiol 113, 735-753.

Breakspear, M., Terry, J.R. and Friston, K.J., 2003. Modulation of excitatory synaptic coupling facilitates synchronization and complex dynamics in a biophysical model of neuronal dynamics. Network 14, 703-732.

Breakspear, M. and Jirsa, V.K., 2006. Neuronal dynamics and brain connectivity. In: McIntosh, A.R. and Jirsa, V.K. (Eds.), Handbook of brain connectivity. Springer, Berlin.

Bruns, A., 2004. Fourier-, Hilbert- and wavelet-based signal analysis: are they really different approaches? J Neurosci Methods 137, 321-332.

Cabeza, R. and Kingstone, A. (Eds.), 2001. Handbook of functional neuroimaging of cognition. MIT Press, Cambridge, Massachusetts.

Campbell, K. and Colrain, I., 2002. Event-related potential measures of the inhibition of information processing: II. The sleep onset period. Int J Psychophysiol 46, 197-214.

Cantero, J., Atienza, M., Gomez, C. and Salas, R., 1999. Spectral structure and brain mapping of human alpha activities in different arousal states. Neuropsychobiol 39, 110-116.

Cantero, J., Atienza, M. and Salas, R., 2002. Human alpha oscillations in wakefulness, drowsiness period, and REM sleep: different electroencephalographic phenomena within the alpha band. Neurophys Clin 32, 54-71.

Carr, L.J., Harrison, L.M. and Stephens, J.A., 1994. Evidence for bilateral innervation of certain homologous motoneuron oools in man. J Physiol 475, 217-227.

Carson, R.G., 2005. Neural pathways mediating bilateral interactions between the upper limbs. Brain Res Brain Res Rev 49, 641-662.

Carson, R.G. and Kelso, J.A.S., 2004. Governing coordination: behavioural principles and neural correlates. Exp Brain Res 154, 267-274.

Carson, R.G. and Riek, S., 2001. Changes in muscle recruitment patterns during skill acquisition. Exp Brain Res 138, 71-87.

Cassim, F., Monaca, C., Szurhaj, W., Bourriez, J.L., Defebvre, L., Derambure, P. and Guieu, J.D., 2001. Does post-movement beta synchronization reflect an idling motor cortex? Neuroreport 12, 3859-3863.

Chapman, R.M. and McCrary, J.W., 1995. EP component identification and measurement by principal components analysis. Brain Cogn 27, 288-310.

Chatfield, C., 2004. The analysis of time-series: an introduction. CRC Press, Florida.

Chavez, M., Besserve, M., Adam, C. and Martinerie, J., 2006. Towards a proper estimation of phase synchronization from time series. J Neurosci Methods 154, 149-160.

Cheyne, D., Bakhtazad, L. and Gaetz, W., 2006. Spatiotemporal mapping of cortical activity accompanying voluntary movements using an event-related beamforming approach. Hum Brain Mapp 27, 213-229.

Cheyne, D., Endo, H., Takeda, T. and Weinberg, H., 1997. Sensory feedback contributes to early movement-evoked fields during voluntary finger movements in humans. Brain Res 771, 196-202.

Cheyne, D. and Weinberg, H., 1989. Neuromagnetic fields accompanying unilateral finger movements: pre-movement and movement-evoked fields. Exp Brain Res 78, 604-612.

Christakos, C.N., 1997. On the detection and measurement of synchrony in neural populations by coherence analysis. J Neurophysiol 78, 3453-3459.

Christakos, C.N., Papadimitriou, N.A. and Erimaki, S., 2006. Parallel neuronal mechanisms underlying physiological force tremor in steady muscle contractions of humans. J Neurophysiol 95, 53-66.

Christou, E.A., Rudroff, T., Enoka, J.A., Meyer, F. and Enoka, R.M., 2006. Discharge rate during low-force isometric contractions influences motor unit coherence below 15 Hz but not motor unit synchronization. Exp Brain Res 178, 285-295.

Churchland, P.S., 1980. A perspective on mind-brain research. J Philos 77, 185-207.

Clark, A., 1998. Time and mind. J Philos 95, 354-376.

Cohen, J., 1988. Statistical power analysis for the behavioral sciences. Erlbaum, Hillsdale, NJ.

Conway, B.A., Halliday, D.M., Farmer, S.F., Shahani, U., Maas, P., Weir, A.I. and Rosenberg, J.R., 1995. Synchronization between motor cortex and spinal motoneuronal pool during the performance of a maintained motor task in man. J Physiol 489, 917-924.

Corsi-Cabrera, M., Arce, C., Del Rio-Portilla, I.Y., Perez-Garci, E. and Guevara, M.A., 1999. Amplitude reduction in visual event-related potentials as a function of sleep deprivation. Sleep 22, 181-189.

Cresswell, A.G. and Loscher, W.N., 2000. Significance of peripheral afferent input to the alpha-motoneurone pool for enhancement of tremor during an isometric fatiguing contraction. Eur J Appl Physiol 82, 129-136.

Crone, N.E., Miglioretti, D.L., Gordon, B. and Lesser, R.P., 1998a. Functional mapping of human sensorimotor cortex with electrocorticographic spectral analysis. II. Event-related synchronization in the gamma band. Brain 121, 2301-2315.

Crone, N.E., Miglioretti, D.L., Gordon, B., Sieracki, J.M., Wilson, M.T., Uematsu, S. and Lesser, R.P., 1998b. Functional mapping of human sensorimotor cortex with electrocorticographic spectral analysis. I. Alpha and beta event-related desynchronization. Brain 121, 2271-2299.

Daffertshofer, A., Boonstra, T.W. and Beek, P.J., 2007. Cortical beta synchronization is related to low-order motor parameters. Int Congress Series 1300, 329-332.

Daffertshofer, A., Lamoth, C.J., Meijer, O.G. and Beek, P.J., 2004. PCA in studying coordination and variability: a tutorial. Clin Biomech 19, 415-428.

Daffertshofer, A., Peper, C.E. and Beek, P.J., 2000a. Spectral analyses of event-related encephalographic signals. Phys Lett A 266, 290-302.

Daffertshofer, A., Peper, C.E. and Beek, P.J., 2005. Stabilization of bimanual coordination due to active interhemispheric inhibition: a dynamical account. Biol Cybern 92, 101-109.

Daffertshofer, A., Peper, C.E., Frank, T.D. and Beek, P.J., 2000b. Spatio-temporal patterns of encephalographic signals during polyrhythmic tapping. Hum Mov Sci 19, 475-498.

David, O., Harrison, L. and Friston, K.J., 2005. Modelling event-related responses in the brain. Neuroimage 25, 756-770.

Davies, P., 1995. Algorithmic compressibility, fundamental and phenomenological laws. In: Weinert, F. (Ed.), Laws of nature: essays on the philosophical, scientific and historical dimensions. Walter de Gruyter & Co, Berlin, pp. 248-267.

De Gennaro, L., Ferrara, M., Curcio, G. and Cristiani, R., 2001. Antero-posterior EEG changes during the wakefulness-sleep transition. Clin Neurophysiol 112, 1901-1911.

De Luca, C.J. and Erim, Z., 1994. Common drive of motor units in regulation of muscle force. Trends Neurosci 17, 299-305.

De Luca, C.J. and Erim, Z., 2002. Common drive in motor units of a synergistic muscle pair. J Neurophysiol 87, 2200-2204.

De Luca, C.J. and Forrest, W.J., 1973. Some properties of motor unit action potential trains recorded during constant force isometric contractions in man. Kybernetik 12, 160-168.

De Luca, C.J., LeFever, R.S., McCue, M.P. and Xenakis, A.P., 1982. Control scheme governing concurrently active human motor units during voluntary contractions. J Physiol 329, 129-142.

de Oliveira, S.C., Gribova, A., Donchin, O., Bergman, H. and Vaadia, E., 2001. Neural interactions between motor cortical hemispheres during bimanual and unimanual arm movements. Eur J Neurosci 14, 1881-1896.

Debaere, F., Swinnen, S.P., Beatse, E., Sunaert, S., Van Hecke, P. and Duysens, J., 2001. Brain areas involved in interlimb coordination: a distributed network. Neuroimage 14, 947-958.

Dimitrova, N.A. and Dimitrov, G.V., 2003. Interpretation of EMG changes with fatigue: facts, pitfalls, and fallacies. J Electromyogr Kinesiol 13, 13-36.

Doumas, M., Praamstra, P. and Wing, A.M., 2005. Low frequency rTMS effects on sensorimotor synchronization. Exp Brain Res 167, 238-245.

Doyle, L.M., Yarrow, K. and Brown, P., 2005. Lateralization of event-related beta desynchronization in the EEG during pre-cued reaction time tasks. Clin Neurophysiol 116, 1879-1888.

Drake, C., Moran, J., Scofield, H., Tepley, N. and Roth, T., 2004. MEG imaged brain activation during the transition from wake to sleep. In: Halgren, E. et al. (Eds.). Proceedings of the proceedings of the 14th international conference on biomagnetism. Biomag 2004 Ltd., Boston, Mass., pp. 211.

Drummond, S.P., Brown, G.G., Stricker, J.L., Buxton, R.B., Wong, E.C. and Gillin, J.C., 1999. Sleep deprivation-induced reduction in cortical functional response to serial subtraction. Neuroreport 10, 3745-3748.

Duzel, E., Habib, R., Schott, B., Schoenfeld, A., Lobaugh, N., McIntosh, A.R., Scholz, M. and Heinze, H.J., 2003. A multivariate, spatiotemporal analysis of electromagnetic time-frequency data of recognition memory. Neuroimage 18, 185-197.

Ebenbichler, G.R., Kollmitzer, J., Erim, Z., Loscher, W.N., Kerschan, K., Posch, M., Nowotny, T., Kranzl, A., Wober, C. and Bochdansky, T., 2000. Load-dependence of fatigue related changes in tremor around 10 Hz. Clin Neurophysiol 111, 106-111.

Ebenbichler, G.R., Kollmitzer, J., Glockler, L., Bochdansky, T., Kopf, A. and Fialka, V., 1998. The role of the biarticular agonist and cocontracting antagonist pair in isometric muscle fatigue. Muscle Nerve 21, 1706-1713.

Eckhorn, R., Bauer, R., Jordan, W., Brosch, M., Kruse, W., Munk, M. and Reitboeck, H.J., 1988. Coherent oscillations - A mechanism of feature linking in the visual cortex - Multiple electrode and correlation analyses in the cat. Biol Cybern 60, 121-130.

Elble, R.J. and Randall, J.E., 1976. Motor-unit activity responsible for 8- to 12-Hz component of human physiological finger tremor. J Neurophysiol 39, 370-383.

Engel, A.K., Konig, P., Kreiter, A.K., Schillen, T.B. and Singer, W., 1992. Temporal coding in the visual cortex: new vistas on integration in the nervous system. Trends Neurosci 15, 218-226.

Engel, A.K., Konig, P., Kreiter, A.K. and Singer, W., 1991. Interhemispheric synchronization of oscillatory neuronal responses in cat visual cortex. Science 252, 1177-1179.

Farina, D., Merletti, R. and Enoka, R.M., 2004. The extraction of neural strategies from the surface EMG. J Appl Physiol 96, 1486-1495.

Farmer, S.F., 1998. Rhythmicity, synchronization and binding in human and primate motor systems. J Physiol 509, 3-14.

Farmer, S.F., 1999. Pulsatile central nervous control of human movement. J Physiol 517, 3-3.

Farmer, S.F., Bremner, F.D., Halliday, D.M., Rosenberg, J.R. and Stephens, J.A., 1993. The frequency content of common synaptic inputs to motoneurones studied during voluntary isometric contraction in man. J Physiol 470, 127-155.

Feige, B., Aertsen, A. and Kristeva-Feige, R., 2000. Dynamic synchronization between multiple cortical motor areas and muscle activity in phasic voluntary movements. J Neurophysiol 84, 2622-2629.

Feige, B., Kristeva-Feige, R., Rossi, S., Pizzella, V. and Rossini, P.M., 1996. Neuromagnetic study of movement-related changes in rhythmic brain activity. Brain Res 734, 252-260.

Fell, J., Dietl, T., Grunwald, T., Kurthen, M., Klaver, P., Trautner, P., Schaller, C., Elger, C.E. and Fernandez, G., 2004. Neural bases of cognitive ERPs: more than phase reset. J Cogn Neurosci 16, 1595-1604.

Ferrara, M., De Gennaro, L., Ferlazzo, F. and Curcio, G., 2002. Topographical changes in N1-P2 amplitude upon awakening from recovery sleep after slow-wave sleep deprivation. Clin Neurophysiol 113, 1183-1190.

Fife, A.A., Vrba, J., Robinson, S.E., Anderson, G., Betts, K., Burbank, M.B., Cheyne, D., Cheung, T., Govorkov, S., Haid, G., Haid, V., Hunter, C., Kubik, P.R., Lee, S., McKay, J., Reichl, E., Schroyen, C., Sekachev, I., Spear, P., Taylor, B., Tillotson, M. and Sutherling, W., 1999. Synthetic gradiometer systems for MEG. IEEE Trans Appl Supercon 9, 4063-4068.

Fisher, N.I., 1993. Statistical analysis of circular data. Cambridge University Press, Cambridge.

Fodor, J.A., 1975. The language of thought. Crowell, New York.

Foffani, G., Bianchi, A.M., Baselli, G. and Priori, A., 2005. Movement-related frequency modulation of beta oscillatory activity in the human subthalamic nucleus. J Physiol 568, 699-711.

Franz, E.A., Eliassen, J.C., Ivry, R.B. and Gazzaniga, M.S., 1996. Dissociation of spatial and temporal coupling in the bimanual movements of callosotomy patients. Psychol Sci 7, 306-310.

Freeman, W.J., 1975. Mass action in the nervous system. Academic Press, New York.

Fries, P., 2005. A mechanism for cognitive dynamics: neuronal communication through neuronal coherence. Trends Cogn Sci 9, 474-480.

Fries, P., Reynolds, J.H., Rorie, A.E. and Desimone, R., 2001. Modulation of oscillatory neuronal synchronization by selective visual attention. Science 291, 1560-1563.

Friston, K.J., 1994. Functional and effective connectivity in neuroimaging: a synthesis. Hum Brain Mapp 2, 56-78.

Friston, K.J., 1997. Another neural code? Neuroimage 5, 213-220.

Fujii, H., Ito, H., Aihara, K., Ichinose, N. and Tsukada, M., 1996. Dynamical cell assembly hypothesis - Theoretical possibility of spatio-temporal coding in the cortex. Neural Networks 9, 1303-1350.

Gaetz, W. and Cheyne, D., 2006. Localization of sensorimotor cortical rhythms induced by tactile stimulation using spatially filtered MEG. Neuroimage 30, 899-908.

Gare, A., 2002. Process philosophy and the emergent theory of mind: Whitehead, Lloyd Morgan and Schelling. Concrescence 3, 1-12.

Gerloff, C., Richard, J., Hadley, J., Schulman, A.E., Honda, M. and Hallett, M., 1998a. Functional coupling and regional activation of human cortical motor areas during simple, internally paced and externally paced finger movements. Brain 121, 1513-1531.

Gerloff, C., Toro, C., Uenishi, N., Cohen, L.G., Leocani, L. and Hallett, M., 1997. Steady-state movement-related cortical potentials: a new approach to assessing cortical activity associated with fast repetitive finger movements. Electroencephalogr Clin Neurophysiol 102, 106-113.

Gerloff, C., Uenishi, N., Nagamine, T., Kunieda, T., Hallett, M. and Shibasaki, H., 1998b. Cortical activation during fast repetitive finger movements in humans: steady-state movement-related magnetic fields and their cortical generators. Electroencephalogr Clin Neurophysiol 109, 444-453.

Gerstein, G.L., Perkel, D.H. and Subramanian, K.N., 1978. Identification of functionally related neural assemblies. Brain Res 140, 43-62.

Gholson, B. and Barker, P., 1985. Kuhn, Lakatos, and Laudan - Applications in the history of physics and psychology. Am Psychol 40, 755-769.

Gibbs, J., Harrison, L.M. and Stephens, J.A., 1995. Organization of inputs to motoneuron pools in man. J Physiol 485, 245-256.

Glass, L., 2001. Synchronization and rhythmic processes in physiology. Nature 410, 277-284.

Gray, C.M. and Singer, W., 1989. Stimulus-specific neuronal oscillations in orientation columns of cat visual cortex. Proc Natl Acad Sci USA 86, 1698-1702.

Gross, J., Pollok, B., Dirks, M., Timmermann, L., Butz, M. and Schnitzler, A., 2005. Task-dependent oscillations during unimanual and bimanual movements in the human primary motor cortex and SMA studied with magnetoencephalography. Neuroimage 26, 91-98.

Gross, J., Tass, P.A., Salenius, S., Hari, R., Freund, H.J. and Schnitzler, A., 2000. Cortico-muscular synchronization during isometric muscle contraction in humans as revealed by magnetoencephalography. J Physiol 527, 623-631.

Gross, J., Timmermann, L., Kujala, J., Dirks, M., Schmitz, F., Salmelin, R. and Schnitzler, A., 2002. The neural basis of intermittent motor control in humans. Proc Natl Acad Sci USA 99, 2299-2302.

Grosse, P., Cassidy, M.J. and Brown, P., 2002. EEG-EMG, MEG-EMG and EMG-EMG frequency analysis: physiological principles and clinical applications. Clin Neurophysiol 113, 1523-1531.

Hagbarth, K.E. and Young, R.R., 1979. Participation of the stretch reflex in human physiological tremor. Brain 102, 509-526.

Hagg, G.M., 1992. Interpretation of EMG spectral alterations and alteration indexes at sustained contraction. J Appl Physiol 73, 1211-1217.

Haken, H., 1983. Synergetics. An introduction. Springer, Berlin.

Haken, H., 1995. Some basic concepts of synergetics with respect to mulistability in perception, phase transitions and formation of meaning. In: Kruse, P. and Stadler, M. (Eds.), Ambiguity in mind and nature, multistable cognitive phenomena. Springer-Verlag, Berlin, Heidelberg.

Haken, H., 1996. Principles of brain functioning. Springer, Berlin.

Haken, H., 2006. Synergetics of brain function. Int J Psychophysiol 60, 110-124.

Haken, H., Kelso, J.A.S. and Bunz, H., 1985. A theoretical model of phase-transitions in human hand movements. Biol Cybern 51, 347-356.

Halliday, A.M. and Redfearn, J.W., 1956. An analysis of the frequencies of finger tremor in healthy subjects. J Physiol 134, 600-611.

Halliday, D.M., Rosenberg, J.R., Amjad, A.M., Breeze, P., Conway, B.A. and Farmer, S.F., 1995. A framework for the analysis of mixed time series/point process data--theory and application to the study of physiological tremor, single motor unit discharges and electromyograms. Prog Biophys Mol Biol 64, 237-278.

Hämäläinen, M., Hari, R., Ilmoniemi, R.J., Knuutila, J. and Lounasmaa, O.V., 1993. Magnetoencephalography - theory, instrumentation, and applications to noninvasive studies of the working human brain. Rev Mod Phys 65, 413-497.

Harrison, L.M., Ironton, R. and Stephens, J.A., 1991. Cross-correlation analysis of multiunit EMG recordings in man. J Neurosci Methods 40, 171-179.

Harrison, P.J. and Zytnicki, D., 1984. Crossed actions of group I muscle afferents in the cat. J Physiol 356, 263-273.

Hebb, D.O., 1949. The organization of behavior. Wiley, New York.

Heidegger, M. and Fink, E., 1979. Heraclitus seminar. University of Alabama Press, Alabama.

Henneman, E., 1957. Relation between size of neurons and their susceptibility to discharge. Science 126, 1345-1347.

Hermens, H.J., Freriks, B., Disselhorst-Klug, C. and Rau, G., 2000. Development of recommendations for SEMG sensors and sensor placement procedures. J Electromyogr Kinesiol 10, 361-374.

Hertrich, I., Mathiak, K., Lutzenberger, W. and Ackermann, H., 2004. Transient and phase-locked evoked magnetic fields in response to periodic acoustic signals. Neuroreport 15, 1687-1690.

Hodgkin, A.L. and Huxley, A.F., 1952. A quantitative description of membrane current and its application to conduction and excitation in nerve. J Physiol 117, 500-544.

Hoffmann, K., 1989. An introduction to measurement using strain gauges. Hottinger Baldwin Messtechnik GmbH, Darmstadt.

Hoppensteadt, F.C. and Izhikevich, E.M., 1998. Thalamo-cortical interactions modeled by weakly connected oscillators: could the brain use FM radio principles? Biosystems 48, 85-94.

Horne, J.A., 1993. Human sleep, sleep loss and behaviour. Implications for the prefrontal cortex and psychiatric disorder. Br J Psychiatry 162, 413-419.

Houweling, S., Daffertshofer, A., van Dijk, B.W. and Beek, P.J., 2007. Synchronization in perceptual-motor integration. Int Congress Series, 1300, 333-336.

Hoy, K.E., Fitzgerald, P.B., Bradshaw, J.L., Armatas, C.A. and Georgiou-Karistianis, N., 2004. Investigating the cortical origins of motor overflow. Brain Res Brain Res Rev 46, 315-327.

Hurtado, J.M., Lachaux, J.P., Beckley, D.J., Gray, C.M. and Sigvardt, K.A., 2000. Inter- and intralimb oscillator coupling in parkinsonian tremor. Mov Disord 15, 683-691.

Hyvärinen, A., Karhunen, J. and Oja, E., 2001. Independent component analysis. John Wiley & Sons, New York.

Jackson, A., Spinks, R.L., Freeman, T.C., Wolpert, D.M. and Lemon, R.N., 2002. Rhythm generation in monkey motor cortex explored using pyramidal tract stimulation. J Physiol 541, 685-699.

James, W., 1890. The principles of psychology. Holt, New York.

Jansen, B.H., 1996. Nonlinear dynamics and quantitative EEG analysis. Electroencephalogr Clin Neurophysiol Suppl 45, 39-56.

Joliot, M., Ribary, U. and Llinas, R., 1994. Human oscillatory brain activity near 40 Hz coexists with cognitive temporal binding. Proc Natl Acad Sci USA 91, 11748-11751.

Jurkiewicz, M.T., Gaetz, W.C., Bostan, A.C. and Cheyne, D., 2006. Post-movement beta rebound is generated in motor cortex: evidence from neuromagnetic recordings. Neuroimage 32, 1281-1289.

Kadefors, R., Kaiser, E. and Petersen, I., 1968. Dynamic spectrum analysis of myopotentials and with special reference to muscle fatigue. Electromyogr 8, 39-74.

Kandel, E.R., Schwartz, J.H. and Jessell, T.M. (Eds.), 1991. Principles of neural science. Appleton & Lange, East Norwalk, Connecticut.

Karhunen, K., 1946. Zur spektralen Theorie stochastischer Prozesse. Ann Acad Sci Fennicae Ser A 34.

Karni, A., Meyer, G., Rey-Hipolito, C., Jezzard, P., Adams, M.M., Turner, R. and Ungerleider, L.G., 1998. The acquisition of skilled motor performance: fast and slow experience-driven changes in primary motor cortex. Proc Natl Acad Sci USA 95, 861-868.

Kato, M. and Konishi, Y., 2006. Auditory dominance in the error correction process: a synchronized tapping study. Brain Res 1084, 115-122.

Kayser, J. and Tenke, C.E., 2005. Trusting in or breaking with convention: towards a renaissance of principal components analysis in electrophysiology. Clin Neurophysiol 116, 1747-1753.

Keenan, K.G., Farina, D., Meyer, F., Merletti, R. and Enoka, R.M., 2006. Sensitivity of the cross-correlation between simulated surface EMGs for two muscles to detect motor unit synchronization. J Appl Physiol 102, 1193-201.

Keil, F.C., 1981. Constraints on knowledge and cognitive development. Psychol Rev 88, 197-227.

Keil, F.C., Smith, W.C., Simons, D.J. and Levin, D.T., 1998. Two dogmas of conceptual empiricism: implications for hybrid models of the structure of knowledge. Cognition 65, 103-135.

Kelso, J.A., 1984. Phase transitions and critical behavior in human bimanual coordination. Am J Physiol 246, R1000-1004.

Kelso, J.A.S., 1995. Dynamic patterns: the self-organization of brain and behavior. MIT Press, Cambridge, MA.

Kelso, J.A.S., Bressler, S.L., Buchanan, S., DeGuzman, G.C., Ding, M., A., F. and A., H., 1992. A phase transition in human brain and behavior. Phys Lett A 169, 134-144.

Kelso, J.A.S., Fuchs, A., Lancaster, R., Holroyd, T., Cheyne, D. and Weinberg, H., 1998. Dynamic cortical activity in the human brain reveals motor equivalence. Nature 392, 814-818.

Kilner, J.M., Baker, S.N., Salenius, S., Hari, R. and Lemon, R.N., 2000. Human cortical muscle coherence is directly related to specific motor parameters. J Neurosci 20, 8838-8845.

Kilner, J.M., Baker, S.N., Salenius, S., Jousmaki, V., Hari, R. and Lemon, R.N., 1999. Task-dependent modulation of 15-30 Hz coherence between rectified EMGs from human hand and forearm muscles. J Physiol 516, 559-570.

Kirkwood, P.A. and Sears, T.A., 1978. The synaptic connexions to intercostal motoneurones as revealed by the average common excitation potential. J Physiol 275, 103-134.

Kirkwood, P.A., Sears, T.A., Tuck, D.L. and Westgaard, R.H., 1982. Variations in the time course of the synchronization of intercostal motoneurones in the cat. J Physiol 327, 105-135.

Kleine, B.U., Stegeman, D.F., Mund, D. and Anders, C., 2001. Influence of motoneuron firing synchronization on SEMG characteristics in dependence of electrode position. J Appl Physiol 91, 1588-1599.

Klimesch, W., Schack, B., Schabus, M., Doppelmayr, M., Gruber, W. and Sauseng, P., 2004. Phase-locked alpha and theta oscillations generate the P1-N1 complex and are related to memory performance. Brain Res Cogn Brain Res 19, 302-316.

Kornhuber, H.H. and Deecke, L., 1965. Changes in the brain potential in voluntary movements and passive movements in man: readiness potential and reafferent potentials. Pflugers Arch Gesamte Physiol Menschen Tiere 284, 1-17.

Köster, B., Lauk, M., Timmer, J., Winter, T., Guschlbauer, B., Glocker, F.X., Danek, A., Deuschl, G. and Lucking, C.H., 1998. Central mechanisms in human enhanced physiological tremor. Neurosci Lett 241, 135-138.

Koukkou, M. and Lehmann, D., 1983. Dreaming: the functional state-shift hypothesis. A neuropsychophysiological model. Br J Psychiatry 142, 221-231.

Kristeva, R., Patino, L. and Omlor, W., 2007. Beta-range cortical motor spectral power and corticomuscular coherence as a mechanism for effective corticospinal interaction during steady-state motor output. Neuroimage 36, 785-92.

Krogh-Lund, C. and Jorgensen, K., 1993. Myo-electric fatigue manifestations revisited: power spectrum, conduction velocity, and amplitude of human elbow flexor muscles during isolated and repetitive endurance contractions at 30% maximal voluntary contraction. Eur J Appl Physiol Occup Physiol 66, 161-173.

Kruse, P. and Stadler, M. (Eds.), 1995. Ambiguity in mind and nature: multistable cognitive phenomena. Springer - Verlag, Berlin Heidelberg.

Kuhn, T.S., 1962. The structure of scientific revolutions. The University of Chicago Press, Chicago.

Lakatos, I., 1978. The methodology of scientific research programs. Cambridge University Press, Cambridge, England.

Lang, W., Obrig, H., Lindinger, G., Cheyne, D. and Deecke, L., 1990. Supplementary motor area activation while tapping bimanually different rhythms in musicians. Exp Brain Res 79, 504-514.

Laudan, L., 1977. Progress and its problems. University of California Press, Berkeley.

Laughlin, R.B. and Pines, D., 2000. The theory of everything. Proc Natl Acad Sci USA 97, 28-31.

Lauk, M., Koster, B., Timmer, J., Guschlbauer, B., Deuschl, G. and Lucking, C.H., 1999. Side-to-side correlation of muscle activity in physiological and pathological human tremors. Clin Neurophysiol 110, 1774-1783.

Le Van Quyen, M., 2003. Disentangling the dynamic core: a research program for a neurodynamics at the large-scale. Biol Res 36, 67-88.

Le Van Quyen, M., Foucher, J., Lachaux, J., Rodriguez, E., Lutz, A., Martinerie, J. and Varela, F.J., 2001. Comparison of Hilbert transform and wavelet methods for the analysis of neuronal synchrony. J Neurosci Methods 111, 83-98.

Lehmann, D., 1995. Brain electric microstates, and cognitive and perceptual modes. In: Kruse, P. and Stadler, M. (Eds.), Ambiguity in mind and nature: multistable cognitive phenomena. Springer-Verlag, Berlin Heidelberg, pp. 407-420.

Levenez, M., Kotzamanidis, C., Carpentier, A. and Duchateau, J., 2005. Spinal reflexes and coactivation of ankle muscles during a submaximal fatiguing contraction. J Appl Physiol 99, 1182-1188.

Lindstrom, L., Kadefors, R. and Petersen, I., 1977. An electromyographic index for localized muscle fatigue. J Appl Physiol 43, 750-754.

Linkenkaer-Hansen, K., Nikouline, V.V., Palva, J.M. and Ilmoniemi, R.J., 2001. Long-range temporal correlations and scaling behavior in human brain oscillations. J Neurosci 21, 1370-1377.

Lippold, O.C.J., Redfearn, J.W.T. and Vuco, J., 1960. The electromyography of fatigue. Ergonomics 3, 121-131.

Llinas, R.R., 1988. The intrinsic electrophysiological properties of mammalian neurons: insights into central nervous system function. Science 242, 1654-1664.

Lobaugh, N.J., West, R. and McIntosh, A.R., 2001. Spatiotemporal analysis of experimental differences in event-related potential data with partial least squares. Psychophysiol 38, 517-530.

Loève, M., 1945. Fonctions aléatoires du second ordre. Compte Rend Acad Sci 220.

Loève, M., 1948. Fonctions aléatoires du second ordre. In: Lèvy, P. (Ed.), Processus stochastiques et mouvement Brownien. Gauthier Villars, Paris.

Lopes da Silva, F., 1991. Neural mechanisms underlying brain waves: from neural membranes to networks. Electroencephalogr Clin Neurophysiol 79, 81-93.

Lopes da Silva, F.H., Vos, J.E., Mooibroek, J. and van Rotterdam, A., 1980. Relative contributions of intracortical and thalamo-cortical processes in the generation of alpha rhythms, revealed by partial coherence analysis. Electroencephalogr Clin Neurophysiol 50, 449-456.

Loscher, W.N., Cresswell, A.G. and Thorstensson, A., 1996. Excitatory drive to the alpha-motoneuron pool during a fatiguing submaximal contraction in man. J Physiol 491, 271-280.

Makeig, S., Debener, S., Onton, J. and Delorme, A., 2004. Mining event-related brain dynamics. Trends Cogn Sci 8, 204-210.

Makeig, S., Jung, T.P., Bell, A.J., Ghahremani, D. and Sejnowski, T.J., 1997. Blind separation of auditory event-related brain responses into independent components. Proc Natl Acad Sci USA 94, 10979-10984.

Makeig, S., Westerfield, M., Jung, T.P., Covington, J., Townsend, J., Sejnowski, T.J. and Courchesne, E., 1999. Functionally independent components of the late positive event-related potential during visual spatial attention. J Neurosci 19, 2665-2680.

Makeig, S., Westerfield, M., Jung, T.P., Enghoff, S., Townsend, J., Courchesne, E. and Sejnowski, T.J., 2002. Dynamic brain sources of visual evoked responses. Science 295, 690-694.

Mäkinen, V., Tiitinen, H. and May, P., 2005. Auditory event-related responses are generated independently of ongoing brain activity. Neuroimage 24, 961-968.

Mäkinen, V.T., May, P.J. and Tiitinen, H., 2004. Human auditory event-related processes in the time-frequency plane. Neuroreport 15, 1767-1771.

Mardia, K.V., 1972. Statistics of directional data. Academic Press, London.

Marr, D.C. and Poggio, T., 1977. From understanding computation to understanding neural circuitry. Neurosci Res Prog Bull 15, 470-491.

Marsden, C.D., Meadows, J.C., Lange, G.W. and Watson, R.S., 1969. The relation between physiological tremor of the two hands in healthy subjects. Electroencephalogr Clin Neurophysiol 27, 179-185.

Marsden, J.F., Farmer, S.F., Halliday, D.M., Rosenberg, J.R. and Brown, P., 1999. The unilateral and bilateral control of motor unit pairs in the first dorsal interosseous and paraspinal muscles in man. J Physiol 521, 553-564.

Mayville, J.M., Fuchs, A., Ding, M., Cheyne, D., Deecke, L. and Kelso, J.A., 2001. Event-related changes in neuromagnetic activity associated with syncopation and synchronization timing tasks. Hum Brain Mapp 14, 65-80.

McAuley, J.H. and Marsden, C.D., 2000. Physiological and pathological tremors and rhythmic central motor control. Brain 123, 1545-1567.

McAuley, J.H., Rothwell, J.C. and Marsden, C.D., 1997. Frequency peaks of tremor, muscle vibration and electromyographic activity at 10 Hz, 20 Hz and 40 Hz during human finger muscle contraction may reflect rhythmicities of central neural firing. Exp Brain Res 114, 525-541.

McCrea, D.A., 2001. Spinal circuitry of sensorimotor control of locomotion. J Physiol 533, 41-50.

McIntosh, A.R., Bookstein, F.L., Haxby, J.V. and Grady, C.L., 1996. Spatial pattern analysis of functional brain images using partial least squares. Neuroimage 3, 143-157.

McIntosh, A.R. and Lobaugh, N.J., 2004. Partial least squares analysis of neuroimaging data: applications and advances. Neuroimage 23, S250-263.

McKenna, T.M., McMullen, T.A. and Shlesinger, M.F., 1994. The brain as a dynamic physical system. Neuroscience 60, 587-605.

Mellor, R. and Hodges, P., 2005. Motor unit synchronization between medial and lateral vasti muscles. Clin Neurophysiol 116, 1585-1595.

Meunier, C. and Segev, I., 2002. Playing the Devil's advocate: is the Hodgkin-Huxley model useful? Trends Neurosci 25, 558-563.

Miller, W.L. and Sigvardt, K.A., 1998. Spectral analysis of oscillatory neural circuits. J Neurosci Methods 80, 113-128.

Mima, T., Simpkins, N., Oluwatimilehin, T. and Hallett, M., 1999. Force level modulates human cortical oscillatory activities. Neurosci Lett 275, 77-80.

Mima, T., Steger, J., Schulman, A.E., Gerloff, C. and Hallett, M., 2000. Electroencephalographic measurement of motor cortex control of muscle activity in humans. Clin Neurophysiol 111, 326-337.

Monno, A., Chardenon, A., Temprado, J.J., Zanone, P.G. and Laurent, M., 2000. Effects of attention on phase transitions between bimanual coordination patterns: a behavioral and cost analysis in humans. Neurosci Lett 283, 93-96.

Mormann, F., Lehnertz, K., David, P. and Elger, C.E., 2000. Mean phase coherence as a measure for phase synchronization and its application to the EEG of epilepsy patients. Phys D 144, 358-369.

Morris, L.G., Thuma, J.B. and Hooper, S.L., 2000. Muscles express motor patterns of non-innervating neural networks by filtering broad-band input. Nat Neurosci 3, 245-250.

Morrison, M., 1995. The new aspect: symmetries as meta-laws - structural metaphysics. In: Wienert, F. (Ed.), Laws of nature. Essays on the philosophical, scientific and historical dimension. Walter de Gruyter, New York, pp. 157- 188.

Morrison, S., Kavanagh, J., Obst, S.J., Irwin, J. and Haseler, L.J., 2005. The effects of unilateral muscle fatigue on bilateral physiological tremor. Exp Brain Res 167, 609-621.

Mortimer, J.T., Magnusson, R. and Petersen, I., 1970. Conduction velocity in ischemic muscle: effect on EMG frequency spectrum. Am J Physiol 219, 1324-1329.

Mullany, H., O'Malley, M., St Clair Gibson, A. and Vaughan, C., 2002. Agonist-antagonist common drive during fatiguing knee extension efforts using surface electromyography. J Electromyogr Kinesiol 12, 375-384.

Munk, M.H., Roelfsema, P.R., Konig, P., Engel, A.K. and Singer, W., 1996. Role of reticular activation in the modulation of intracortical synchronization. Science 272, 271-274.

Murphy, G.L. and Medin, D.L., 1985. The role of theories in conceptual coherence. Psychol Rev 92, 289-316.

Myers, L.J., Lowery, M., O'Malley, M., Vaughan, C.L., Heneghan, C., St Clair Gibson, A., Harley, Y.X. and Sreenivasan, R., 2003. Rectification and non-linear pre-processing of EMG signals for cortico-muscular analysis. J Neurosci Methods 124, 157-165.

Näätänen, R., Ilmoniemi, R.J. and Alho, K., 1994. Magnetoencephalography in studies of human cognitive brain function. Trends Neurosci 17, 389-395.

Näätänen, R. and Winkler, I., 1999. The concept of auditory stimulus representation in cognitive neuroscience. Psychol Bull 125, 826-859.

Nagamine, T., Kajola, M., Salmelin, R., Shibasaki, H. and Hari, R., 1996. Movement-related slow cortical magnetic fields and changes of spontaneous MEG- and EEG-brain rhythms. Electroencephalogr Clin Neurophysiol 99, 274-286.

Newell, A. and Simon, H.A., 1976. Computer science as empirical inquiry: symbols and search. Commun Ass Comput Machinery 19, 113-126.

Nicolis, G. and Prigogine, I., 1981. Symmetry-breaking and pattern selection in far-from-equilibrium systems. Proc Natl Acad Sci USA 78, 659-663.

Nunez, P.L. (Ed.), 1995. Neocortical dynamics and human EEG rhythms. Oxford University Press, New York.

O'Sullivan, J.D., Rothwell, J., Lees, A.J. and Brown, P., 2002. Bilaterally coherent tremor resembling enhanced physiological tremor: report of three cases. Mov Disord 17, 387-391.

Oda, S., 1997. Motor control for bilateral muscular contractions in humans. Jpn J Physiol 47, 487-498.

Oishi, M., Kameyama, S., Fukuda, M., Tsuchiya, K. and Kondo, T., 2004. Cortical activation in area 3b related to finger movement: an MEG study. Neuroreport 15, 57-62.

Omlor, W., Patino, L., Hepp-Reymond, M.C. and Kristeva, R., 2007. Gamma-range corticomuscular coherence during dynamic force output. Neuroimage 34, 1191-1198.

Palm, G., 1981. Towards a theory of cell assemblies. Biol Cybern 39, 181-194.

Palus, M., 1997. Detecting phase synchronization in noisy systems. Phys Lett A 235, 341-351.

Palva, S., Linkenkaer-Hansen, K., Näätänen, R. and Palva, J.M., 2005. Early neural correlates of conscious somatosensory perception. J Neurosci 25, 5248-5258.

Pantev, C., Makeig, S., Hoke, M., Galambos, R., Hampson, S. and Gallen, C., 1991. Human auditory evoked gamma-band magnetic fields. Proc Natl Acad Sci USA 88, 8996-9000.

Parkes, L.M., Bastiaansen, M.C. and Norris, D.G., 2006. Combining EEG and fMRI to investigate the post-movement beta rebound. Neuroimage 29, 685-696.

Pascual-Leone, A., Grafman, J. and Hallett, M., 1994. Modulation of cortical motor output maps during development of implicit and explicit knowledge. Science 263, 1287-1289.

Pattee, H.H., 1973. The physical basis and origin of hierarchical control. In: Pattee, H. H. (Ed.), Hierarchy theory: the challenge of complex systems. George Braziller, Inc., New York, pp. 71-108.

Penny, W.D., Kiebel, S.J., Kilner, J.M. and Rugg, M.D., 2002. Event-related brain dynamics. Trends Neurosci 25, 387-389.

Peper, C.E., Beek, P.J. and van Wieringen, P.C.W., 1995a. Frequency-induced phase-transitions in bimanual tapping. Biol Cybern 73, 301-309.

Peper, C.E., Beek, P.J. and van Wieringen, P.C.W., 1995b. Multifrequency coordination in bimanual tapping - Asymmetrical coupling and signs of supercriticality. J Exp Psychol Hum 21, 1117-1138.

Peper, C.E. and Carson, R.G., 1999. Bimanual coordination between isometric contractions and rhythmic movements: an asymmetric coupling. Exp Brain Res 129, 417-432.

Perez, M.A., Lundbye-Jensen, J. and Nielsen, J.B., 2006. Changes in corticospinal drive to spinal motoneurones following visuo-motor skill learning in humans. J Physiol 573, 843-855.

Peters, M., 1985. Constraints in the performance of bimanual tasks and their expression in unskilled and skilled subjects. Q J Exp Psychol A 37, 171-196.

Pfurtscheller, G., 1981. Central beta rhythm during sensorimotor activities in man. Electroencephalogr Clin Neurophysiol 51, 253-264.

Pfurtscheller, G. and Aranibar, A., 1978. Occipital rhythmic activity within alpha band during conditioned externally paced movement. Electroencephalogr Clin Neurophysiol 45, 226-235.
Pfurtscheller, G. and Aranibar, A., 1979. Evaluation of event-related desynchronization (ERD) preceding and following voluntary self-paced movement. Electroencephalogr Clin Neurophysiol 46, 138-146.
Pfurtscheller, G. and Lopes da Silva, F.H., 1999. Event-related EEG/MEG synchronization and desynchronization: basic principles. Clin Neurophysiol 110, 1842-1857.
Pfurtscheller, G., Neuper, C., Brunner, C. and Lopez da Silva, F.H., 2005. Beta rebound after different types of motor imagery in man. Neurosci Lett 378, 156-159.
Pfurtscheller, G., Stancak, A., Jr. and Neuper, C., 1996. Post-movement beta synchronization. A correlate of an idling motor area? Electroencephalogr Clin Neurophysiol 98, 281-293.
Pfurtscheller, G., Zalaudek, K. and Neuper, C., 1998. Event-related beta synchronization after wrist, finger and thumb movement. Electroencephalogr Clin Neurophysiol 109, 154-160.
Pikovsky, A., Rosenblum, M. and Kurths, J., 2001. Synchronization: a universal concept in nonlinear sciences. Cambridge University Press, Cambridge.
Pollok, B., Gross, J., Muller, K., Aschersleben, G. and Schnitzler, A., 2005. The cerebral oscillatory network associated with auditorily paced finger movements. Neuroimage 24, 646-655.
Pollok, B., Gross, J. and Schnitzler, A., 2006. How the brain controls repetitive finger movements. J Physiol Paris 99, 8-13.
Pollok, B., Muller, K., Aschersleben, G., Schmitz, F., Schnitzler, A. and Prinz, W., 2003. Cortical activations associated with auditorily paced finger tapping. Neuroreport 14, 247-250.
Popper, K.R., 1972. Conjectures and refutations: the growth of scientific knowledge. Routledge, London.
Port, R.F. and van Gelder, T. (Eds.), 1995. Mind as motion. The MIT Press, Cambridge, MA.
Post, A.A., Peper, C.E. and Beek, P.J., 2000a. Relative phase dynamics in perturbed interlimb coordination: the effects of frequency and amplitude. Biol Cybern 83, 529-542.
Post, A.A., Peper, C.E., Daffertshofer, A. and Beek, P.J., 2000b. Relative phase dynamics in perturbed interlimb coordination: stability and stochasticity. Biol Cybern 83, 443-459.
Praamstra, P., Turgeon, M., Hesse, C.W., Wing, A.M. and Perryer, L., 2003. Neurophysiological correlates of error correction in sensorimotor-synchronization. Neuroimage 20, 1283-1297.
Pradhan, N. and Dutt, D.N., 1993. A nonlinear perspective in understanding the neurodynamics of EEG. Comput Biol Med 23, 425-442.
Prigogine, I., 1978. Time, structure, and fluctuations. Science 201, 777-785.

Psek, J.A. and Cafarelli, E., 1993. Behavior of coactive muscles during fatigue. J Appl Physiol 74, 170-175.

Rabinovich, M.I., Varona, P., Selverston, A.I. and Abarbanel, H.D.I., 2006. Dynamical principles in neuroscience. Rev Mod Phys 78, 1213-1265.

Recanzone, G.H., Merzenich, M.M., Jenkins, W.M., Grajski, K.A. and Dinse, H.R., 1992. Topographic reorganization of the hand representation in cortical area 3b owl monkeys trained in a frequency-discrimination task. J Neurophysiol 67, 1031-1056.

Rescher, N., 1996. Process metaphysics: an introduction to process philosophy. State University of New York Press, Albany.

Ridderikhoff, A., Daffertshofer, A., Peper, C.L. and Beek, P.J., 2005a. Mirrored EMG activity during unimanual rhythmic movements. Neurosci Lett 381, 228-233.

Ridderikhoff, A., Peper, C.E. and Beek, P.J., 2005b. Unraveling interlimb interactions underlying bimanual coordination. J Neurophysiol 94, 3112-3125.

Riecker, A., Wildgruber, D., Mathiak, K., Grodd, W. and Ackermann, H., 2003. Parametric analysis of rate-dependent hemodynamic response functions of cortical and subcortical brain structures during auditorily cued finger tapping: a fMRI study. Neuroimage 18, 731-739.

Rodriguez, E., George, N., Lachaux, J.P., Martinerie, J., Renault, B. and Varela, F.J., 1999. Perception's shadow: long-distance synchronization of human brain activity. Nature 397, 430-433.

Rosenberg, J.R., Amjad, A.M., Breeze, P., Brillinger, D.R. and Halliday, D.M., 1989. The Fourier approach to the identification of functional coupling between neuronal spike trains. Prog Biophys Mol Biol 53, 1-31.

Rosenblum, M., Pikovsky, A. and Kurths, J., 1996. Phase synchronization of chaotic oscillators. Phys Rev Lett 76, 1804-1807.

Rudrauf, D., Douiri, A., Kovach, C., Lachaux, J.P., Cosmelli, D., Chavez, M., Adam, C., Renault, B., Martinerie, J. and Le Van Quyen, M., 2006. Frequency flows and the time-frequency dynamics of multivariate phase synchronization in brain signals. Neuroimage 31, 209-227.

Russell, B., 1946. History of western philosophy and its connection with political and social circumstances from the earliest times to the present day. George Allen & Unwin Ltd., London.

Sadato, N., Yonekura, Y., Waki, A., Yamada, H. and Ishii, Y., 1997. Role of the supplementary motor area and the right premotor cortex in the coordination of bimanual finger movements. J Neurosci 17, 9667-9674.

Salenius, S., Portin, K., Kajola, M., Salmelin, R. and Hari, R., 1997. Cortical control of human motoneuron firing during isometric contraction. J Neurophysiol 77, 3401-3405.

Salinas, E. and Sejnowski, T.J., 2001. Correlated neuronal activity and the flow of neural information. Nat Rev Neurosci 2, 539-550.

Salmelin, R., Hämäläinen, M., Kajola, M. and Hari, R., 1995. Functional segregation of movement-related rhythmic activity in the human brain. Neuroimage 2, 237-243.

Sanes, J.N. and Donoghue, J.P., 2000. Plasticity and primary motor cortex. Annu Rev Neurosci 23, 393-415.
Sayers, B.M. and Beagley, H.A., 1974. Objective evaluation of auditory evoked EEG responses. Nature 251, 608-609.
Sayers, B.M., Beagley, H.A. and Henshall, W.R., 1974. The mechansim of auditory evoked EEG responses. Nature 247, 481-483.
Schaefer, M., Flor, H., Heinze, H.J. and Rotte, M., 2005. Dynamic shifts in the organization of primary somatosensory cortex induced by bimanual spatial coupling of motor activity. Neuroimage 25, 395-400.
Schanze, T. and Eckhorn, R., 1997. Phase correlation among rhythms present at different frequencies: spectral methods, application to microelectrode recordings from visual cortex and functional implications. Int J Psychophysiol 26, 171-189.
Schlaug, G., Knorr, U. and Seitz, R., 1994. Inter-subject variability of cerebral activations in acquiring a motor skill: a study with positron emission tomography. Exp Brain Res 98, 523-534.
Schmidt, R.C., Treffner, P.J., Beek, P.J. and Turvey, M.T., 1991. Dynamic substructure of coordinated rhythmic movements. J Exp Psychol Hum 17, 635-651.
Schoffelen, J.M., Oostenveld, R. and Fries, P., 2005. Neuronal coherence as a mechanism of effective corticospinal interaction. Science 308, 111-113.
Sears, T.A. and Stagg, D., 1976. Short-term synchronization of intercostal motoneurone activity. J Physiol 263, 357-381.
Semmler, J.G., 2002. Motor unit synchronization and neuromuscular performance. Exerc Sport Sci Rev 30, 8-14.
Serrien, D.J. and Brown, P., 2004. Changes in functional coupling patterns during bimanual task performance. Neuroreport 15, 1387-1390.
Serrien, D.J., Ivry, R.B. and Swinnen, S.P., 2006. Dynamics of hemispheric specialization and integration in the context of motor control. Nat Rev Neurosci 7, 160-166.
Sharott, A., Marsden, J. and Brown, P., 2003. Primary orthostatic tremor is an exaggeration of a physiological response to instability. Mov Disord 18, 195-199.
Sherrington, C., 1925. Remarks on some aspects of reflex inhibition. Proc R Soc Lond B 97, 19-45.
Shin, C.W. and Kim, S., 2006. Self-organized criticality and scale-free properties in emergent functional neural networks. Phys Rev E 74, 045101.
Singer, W., 1993. Synchronization of cortical activity and its putative role in information processing and learning. Ann Rev Physiol 55, 349-374.
Singer, W., 1999. Neuronal synchrony: a versatile code for the definition of relations? Neuron 24, 49-65, 111-125.
Solomonow, M., Baratta, R., Zhou, B.H. and D'Ambrosia, R., 1988. Electromyogram coactivation patterns of the elbow antagonist muscles during slow isokinetic movement. Exp Neurol 100, 470-477.

Spencer, R.M.C., Ivry, R.B., Cattaert, D. and Semjen, A., 2005. Bimanual coordination during rhythmic movements in the absence of somatosensory feedback. J Neurophysiol 94, 2901-2910.

Sporns, O., Tononi, G. and Edelman, G.M., 2000. Theoretical neuroanatomy: relating anatomical and functional connectivity in graphs and cortical connection matrices. Cereb Cortex 10, 127-141.

Stam, C.J., 2004. Functional connectivity patterns of human magnetoencephalographic recordings: a 'small-world' network? Neurosci Lett 355, 25-28.

Stam, C.J., 2005. Nonlinear dynamical analysis of EEG and MEG: review of an emerging field. Clin Neurophysiol 116, 2266-2301.

Stam, C.J., 2006. Nonlinear brain dynamics. Nova Science Publishers, Inc., New York.

Stam, C.J., Nolte, G. and Daffertshofer, A., 2007. Phase lag index: assessment of functional connectivity from multi channel EEG and MEG with diminished bias from common sources. Hum Brain Mapp. DOI: 10.1002/hbm.20346.

Stam, C.J., van Cappellen van Walsum, A.M., Pijnenburg, Y.A., Berendse, H.W., de Munck, J.C., Scheltens, P. and van Dijk, B.W., 2002. Generalized synchronization of MEG recordings in Alzheimer's disease: evidence for involvement of the gamma band. J Clin Neurophysiol 19, 562-574.

Stam, C.J. and van Dijk, B.W., 2002. Synchronization likelihood: an unbiased measure of generalized synchronization in multivariate data sets. Phys D 163, 236-251.

Stent, G.S., 1975. Limits to the scientific understanding of man. Science 187, 1052-1057.

Suffczynski, P., Kalitzin, S., Pfurtscheller, G. and Lopes da Silva, F.H., 2001. Computational model of thalamo-cortical networks: dynamical control of alpha rhythms in relation to focal attention. Int J Psychophysiol 43, 25-40.

Summers, J.J., Ford, S.K. and Todd, J.A., 1993a. Practice effects on the coordination of the 2 hands in a bimanual tapping task. Hum Mov Sci 12, 111-133.

Summers, J.J., Rosenbaum, D.A., Burns, B.D. and Ford, S.K., 1993b. Production of polyrhythms. J Exp Psychol Hum 19, 416-428.

Swinnen, S.P., Jardin, K. and Meulenbroek, R., 1996. Between-limb asynchronies during bimanual coordination: effects of manual dominance and attentional cueing. Neuropsychologia 34, 1203-1213.

Swinnen, S.P., Walter, C.B., Lee, T.D. and Serrien, D.J., 1993. Acquiring bimanual skills: contrasting forms of information feedback for interlimb decoupling. J Exp Psychol Learn Mem Cogn 19, 1328-1344.

Tallon-Baudry, C. and Bertrand, O., 1999. Oscillatory gamma activity in humans and its role in object representation. Trends Cogn Sci 3, 151-162.

Taniguchi, M., Kato, A., Fujita, N., Hirata, M., Tanaka, H., Kihara, T., Ninomiya, H., Hirabuki, N., Nakamura, H., Robinson, S.E., Cheyne, D. and Yoshimine, T., 2000. Movement-related desynchronization of the cerebral cortex studied with spatially filtered magnetoencephalography. Neuroimage 12, 298-306.

Tass, P., Rosenblum, M.G., Weule, J., Kurths, J., Pikovsky, A., Volkmann, J., Schnitzler, A. and Freund, H.J., 1998. Detection of n:m phase locking from noisy data: application to magnetoencephalography. Phys Rev Lett 81, 3291-3294.

Tass, P.A., 1999. Phase resetting in medicine and biology: stochastic modelling and data analysis. Springer-Verlag Berlin, Heidelberg.

Tass, P.A., 2003. Stochastic phase resetting of two coupled phase oscillators stimulated at different times. Phys Rev E 67, 051902.

Tass, P.A., 2004. Transmission of stimulus-locked responses in two coupled phase oscillators. Phys Rev E 69, 051909.

ter Hark, M., 2003. Searching for the searchlight theory: from Karl Popper to Otto Selz. J Hist Ideas 64, 465-487.

Thompson, E. and Varela, F.J., 2001. Radical embodiment: neural dynamics and consciousness. Trends Cogn Sci 5, 418-425.

Tiitinen, H., Sinkkonen, J., Reinikainen, K., Alho, K., Lavikainen, J. and Näätänen, R., 1993. Selective attention enhances the auditory 40-Hz transient response in humans. Nature 364, 59-60.

Toma, K., Mima, T., Matsuoka, T., Gerloff, C., Ohnishi, T., Koshy, B., Andres, F. and Hallett, M., 2002. Movement rate effect on activation and functional coupling of motor cortical areas. J Neurophysiol 88, 3377-3385.

Toni, I., Krams, M., Turner, R. and Passingham, R.E., 1998. The time course of changes during motor sequence learning: a whole-brain fMRI study. Neuroimage 8, 50-61.

Tononi, G., Edelman, G.M. and Sporns, O., 1998. Complexity and coherency: integrating information in the brain. Trends Cogn Sci 2, 474-484.

Treffner, P.J. and Turvey, M.T., 1996. Symmetry, broken symmetry, and handedness in bimanual coordination dynamics. Exp Brain Res 107, 463-478.

Turvey, M.T., 1990. Coordination. Am Psychol 45, 938-953.

Vaillancourt, D.E. and Newell, K.M., 2000. Amplitude changes in the 8-12, 20-25, and 40 Hz oscillations in finger tremor. Clin Neurophysiol 111, 1792-1801.

Varela, F., Lachaux, J.P., Rodriguez, E. and Martinerie, J., 2001. The brainweb: phase synchronization and large-scale integration. Nat Rev Neurosci 2, 229-239.

Viitasalo, J.H. and Komi, P.V., 1977. Signal characteristics of EMG during fatigue. Eur J Appl Physiol Occup Physiol 37, 111-121.

Virtanen, J., Ahveninen, J., Ilmoniemi, R.J., Näätänen, R. and Pekkonen, E., 1998. Replicability of MEG and EEG measures of the auditory N1/N1m-response. Electroencephalogr Clin Neurophysiol 108, 291-298.

Virtanen, J., Rinne, T., Ilmoniemi, R.J. and Näätänen, R., 1996. MEG-compatible multichannel EEG electrode array. Electroencephalogr Clin Neurophysiol 99, 568-570.

von der Malsburg, C., 1999. The what and why of binding: the modeler's perspective. Neuron 24, 95-104, 111-125.

von Holst, E., 1937/1973. On the nature of order in the central nervous system. The behavioural physiology of animals and man, Vol.1. University of Miami Press, Coral Cables, FL, pp. 3-32.

Vrba, J., 2002. Magnetoencephalography: the art of finding a needle in a haystack. Phys C 368, 1-9.

Vrba, J., Haid, G., Lee, S., Taylor, B., Fife, A.A., Kubik, P., McCubbin, J. and Burbank, M.B., 1991. Biomagnetometers for unshielded and well shielded environments. Clin Phys Physiol Meas 12 Suppl B, 81-86.

Vrba, J. and Robinson, S.E., 2001. Signal processing in magnetoencephalography. Methods 25, 249-271.

Walter, D.O., 1971. Objectivity revised: models from 20th-century physical science for use in the human sciences. Int J Neurosci 1, 243-250.

Weinberg, H., Brickett, P.A., Vrba, J., Fife, A.A. and Burbank, M.B., 1984. The use of a squid third order spatial gradiometer to measure magnetic fields of the brain. Ann NY Acad Sci 425, 743-752.

Weinberg, H., Cheyne, D. and Crisp, D., 1990. Electroencephalographic and magnetoencephalographic studies of motor function. Adv Neurol 54, 193-205.

Werth, E., Achermann, P. and Borbely, A.A., 1996. Brain topography of the human sleep EEG: antero-posterior shifts of spectral power. Neuroreport 8, 123-127.

Wilson, H.R. and Cowan, J.D., 1972. Excitatory and inhibitory interactions in localized populations of model neurons. Biophys J 12, 1-24.

Wing, A.M. and Kristofferson, A.B., 1973. Response delays and timing of discrete motor responses. Percept Psychophys 14, 5-12.

Woldag, H., Waldmann, G., Schubert, M., Oertel, U., Maess, B., Friederici, A. and Hummelsheim, H., 2003. Cortical neuromagnetic fields evoked by voluntary and passive hand movements in healthy adults. J Clin Neurophysiol 20, 94-101.

Woldorff, M.G., Tempelmann, C., Fell, J., Tegeler, C., Gaschler-Markefski, B., Hinrichs, H., Heinze, H.J. and Scheich, H., 1999. Lateralized auditory spatial perception and the contralaterality of cortical processing as studied with functional magnetic resonance imaging and magnetoencephalography. Hum Brain Mapp 7, 49-66.

Xiang, J., Hoshiyama, M., Koyama, S., Kaneoke, Y., Suzuki, H., Watanabe, S., Naka, D. and Kakigi, R., 1997. Somatosensory evoked magnetic fields following passive finger movement. Brain Res Cogn Brain Res 6, 73-82.

Yamagishi, N., Callan, D.E., Goda, N., Anderson, S.J., Yoshida, Y. and Kawato, M., 2003. Attentional modulation of oscillatory activity in human visual cortex. Neuroimage 20, 98-113.

Yates, F.E., 1980. Physical causality and brain theories. Am J Physiol 238, R277-290.

Zhuang, P., Toro, C., Grafman, J., Manganotti, P., Leocani, L. and Hallett, M., 1997. Event-related desynchronization (ERD) in the alpha frequency during development of implicit and explicit learning. Electroencephalogr Clin Neurophysiol 102, 374-381.

Zijdewind, I. and Kernell, D., 2001. Bilateral interactions during contractions of intrinsic hand muscles. J Neurophysiol 85, 1907-1913.
Zola-Morgan, S., 1995. Localization of brain function: the legacy of Franz Joseph Gall (1758-1828). Annu Rev Neurosci 18, 359-383.

Summary

The present thesis addresses the question how cognitive processes influence the neural control of action. Cognition was expected to modulate neural dynamics, in general, and oscillatory activity and its synchronization, in particular. To investigate this general expectation, several experiments were conducted in which task-related variables like force level, central and peripheral fatigue, movement tempo, and task difficulty, were varied to induce changes in the accompanying neural synchronization. Neural activity was recorded using electromyography (EMG) and magnetoencephalography (MEG), while participants performed either static isometric or dynamic rhythmic tasks.

In Chapter 1, basic concepts of synchronization in brain activity are introduced. It is argued that a focus on synchronization stands in the scientific tradition that considers processes as fundamental and is therefore complementary to more structure-oriented approaches that try to identify modular processes of specialized brain regions. Next, a concise sketch of the theory of complex systems is provided because this theory provides an adequate conceptual framework for studying the behavior and coupling of dynamical compounds like neural oscillators, as has been amply demonstrated in the field of neuroscience. This sketch is followed by a brief discussion of the pertinent literature on neural synchronization showing that synchronization can provide mechanisms of feature binding or motor integration. Finally, the thesis' main threads are outlined by introducing the investigated experimental tasks and applied data analysis methods.

In Chapter 2, two experiments are discussed that examined the effects of muscle fatigue on motor-unit (MU) synchronization between the quadriceps muscles of both legs. Muscle fatigue was expected to result in an increased common drive to different MUs of synergists within a leg and, hence, to increased MU synchronization. It was further expected that fatigue-related motor overflow may cause MU synchronization of homologous muscles of both legs, although to a lesser extent than for synergists within a leg. In the first experiment, different levels of fatigue were induced by varying posture (knee angle), while in the second experiment fatigue was induced by having participants produce different force levels in a fixed posture. Synchronization, quantified in terms of coherence between surface EMG, was found in two distinct frequency bands (6-11 and 13-18 Hz), more prominently so within a leg than between legs. The inter-limb synchronization in the 6-11 Hz

frequency band increased with fatigue and resembled increased motor overflow during unimanual contractions. As such, the two phenomena may be related in that they both indicate a fatigue-induced increase in bilateral coupling. MU synchronization at 13-18 Hz was clearly different and depended on posture.

Chapter 3 reports a similar experiment that was designed to study the relation between bilateral MU synchronization and motor overflow. The bilateral coupling between homologous arm muscles was compared during fatiguing elbow flexion and extension contractions. Similar to the results of Chapter 2, MU synchronization was found in the 8-12 Hz frequency band, more strongly so when fatigued. This fatigue-related increase in bilateral MU synchronization was stronger between extensor than between flexor muscles, which appeared consistent with the literature on mirror movements and supported the alleged link between bilateral MU synchonization and fatigue-related motor overflow. In contrast to the study on leg muscles in Chapter 2, the arm muscles did not exhibit MU synchronization in the 13-18 Hz frequency band, which seemed consistent with the hypothesis that MU synchronization in the higher frequency band, as described in Chapter 2, was linked to balance maintenance. The results are discussed in terms of common bilateral input and substantiate the idea that common input is functionally organized.

The experiment reported in Chapter 4 deals with the effects of sleep deprivation (SD) on cortical brain activity during acoustically paced rhythmic force production. MEG was recorded during a rhythmic motor task that was conducted at two consecutive days between which SD was induced by keeping participants awake, i.e. participants did not sleep for at least 24 hours. Effects of SD on brain activity were examined via spatial distribution of spectral power over the scalp at different frequency bands and via auditory- and motor-evoked fields. For the latter, principal component analysis (PCA) revealed that auditory- and motor-evoked fields were attenuated after SD. Furthermore, an anterior shift of alpha power towards more frontal channels was found. At the behavioral level, SD resulted in a reduction of the lag (negative asynchrony) between produced forces and acoustic stimuli at higher movement tempos. Conjointly, these results are interpreted in terms of a change of central processing of afferent sensory input due to SD.

In Chapter 5, the event-related brain activity associated with the performance of an acoustically paced synchronization task is further examined. To gain insight into the neural dynamics causing the auditory- and motor-related activity, the amplitude and phase dynamics inherent in MEG signals

were analyzed across frequency bands. By comparing amplitude and phase dynamics, a distinction was made between so-called evoked and induced responses. Again, PCA was used, this time, however, to compare amplitude and phase changes during mere listening, paced and unpaced tapping. Using PCA allowed for a separation of brain activity related to motor and auditory processes, respectively. Motor performance was accompanied by phasic amplitude changes and increased phase locking with the taps in the beta band. Auditory processing of acoustic stimuli resulted in a simultaneous increase of amplitude and phase locking with those stimuli in the theta and alpha band. The temporal overlap of auditory-related amplitude changes and phase locking indicated an evoked response, in accordance with previous studies on auditory perception. The temporal difference of movement-related amplitude and phase dynamics in the beta band, on the other hand, suggested a change in ongoing brain activity, i.e. an induced response supporting previous results on motor-related brain dynamics in the beta band.

Chapter 6 concerns a study on the changes in neural synchronization during motor learning. To this end, MEG and EMG activity was recorded while participants learned to perform a 5:3 polyrhythm. As this task involved bimanual rhythmic activity at distinct movement tempos, it was expected to elicit neural activity in bilateral motor cortices that could be readily disentangled. Building on the results of Chapter 5 regarding motor-related fields, synthetic aperture magnetometry (SAM) analysis was used in focusing on the beta band in order to separate bilateral activity in both motor cortices. On a behavioral level, performance converged onto the to-be-learned 5:3 polyrhythm in the course of the experiment. The SAM-based reconstruction of the activity of the motor cortices revealed phasic changes in beta activity related to force production of the contralateral finger. The degree of beta modulation increased during the experiment and was positively correlated with motor performance, in particular for the motor cortex contralateral to the slow hand. These findings support the view that activity in motor cortex co-varies closely with behavioral changes in the course of learning.

In Chapter 7, the epilogue, the theoretical framework presented in Chapter 1 is recalled in order to discuss the implications of the experimental results for the understanding of brain dynamics. It is concluded from those results that neural synchronization is ubiquitous during the execution of motor tasks. In particular, two distinct synchronization patterns stood out in the various experimental settings: the 10 Hz synchronization between bilateral EMGs and the beta modulation above the contralateral motor cortex during rhythmic motor tasks. Moreover, neural synchronization was consistently

modulated by various task parameters, in line with the alleged functional role of neural synchronization. Neural synchronization therefore appears to be a significant characteristic of the neural dynamics of motor control and an essential vehicle for the understanding of the temporal aspects of neural motor control. The collective results are thus consistent with the theoretical framework capitalized upon in this thesis and contribute to current discussions as to how the brain processes information in general. Especially the absence of beta synchronization during rhythmic motor performance is deemed revealing in this regard, i.e. cortical beta activity was attenuated during periods of phasic motor control and corticospinal synchronization was largely absent during rhythmic motor control. These findings suggest that instances of rhythmic and static motor control differ fundamentally. Apparently, periodic synchronized behavior does not serve as a means for motor-related information transfer between cortical and spinal areas during rhythmic motor performance. In this context, recent literature is discussed on the mode of information processing employed by the central nervous system and possible other forms of synchronization that may be present during dynamic motor control. Based on this discussion, new directions for future research are suggested that can experimentally test these extensions of the initiated research program.

Samenvatting

Neurale dynamica van de bewegingssturing

De mens is in staat om met grote precisie naar doelen te bewegen, ritmische patronen te produceren, krachten op de omgeving uit te oefenen en voorwerpen op te pakken. Deze motorische vaardigheden komen tot stand dankzij een gecoördineerd samenspel van onze spieren. Bij dit samenspel is een groot aantal neurale structuren betrokken, waaronder het ruggenmerg, de basale kernen en de cerebrale cortex. Hoe deze neurale structuren elkaar via informatie-uitwisseling beïnvloeden wordt al geruime tijd onderzocht, maar dit heeft nog niet tot algemeen aanvaarde antwoorden geleid. De in dit proefschrift beschreven experimenten hadden tot doel meer inzicht te verschaffen in de interacties tussen de neurale structuren die bij bewegingssturing betrokken zijn. In deze experimenten werden factoren gemanipuleerd die de taakuitvoering beïnvloeden, zoals spiervermoeidheid, slaapdeprivatie, bewegingssnelheid en de moeilijkheidsgraad van de taak. Verwacht werd dat deze manipulaties zouden leiden tot modulaties in neurale activiteit, zoals gemeten met electromygrafie (EMG) en magneto-encephalografie (MEG). Gedetailleerde analyse van deze modulaties zou vervolgens inzicht moeten geven in de aard en functie van de bestudeerde activiteit.

In hoofdstuk 1 wordt het theoretisch kader van het onderzoek geschetst. Binnen het onderzoek naar de relatie tussen hersenen en gedrag zijn verschillende benaderingen te onderscheiden, elk met hun eigen uitgangspunten. Enerzijds zijn er benaderingen waarin voornamelijk geprobeerd wordt de verschillende hersenstructuren, die betrokken zijn bij de sturing van bewegingen, in kaart te brengen om zo een idee te krijgen van hun functies. Andere benaderingen richten zich juist op het samenspel van activiteit tussen deze hersenstructuren. Het onderzoek in dit proefschrift behoort tot de tweede categorie en volgt een benadering die stoelt op de dynamische-systeemtheorie. Vanuit deze invalshoek wordt de neurale activiteit beschouwd in termen van gekoppelde neurale oscillatoren. Wiskundig gezien kunnen dergelijke systemen allerlei gedragingen vertonen waarin verschillende regimes zijn te onderscheiden. Zo blijkt uit empirisch onderzoek dat verschillende neuronen of groepen van neuronen synchroon gedrag vertonen dat beïnvloed wordt door wat de proefpersoon waarneemt of doet. In hoofdstuk 1 wordt kort de literatuur over het centrale begrip neurale synchronisatie en de

functionele betekenis daarvan besproken. Om meer inzicht te krijgen in de rol van synchronisatie bij bewegingssturing werd een reeks van experimenten uitgevoerd, waarin, zoals gezegd, verschillende variabelen werden gemanipuleerd om de effecten daarvan op de neurale synchronisatie te bestuderen.

In hoofdstuk 2 worden twee experimenten behandeld waarin het effect van spiervermoeidheid op de synchronisatie tussen motorische eenheden wordt onderzocht. Een motorische eenheid bestaat uit een motorneuron in het ruggenmerg en de spiervezels die door dit neuron worden aangestuurd. Motorneuronen worden op hun beurt aangestuurd door hoger gelegen neurale structuren. De verwachting was dat de gezamenlijke aansturing van verschillende motorische eenheden, en daarmee de mate van hun synchronisatie, zou toenemen bij toenemende spiervermoeidheid.

In beide experimenten voerden de proefpersonen een taak uit waarin zij continu een bepaalde kracht moesten leveren door de kniestrekkers in beide benen isometrisch aan te spannen. In het eerste experiment werd spiervermoeidheid geïnduceerd door de lichaamshouding van de proefpersoon te veranderen, zodat het steeds moeilijker werd om deze houding vol te houden. In het tweede experiment moest de geproduceerde kracht verhoogd worden bij dezelfde houding. Synchronisatie werd gekwantificeerd in termen van de coherentie tussen oppervlakte-EMG's. In twee frequentiebanden werd synchronisatie gevonden, namelijk tussen 6 en 11 Hz en tussen 13 en 18 Hz. Deze synchronisatie was sterker tussen de activiteit van spieren binnen één been dan tussen dezelfde (homologe) spieren van beide benen. Naarmate proefpersonen vermoeider raakten nam ook de synchronisatie tussen de activiteit van de homologe spieren toe in de frequentieband van 6 tot 11 Hz. Dit verschijnsel is vergelijkbaar met het 'motor overflow'-fenomeen, waarbij aanspanning van een enkele ledemaat leidt tot spieractiviteit in de andere ledemaat. De toegenomen synchronisatie en het 'motor overflow'-fenomeen hangen mogelijk met elkaar samen, omdat beide optreden tijdens spiervermoeidheid en tevens duiden op een toenemende koppeling tussen ledematen. De waargenomen synchronisatie tussen motorische eenheden in de frequentieband van 13 tot 18 Hz vertoonde echter geen duidelijke verandering met spiervermoeidheid, maar leek meer beïnvloed te worden door de ingenomen houding.

In hoofdstuk 3 wordt de relatie tussen 'motor overflow' en de synchronisatie tussen motorische eenheden van homologe spieren verder onderzocht. Dit

gebeurt aan de hand van een experiment waarin de synchronisatie tussen motorische eenheden van (vermoeide) homologe bovenarmspieren werd vergeleken bij buiging en strekking van de elleboog. Net als in hoofdstuk 2 werd synchronisatie gevonden in de frequentieband van 8 tot 12 Hz en deze nam weer toe met spiervermoeidheid. De toename in synchronisatie met vermoeidheid was sterker voor de elleboogstrekkers dan voor de -buigers. Deze bevinding komt overeen met de onderzoeksresultaten van eerdere studies waarin een sterkere 'motor overflow' wordt gerapporteerd voor strekkers dan voor buigers.

In tegenstelling tot het onderzoek uit hoofdstuk 2 werd geen synchronisatie gevonden in de frequentieband van 13 tot 18 Hz. Dit is in overeenstemming met het idee dat synchronisatie in deze frequentieband gerelateerd is aan balanshandhaving en dus niet zal optreden tussen bovenarmspieren. De resultaten ondersteunen het idee dat de gezamenlijke aansturing van homologe spieren functioneel georganiseerd is.

Het in hoofdstuk 4 gerapporteerde experiment beschrijft het effect van slaapdeprivatie op hersenactiviteit tijdens een taak waarin proefpersonen op geleide van auditieve signalen ritmisch kracht moesten produceren. Tijdens de uitvoering van deze taak werd MEG-activiteit gemeten. Het experiment vond plaats op twee opeenvolgende dagen. Gedurende de hele nacht tussen beide dagen werden de proefpersonen wakker gehouden, zodat ze op de tweede dag tenminste 24 uur niet geslapen hadden. Het effect hiervan op de hersenactiviteit werd bepaald aan de hand van de distributie van spectraal vermogen en de sterkte van de corticale activiteit in aan het gehoor en de motoriek gerelateerde velden. Principale Componenten Analyse (PCA) toonde aan dat de activiteit in deze velden een kleinere amplitude had na slaapdeprivatie. Verder verschoof het vermogen in de alpha-frequentieband van meer occipitale naar meer frontale MEG-kanalen.

Uit de gedragsdata bleek dat de maxima in krachtproductie aan de tonen voorafgingen, hetgeen er op wijst dat de proefpersonen op de auditieve stimuli anticipeerden. Slaapdeprivatie resulteerde in een afname van deze anticipatie bij hogere bewegingstempi. Deze resultaten wijzen alle op een verandering van de centrale verwerking van sensorische informatie als gevolg van slaapdeprivatie.

In hoofdstuk 5 werden de aan het gehoor en de motoriek gerelateerde velden van neurale activiteit nader onderzocht door de amplitude- en fasedynamica van de MEG-signalen te analyseren in verschillende frequentiebanden. Wederom werd PCA gebruikt om de MEG-activiteit tussen de verschillende

experimentele condities te vergelijken, te weten: a) luisteren naar een ritme, b) met de vinger meetikken met het ritme, en c) het aangeboden ritme blijven produceren nadat de auditieve stimulus is weggevallen. Door de veranderingen in amplitude en fase te vergelijken bleek het mogelijk om geïnduceerde (induced) MEG-activiteit te onderscheiden van opgewekte (evoked) MEG-activiteit. Bij opgewekte reacties treden amplitudemodulatie en fasekoppeling met een gebeurtenis gelijktijdig op, terwijl dit bij geïnduceerde activiteit niet het geval is.

De resultaten van de PCA maakten het mogelijk om verschillende reacties in de hersenactiviteit te onderscheiden, die gerelateerd waren aan auditieve en motorische processen. Bewegingssturing ging samen met veranderingen in amplitude- en faseverdeling in de bèta-frequentieband binnen een bewegingscyclus. Het verwerken van de auditieve stimuli leidde tot een gelijktijdige toename van amplitude en fasekoppeling met deze stimuli in de thèta- en alpha-band, hetgeen wees op een opgewekte reactie. Dit resultaat kwam overeen met eerdere bevindingen in het onderzoek naar auditieve informatieverwerking. De aan motoriek gerelateerde veranderingen in amplitude en fasekoppeling met de beweging vonden niet gelijktijdig plaats, hetgeen wees op een geïnduceerde reactie. Geconcludeerd werd daarom dat de verschillende waargenomen veranderingen in hersenactiviteit werden teweeggebracht door verschillende onderliggende processen.

In hoofdstuk 6 wordt een studie beschreven naar de veranderingen in neurale synchronisatie tijdens het leren van een motorische taak. MEG- en EMG-activiteit werden gemeten terwijl de proefpersonen een 5:3-polyritme aanleerden, hetgeen inhoudt dat beide handen met een verschillend tempo dienden te bewegen in een frequentieverhouding van vijf staat tot drie. Omdat de bewegingsfrequenties van beide handen verschilden, was de neurale activiteit van beide motorcortices makkelijk te onderscheiden in de MEG-signalen. Voortbordurend op de resultaten van hoofdstuk 5 over de aan motoriek gerelateerde velden, werd Synthetic Aperture Magnetometry (SAM) analyse toegepast om de bilaterale activiteit van beide motorcortices in de bèta-band te scheiden. Deze analyse toonde een snelle verandering van bèta-activiteit in beide motorcortices, die gerelateerd was aan de activiteit van de contralaterale hand. Dit is in overeenstemming met het anatomische gegeven dat de linker motorcortex verbonden is met de spieren aan de rechter kant van het lichaam en vice versa. De mate van bèta-modulatie nam toe gedurende het experiment en was positief gecorreleerd met het succes waarmee de proefpersonen het 5:3-polyritme uitvoerden. Deze correlatie was het sterkst

voor de motorcortex contralateraal van de langzame hand. Dit komt overeen met resultaten van gedragsstudies die aantoonden dat een polyritme wordt geleerd door het op de juiste manier timen van de bewegingen van de langzame hand ten opzichte van die van de snelle hand.

In hoofdstuk 7, de epiloog, worden de resultaten van de experimenten geïnterpreteerd in termen van het in hoofdstuk 1 geïntroduceerde theoretische kader. Geconcludeerd wordt dat neurale synchronisatie een belangrijk kenmerk is van de hersenactiviteit die gepaard gaat met de uitvoering van motorische taken. Met name twee synchronisatiepatronen waren duidelijk te onderscheiden, te weten de 10 Hz-synchronisatie tussen homologe spieractiviteit (hoofdstuk 2 en 3) en de bèta-modulatie van activiteit van de contralaterale motorcortex gedurende ritmische taken (hoofdstuk 5 en 6). Deze synchronisatiepatronen werden bovendien systematisch beïnvloed door veranderingen in verschillende taakfactoren, hetgeen er op duidt dat synchronisatie een functionele rol speelt. De onderzoeksresultaten zijn in overeenstemming met het geadopteerde theoretische kader en dragen bij aan de huidige discussie over informatieverwerking in het brein. Met name de afname van bèta-synchronisatie gedurende ritmische bewegingstaken is wat dat betreft opmerkelijk: corticale bèta-activiteit werd onderdrukt gedurende korte episodes van bewegingssturing en corticospinale synchronisatie was grotendeels afwezig gedurende ritmische taken. Deze resultaten suggereren dat neurale bewegingssturing verschillend is voor dynamische en statische taken: bij laatstgenoemde taken werd, zoals beschreven in hoofdstuk 1, consistent corticospinale synchronisatie gevonden in de bèta-band. Blijkbaar speelt synchronisatie geen prominente rol bij de uitwisseling van motorische informatie tussen corticale en spinale gebieden tijdens de uitvoering van ritmische taken.

De bevindingen uit het onderzoek worden in de epiloog verder gerelateerd aan recente literatuur over informatieverwerking door het zenuwstelsel en de verschillende vormen van synchronisatie die daarbij kunnen optreden. Gebaseerd op deze discussie worden uitbreidingen van het oorspronkelijke theoretisch kader voorgesteld en mogelijkheden besproken om deze experimenteel te toetsen.

Dankwoord

Wetenschap heeft mij altijd sterk geïnteresseerd. Het vormt een eindeloos labyrint van ideeën, theorieën en onderzoeken van scherpzinnige mensen die een groot deel van hun leven besteden aan het zoeken naar antwoorden op de grote vragen van het leven. Ik heb het voorrecht gehad met meerdere fascinerende wetenschappers te mogen samenwerken, met wie ik van gedachten heb gewisseld over de vele intrigerende onderwerpen die de wetenschap rijk is. Zonder hen was het nooit mogelijk geweest om dit proefschrift te schrijven.

Allereerst natuurlijk Andreas Daffertshofer, met wie ik zeer intensief heb samengewerkt tijdens mijn promotieonderzoek. Ik heb het getroffen met jou als dagelijks begeleider. Niet alleen heb je een brede wetenschappelijke interesse en een buitengewone kennis van complexe dynamische systemen, je was ook altijd bereid deze met me te delen en me te helpen bij de vele vragen die ik had. Ik waardeer ook het rotsvaste vertrouwen dat je had in ons project. Ik denk met veel plezier terug aan al onze discussies in de kroeg waar we, naarmate de avond vorderde, steeds extremere ideeën bedachten en je drang om niet te winnen weddenschappen af te sluiten steeds groter werd. Dat je daarbij soms koppig en tegendraads bent, kan ik alleen maar appreciëren. Ik hoop dat we onze samenwerking in de toekomst kunnen voortzetten, ook al zit ik de komende jaren een eind verwijderd van Amsterdam.

Peter Beek, als promotor was je zowel betrokken bij de grote lijn van mijn promotieonderzoek als bij de meest minutieuze details. Je uitgebreide kennis van de bewegingswetenschappen, je gevoel voor het wetenschappelijk argument en je aanstekelijke lach, maakte dat het altijd een genoegen was om met je samen te werken. Ik heb veel geleerd wanneer we samen mijn manuscripten doornamen en jij uitgebreid verschillende varianten van de tekst in overweging nam om de boodschap zo duidelijk en nauwkeurig mogelijk te formuleren. Je consistente visie op de dynamische aspecten van de bewegingssturing was een inspiratiebron voor mij.

Michael Breakspear, thank you for giving me the opportunity to visit your lab in Sydney. I greatly enjoyed those months at the Black Dog Institute, talking about grand analysis methods and listening to your inspiring ideas on new scientific directions. I'm looking forward to return to Sydney, continue our collaboration and improve my lousy surfing skills.

Ik heb veel plezier gehad op de Faculteit der Bewegingswetenschappen met de vele collega's met wie ik heb samengewerkt, of modder gehapt op de fiets in de Ardennen. Het was een genoegen om te werken in een open sfeer

waar je bij iedereen binnen kunt lopen met vragen en waar een uitmuntende technisch dienst is. Lieke Peper, dankzij jou ben ik met deze faculteit in contact gekomen en heb ik hier gesolliciteerd. Bert Clairbois, bedankt voor al je hulp bij het aansluiten van alle apparatuur aan het MEG systeem en het ontwikkelen van de MEG sensor wat leidde tot ons eerste artikel. Bert Coolen, bedankt dat je me hebt geholpen om alle experimentele protocollen te kunnen implementeren. Verder bedank ik mijn kamergenoten, Hemke van Doorn, Rob Withagen en Martijn Niessen, met wie ik onder de mom van wetenschap onze kamer heb omgebouwd tot een oerwoud en de beurs dagelijks onveilig heb gemaakt met opties, aandelen en turbo's. Hemke, ook al hebben we met onze gezamenlijke rekening grote hoogtes, maar vooral ook dieptepunten bereikt, en zijn we er uiteindelijk nauwelijks wijzer van geworden, ik vond het een mooi avontuur. Behalve mijn kamergenoten zijn er nog vele collega's die ik zal missen: Melvyn, Harjo, Anke, Rolf, Dinant, Joost, Johan, Claudine, Arne, Nicolette, Floor, Rita, Sanne, John, Alistair, Jan en Maarten bedankt voor alle discussies en fijne weekenden.

Gedurende mijn studie psychologie heb ik meerdere mensen ontmoet die mij hebben geïntroduceerd in de theoretische standpunten, waarvan er verschillende zijn terug te vinden in dit proefschrift: Loet Leydesdorff, die mij in het eerste jaar van mijn studie al in contact bracht met wetenschapsdynamica en autopoiesis, Cees van Leeuwen, die mij stuurde in de richting van dynamische systemen, intermittency en zelforganisatie, Robert Shaw and Michael Turvey, from who I learned everything about ecological psychology, quantum mechanics, any many other topics over a beer next to the pool or during Friday night pub, en Han van der Maas en Ingmar Visser, die bij begeleidden bij mijn afstuderen.

Wetenschap is natuurlijk allemaal leuk en aardig, maar er zijn ook nog andere dingen in het leven. Daarom ben ik heel blij dat ik zoveel goede vrienden heb met wie ik lekker een biertje (of een cocktail) kan drinken, op wintersport ga of een week zeilen, weekendjes weg naar Berlijn, de Bourgogne, of Toscane, en met wie ik alle andere mooie en minder mooie dingen in het leven kan delen. Ik zal jullie allemaal erg gaan missen in Sydney, er staat altijd een biertje voor jullie koud. In het bijzonder wil ik nog Ruben bedanken voor het vette design van mijn proefschrift, Jan voor zijn taalkundige visie, en natuurlijk mijn paranimfen, Chris, mijn eeuwige partner in crime, en Job, die mij straks gegarandeerd van mijn stress afhelpt als ik dit proefschrift moet verdedigen.

En dan mijn broer en ouders die altijd geïnteresseerd zijn in wat ik doe en mij altijd steunen ook al maak ik plannen om drie jaar naar Sydney te gaan. Jullie betekenen heel veel voor me en ik ga jullie erg missen.

Tenslotte natuurlijk Jesse: Wat ben ik blij met dit leven met jou! Ik heb heel veel zin in ons nieuwe avontuur in Sydney en de vele die nog komen gaan.

List of publications

Part of this thesis

T.W. Boonstra, H.E. Clairbois, A. Daffertshofer, J. Verbunt, B.W. van Dijk and P.J. Beek (2004). MEG-compatible force sensor. *Journal of Neuroscience Methods 144*, 193-196.

T.W. Boonstra, A. Daffertshofer and P.J. Beek (2005). Effects of sleep deprivation on event-related fields and alpha activity during rhythmic force production. *Neuroscience Letters 388*, 27-32.

T.W. Boonstra, A. Daffertshofer, C.E. Peper and P.J. Beek (2006). Amplitude and phase dynamics associated with acoustically-paced finger tapping. *Brain Research 109,* 60-69.

T.W. Boonstra, A. Daffertshofer, E. van As, S. van der Vlugt and P.J. Beek (2007). Bilateral motor unit synchronization is functionally organized. *Experimental Brain Research 178*, 79-88.

T.W. Boonstra, A. Daffertshofer, J.C. van Ditshuizen, M.R.C. van den Heuvel, C. Hofman, N.W. Willigenburg and P.J. Beek (2007). Fatigue-related changes in motor-unit synchronization of quadriceps muscles within and across legs. *Journal of Electromyography and Kinesiology*. DOI:10.1016/j.jelekin.2007.03. 005.

T. W. Boonstra, A. Daffertshofer, M. Breakspear, P. J. Beek (2007). Multivariate time-frequency analysis of electromagnetic brain activity during bimanual motor learning. *NeuroImage* 36, 370-377.

Other

T.W. Boonstra, J.F. Stins, A. Daffertshofer, P.J. Beek (2007). Effects of sleep deprivation on neural functioning: an integrative review. *Cellular and Molecular Life Sciences 64*, 934-46.

A. Daffertshofer, T.W. Boonstra, P.J. Beek (2007). Cortical beta synchronization is related to low-order motor parameters. *International Congress Series 1300*, 329-332.